Studies on Synthesis and Evaluation of Novel Ratiometric Fluorescent Chemosensors Based on Hexahomotrioxacalix[3]arenes

September 2016

Division of Energy and Material Science

Graduate School of Science and Engineering

Saga University

Jiang XueKai

Studies on Synthesis and Evaluation of Novel Ratiometric Fluorescent Chemosensors Based on Hexahomotrioxacalix[3]arenes

A dissertation presented to the Graduate School of Science and Engineering of Saga University in partial fulfillment of the requirements for the degree of Doctor of Philosophy

September 2016

By:

Jiang XueKai

Supervisor:

Professor Dr. Takehiko Yamato

CERTIFICATE OF APPROVAL

Ph.D Dissertation

This is to certify that the Ph.D Dissertation of

Jiang XueKai

has been approved by the Examining Committee for the dissertation requirement for the Doctor of Philosophy degree in Chemistry at the September, 2016 graduation.

Dissertation committee:_____

Supervisor: Prof. Takehiko Yamato

_____

Member, Prof. Tsugio Kitamura

_____

Member, Prof. Takeshi Hanamoto

_____

Member, Prof. Mishinori Takeshita

ACKNOWLEDGEMENTS

First, I would like to express my sincere thanks to my supervisor, Professor Takehiko Yamato, without his support, guidance, helping, this thesis would be impossible, thank you very much. I hope my supervisor will be health forever and create much brilliant on chemical research field.

I also would like to express deepest gratitude to Professor Tsugio Kitamura, Professor Mishinori Takeshita, Professor Takeshi Hanamoto and Professor Keisuke Ohto. I also want to show my deepest gratitude to, Professor Xi Zeng and Professor Lan Mou in Guizhou University, Guiyang, China, who recommended me to Saga University for doctor course in the year of 2012.

I would like to express deep gratitude to all of the members in Yamato Lab, especially to Dr. Xin-Long Ni, Dr. Xing Feng, Dr. Ummey Rayhan, Dr. Hang Cong, Dr. Cheng-Cheng Jin, Dr. Md. Monarul Islam, Dr. Hirotsugu Tomiyasu, Dr. Zannatul Kowser Jiang-Lin Zhao, Nobuyuki Seto, Chong Wu, Chuan-Zeng Wang, Yusuke Ikejiri, who always give me suggestion and make my doctor life more enjoyable.

Finally, I would like to express my deep appreciation to my farther, Dao-Fu Jiang, mother, You-Lan Wang, wife, Wei-Li Hu. Their silent support is my driving force to go bravely forward. I hope my father and mother will be health forever and my wife will have a good future.

ABSTRACT

Over the past three decades, calix[n]arenes have become one of the preeminent classes of molecular receptors, owing to their excellent abilities to act as host molecules for a wide variety of neutral or charged species. For the elaboration of the molecular receptor, the use of cavity-based calix[n]arenes is particularly attractive because, in strong relation to natural systems, it can be expected that the cavity will ensure very high selectivity. Thus, against this background, several kinds of fluorescent chemosensors for heavy metal ions, anions, ammonium ions were designed and synthesized based on calixarene in this dissertation. The sensitivity and selectivity properties of these receptors to the target analyte were carefully evaluated.

In this research, *O*-Alkylation of hexahomooxacalix[3]arene (**1**H_3) with 9-chloromethyl- anthracene was carried out under the different reaction conditions. Interestingly, by using acetone/benzene (1:1 v/v) mixed solvent system, the *cone*-**4**An_3 was succeeded to synthesize. These results suggest that the solvent can also control the conformation of the *O*-alkylation products.

On the other hand, a novel type of selective and sensitive fluorescent sensor (**L**) having triazole rings as the binding sites on the lower rim of a hexahomotrioxacalix[3]arene scaffold in a *cone* conformation have been synthesized. This sensor has desirable properties for practical applications, including selectivity for detecting Zn^{2+} and Cd^{2+} in the presence of excess competing metal ions at low ion concentration or as a fluorescence enhancement type chemosensor.

Meanwhile, this compound also exhibits the high selective recognition towards alkylammonium cations, which can be also confirmed by enhancement of fluorescence spectra. The calix cavity changed from a “flattened-cone” to a more-upright form, and addition of n-$BuNH_3^+$ to **L** resulted in the formation of endo-cavity inclusion complexes. Interestingly, upon addition of Zn^{2+} to this system, chemosensor **L** can be capable of binding a metal ions and alkylammonium cations simultaneously through positive allosteric effect.

In summary, homooxacalix[3]arene have two conformation isomers, and the cone results can formed when a template metal is present in the reaction system or using solvent effect. Chemosensor **L** in cone conformation were designed and synthesized based on hexahomotrioxacalix[3]arene, Click chemistry. It has been use to recognize metal cation and ammonium cations. In these research fields, there are relativity few example and will open a gate for chemical research on chemosensors based on calixarene.

TABLE OF CONTENTS

ACKNOWLEDGEMENTS I

ABSTRACT II

TABLE OF CONTENTS III

Chapter 1

Development of Fluorescent Chemosensors Recently Based on Calixarene 1

1.1 General Introduction 2

1.2 Photophysics of fluorescent chemosensors 4

1.2.1 Principle of fluorescent chemosensor 4

1.2.2 Photoinduced electron transfer (PET) 5

1.2.3 Excimer formation 7

1.2.4 Photoinduced Charge Transfer(PCT) 7

1.2.5 Fluorescence Resonance Energy Transfer (FRET) 8

1.3 Fluorescent probes based on calixarene 9

1.3.1Calixarene-derived sensors for cations 9

1.3.3 Heteroditopic receptors for simultaneous cation–anion complexation 23

1.4 Conclusions 26

1.5 References 26

Chapter 2

Synthesis and structures of *O*-anthrylmethyl substituted hexahomotrioxacalix[3]arenes 32

2.1 Introduction 33

2.2 Results and discussion 34

2.2.1 Synthesis 34

2.2.2 Structure Assignment 36

2.2.3 Partial-cone and cone conformation 42

2.3 Conclusions 45

2.4 Experimental Section 46

2.5 References 50

Chapter 3

Synthesis and evaluation of a novel fluorescent sensors based on hexahomotrioxacalix[3]arene for Zn^{2+} and Cd^{2+} 54

3.1 Introduction 55

3.2. Results and discussion 57

3.2.1 Fluorescent spectroscopy studies 58

3.2.3 HPLC spectroscopy studies 67

3.2.4 ^{1}H NMR titration studies 67

3.3. Conclusions 69

3.4. Experimental section 69

3.4.1. General 69

3.4.2. Materials 70

3.5 References and notes 71

Chapter 4

Ratiometric fluorescent receptor for both Zn^{2+} and ammonium ions: based on a anthryl-linked triazole-modified homooxacalix[3]arene 74

4.1 Introduction 75

4.2 Result and discussion 76

4.2.1 Fluorescent Receptor for Ammonium Ions 76

4.2.2 Fluorescent receptor for both Zn^{2+} and ammonium ions 85

4.3. Conclusions 91

4.4. References 91

Summary 94

Publications 97

Chapter 1

Development of Fluorescent Chemosensors Recently Based on Calixarene

In this chapter we will introduce the fundamental research on calixarene and a shortly review of the recently development of fluorescent receptors for cations and anions based on calixarene.

1.1 General Introduction

Molecular recognition [1-2] is the core concepts of supramolecular chemistry, and in molecular recognition domain, with molecular devices properties of fluorescent recognition reagent (namely fluorescence probe) is a kind of abiotic "molecular devices". It selectively bonds with the target material, and then effectively recognizing of certain ions or molecules by the fluorescence signal. A fluorescent probe [3-6] consists of an ion recognition unit and a fluorogenic unit, which converts the actuating signal from the ionophore unit into a light signal. The recognition unit is deciding selectivity of the different objects, fluorogenic signal unit play a role in change the information of identification into a fluorescent signal. Fluorescent probe is an excellent molecular sensor, such as: high selectivity, high sensitivity, real-time in situ detection, and has been widely used in clinical diagnosis, biological analysis, environmental monitoring, materials science and other fields.

Recognition unit is the key part for designing of fluorescent probe. [7] Calixarenes with appropriately appended groups are good chemosensor candidates for recognition of cations anions and neutral moleculaes.

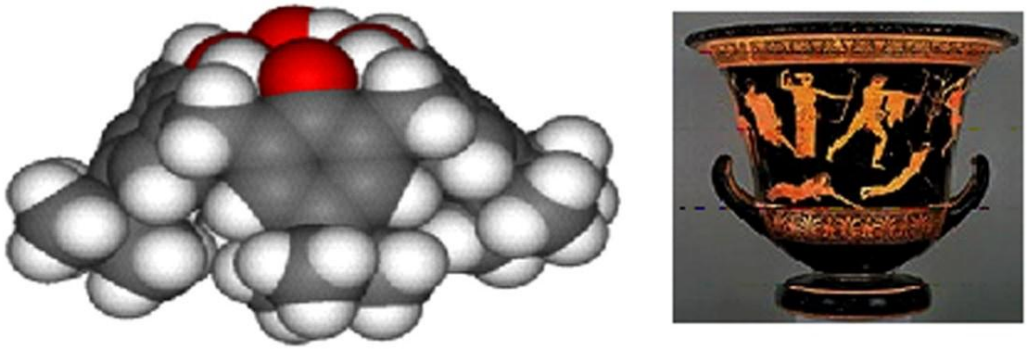

Figure 1.1. p-tert-Butyl-calix[4]arene resembles a calix crater vase in shape.

Calixarenes are one of the macrocyclic receptors known to date besides crown ethers, cyclodextrins, cryptands, and cucurbiturils [8], which was introduced by Gustche8 for cyclic oligomers, which was obtained from the condensation of formaldehyde with *p*-alkylphenols under alkaline conditions. The use of this word “calix” means “beaker” in Latin and Greek, Figure 1, was suggested in particular by the shape of the tetramer, which can (and generally) adopt a bowl- or beaker-like

conformation which indicates the possibility of the inclusion of "guest" molecules. Calixarenes are macrocyclic molecules, like crown ether and cyclodextrin.

Two regions can be distinguished in calixarenes, *viz.* the phenolic OH groups and the *para* positions of the aromatic rings, which are called respectively the "lower rim" and the "upper rim" of the calix (both rims can easily be selectively functionalized) as shown in Figure 3. In calix[4]arene, adjacent nuclei have been named "proximal" or (1,2) whereas the opposite ones are in "distal" or diametrical" (1,3) positions.

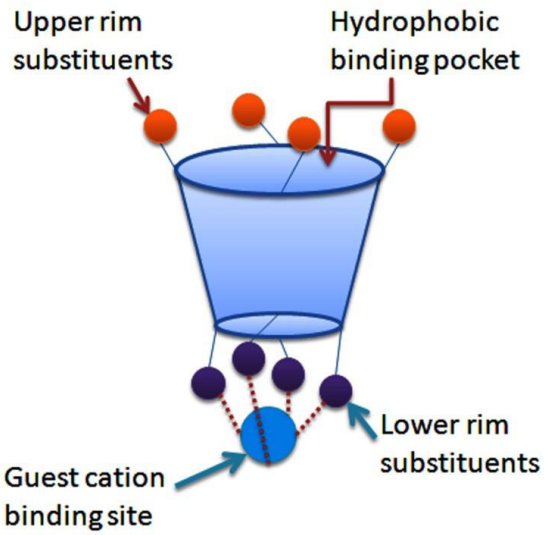

Figure 1.2. Anatomy of a calix[4]arene in the cone conformation.

Calixarenes made up the phenol and methylene units have many conformational isomers because of two possible rotational modes of the phenol unit, the oxygen-through-the annulus rotation and the para-substituent-through-the annulus rotation. Due to free rotation about the bonds of Ar-C-Ar groups, one of the most fascinating aspects of calixarenes is conformations. In the case of calix[4]arenes, there exists four possible conformational isomers in calix[4]arenes; i.e. *cone*, *partial-cone*, 1,2-*alternate* and 1,3-*alternate*. They differ with respect to the position of the phenolic OH groups (and the *p*-positions) with respect to the molecular plane (here easily define by the C, atoms of the methylene bridges).

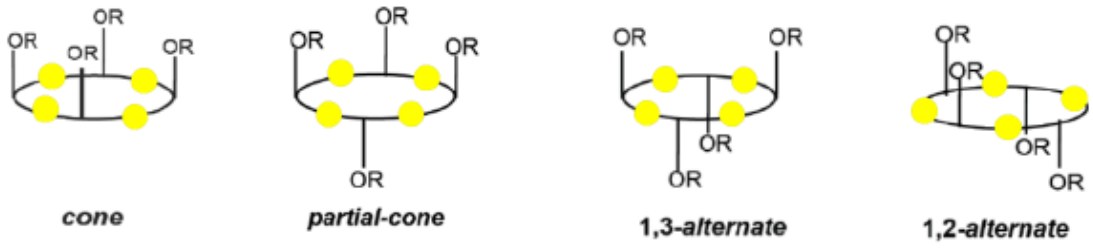

Figure 1.3. Four stable conformations of calix[4]arenes.

Calixarenes are 2,6-metacyclophanes with a methylene bridge between their phenolic groups, as shown in Figure 1. In 1994, the term "homocalixarene" was coined by Brodesser and Vögtle to describe analogues of calixarenes with two or more methylene groups between the aromatic moieties. [9] When one or more CH_2 bridges are replaced by CH_2OCH_2 groups the macrocycles are known as homooxacalixarenes, or simply oxacalixarenes. The presence of the heteroatom is reflected in the name of the compound, for example, p-tertbutylcalix[4]arene with a CH_2OCH_2 group instead of a CH_2 bridge is p-tert-butyldihomooxacalix[4]arene. [10] "Dihomo" implies two additional atoms in the bridge and "oxa" that one of them is oxygen.

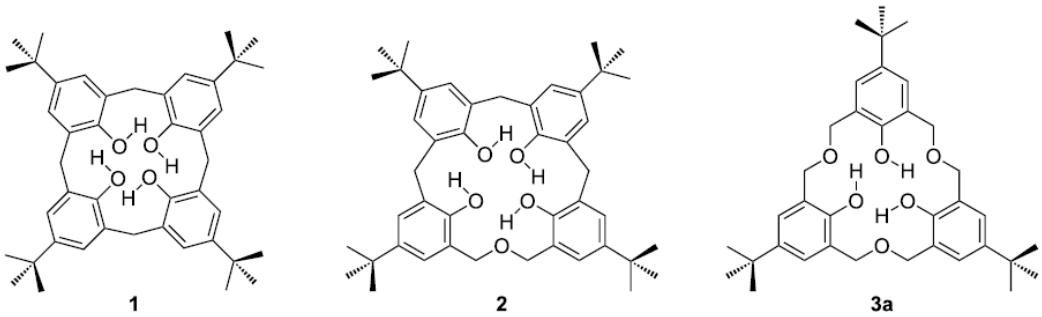

Figure 1.4. Calixarenes and expanded calixarenes: *p-tert*-Butylcalix[4]arene (**1**), *p-tert*-butyldihomooxacalix[4]arene (**2**), *p-tert*-butylhexahomotrioxacalix[3]arene (**3a**).

In comparison with the structural characteristics of the calixarene family, Oxacalix[3]arenes have received significant attention as receptors, mainly due to their structural features: A cavity formed by a 18-membered ring, only two basic conformations (*cone* and *partial-cone*), and a C_3-symmetry. [11] This last feature can provide a suitable binding site for species that require trigonal-planar, tetrahedral or octahedral coordination environments. The flexibility of the macrocycles can allow them to establish ideal bond distances and angles to bind such species.

1.2 Photophysics of fluorescent chemosensors

1.2.1 Principle of fluorescent chemosensor

The main issue in the design of any effective chemosensor is the association of a selective molecular recognition event with a physical signal highly sensitive to its occurrence. As shown in Figure 9, an effective fluorescent chemosensor includes an ion recognition unit (ionophore) and a fluorogenic unit (fluorophore), both moieties

generally can be independent species or covalently linked by a spacer.[12-13] The ionophore is required for selective binding of the substrate, while the fluorophore provides the means of or inhibition. Mechanisms which control the response of a fluorophore to substrate binding include photoinduced electron transfer (PET),[14-20] photoinduced charge transfer (PCT),[21-29] excimer/exciplex formation or extinction,[30-31] and Fluorescence (FoÖrster) resonance energy transfer (FRET).[32-34]

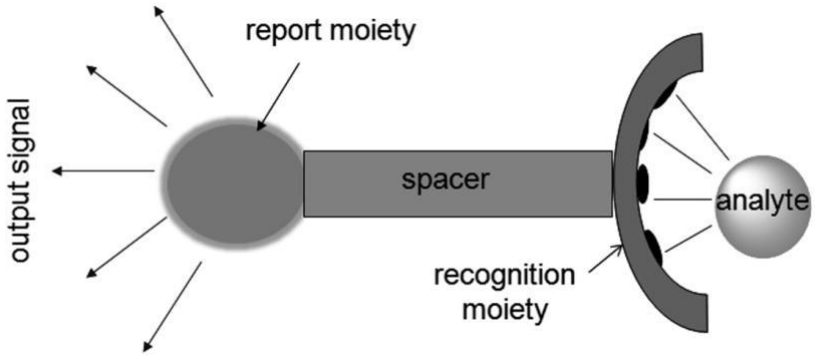

Figure 1.5. Diagram of an effective fluorescent chemosensor.

In that case, Changes in both the absorption and emission of light can be utilized as signals provided by appropriate chromophores or fluorophores, and two important classes of sensors are those of the optical and fluorimetric types. While spectrophotometry and fluorimetry are both relatively simple techniques which are rapidly performed, nondestructive and suited to multicomponent analysis, fluorimetry is considered superior commonly, principally because of its greater sensitivity.[35-40] Moreover absorbance measurements can at best determine concentrations down to 0.1 μM, fluorescence techniques can accurately measure concentrations 1 million times smaller. An additional advantage of fluorimetry is that discrimination between analytes is possible by time resolved measurements.[41]

1.2.2 Photoinduced electron transfer (PET)

In the simplest cases, emission of a photon, fluorescence, follows HOMO to LUMO excitation of an electron in a molecule. Where this emission is efficient, the molecule may be termed a fluorophore. Vibrational deactivation of the excited state prior to emission usually gives rise to a “Stokes shift” in that the wavelength of the emitted radiation is less than that of the exciting radiation.[42] Various other interactions may also modify the emission process, and these are of considerable importance in regard to analytical applications of fluorescence. Thus, when a lone electron pair is located in an orbital of the fluorophore itself or an adjacent molecule and the energyof this orbital lies between those of the HOMO and LUMO, efficient electron transfer of one electron of the pair to the hole in the HOMO created by light absorption may occur, followed by transfer of the initially excited electron to the lone pair orbital.

Such PET provides a mechanism for nonradiative deactivation of the excited state (Figure 6), leading to a decrease in emission intensity or "quenching" of the fluorescence.[43-44]

Fluorescence lost as a result of PET may be recovered if it is possible to involve the lone pair in a bonding interaction. Thus, protonation or binding of a metal ion effectively placesthe electron pair in an orbital of lower energy and inhibits the electron-transfer process. The excited-state energy may then again be lost by radiative emission. In the case of metal ion binding, this effect is referred to as chelation-enhanced fluorescence (CHEF).[45]

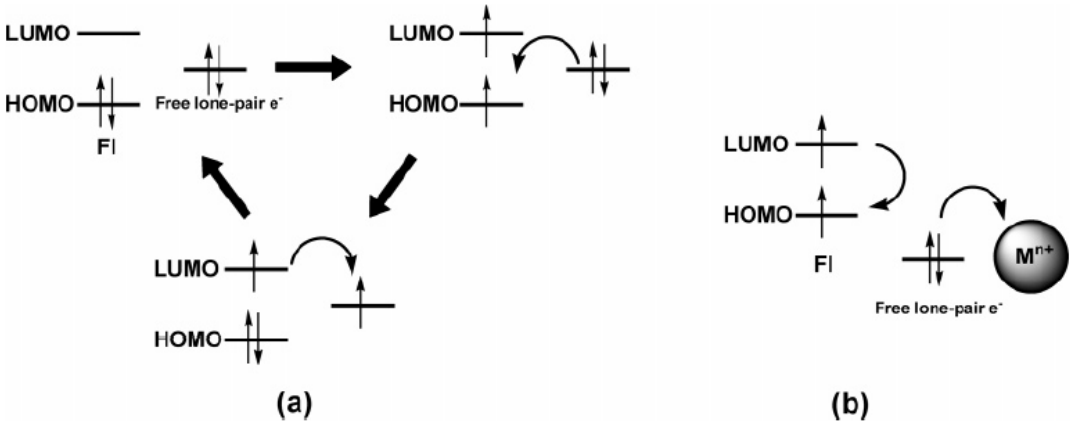

Figure 1.6. Mechanisms for PET (a) and CHEF (b) systems.

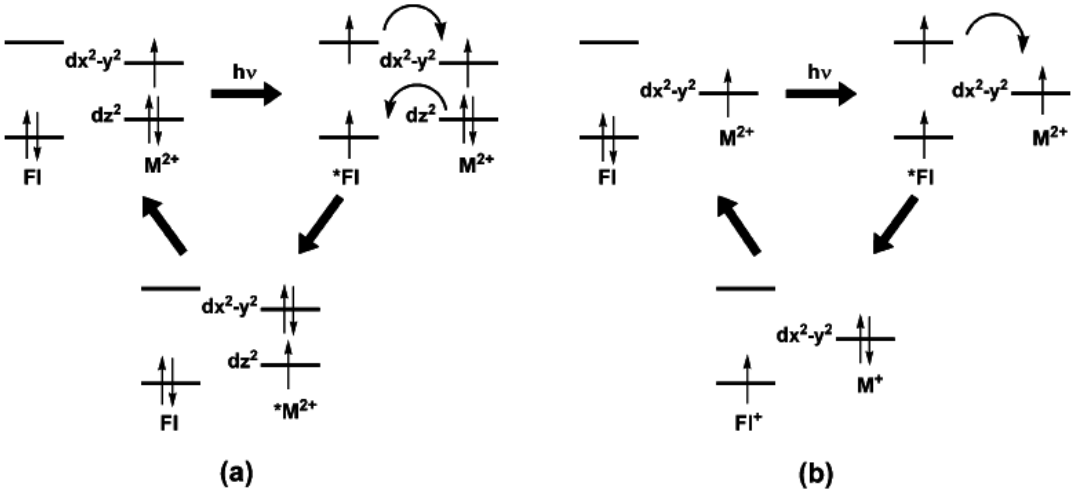

Figure 1.7. Mechanisms for (a) ET and (b) ET in systems containing an excited fluorophore and a d^9 metal ion.

In some cases, complexation of metal ions, Cu(II) and Ni(II), for example,[46-47] does not induce CHEF but causes the fluorescence to be quenched via two well-defined mechanisms, electron transfer (eT) and energy transfer (ET) to the metal ion, that lead to rapid nonradiative decay. While the ET process (Figure 7) involves no formal charge transfer, the eT process does and must therefore be associated with

some spatial reorganization of solvating molecules, so that inhibition of their motions should cause inhibition of eT. Thus, the two processes can be distinguished by comparing the luminescence of liquid and frozen solutions, enhancement of luminescence in the latter indicating that eT must be responsible for quenching in the liquid solution. It has been shown that eT has a weaker dependence on the donoracceptor separation than ET, so that eT tends to dominate for longer separations and ET for shorter.[48-50]

1.2.3 Excimer formation

Where aromatic rings are involved in weak interactions (such as π-stacking) which bring them within van der Waals contact distances, electronic excitation of one ring can cause an enhanced interaction with its neighbor, leading to what is termed an excited-state dimer or "excimer".[51-52] In other words, an excimer is a complex formed by the interaction of an excited fluorophore with another fluorophore in its ground state. Excimer emission typically provides a broad fluorescence band without vibrational structure, with the maximum shifted, in the case of most aromatic molecules,[53] by about 6000 cm^{-1} to lower energies compared to that of the uncomplexed ("monomer") fluorophore emission. An excimer may also form from an excited monomer if the interaction develops within the lifetime of the latter. Thus, it is expected that excimers are more likely to be produced by relatively long-lived monomer excited states.[54-57] Rates of fluorophore diffusion, especially in viscous solvents, are therefore another limit on excimer formation.[58-61] Importantly, the separation and relative orientation of multiple fluorophore units attached to ligands can be controlled by metal ion coordination, so that recognition of a cation can be monitored by the monomer/excimer fluorescenceintensity ratio.

1.2.4 Photoinduced Charge Transfer(PCT)

Electronic excitation necessarily involves some degree of charge transfer, but in fluorophores containing both electronwithdrawing and electron-donating substituents, this charge transfer may occur over long distances and be associated with major dipole moment changes, making the process particularly sensitive to the microenvironment of the fluorophore. Thus, it can be expected that cations or anions in close interaction with the donor or the acceptor moiety will change the photophysical properties of the fluorophore.[62]

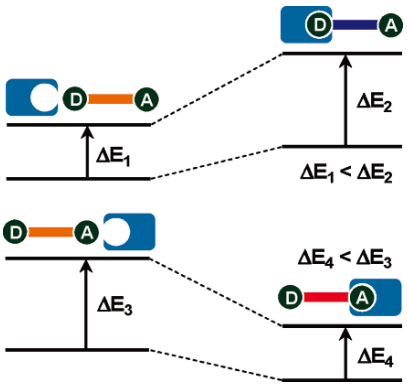

Figure 1.8. PCT system.

Upon, for example, cation complexation of an electron donor group within a fluorophore, the electron-donating character of the donor group will be reduced. The resulting reduction of conjugation causes a blue shift of the absorption spectrum together with a decrease of the molar absorptive. In contrast, metal ion binding to the acceptor group enhances its electron-withdrawing character, and the absorption spectrum is thus red-shifted with an increase in molar absorptive (Figure 8).[63] The fluorescence spectra should be shifted in the same direction as the absorption spectra, and in addition to these shifts, changes in the quantum yields and lifetimes can be observed. All these photophysical effects are obviously dependent on the charge and the size of the cation, and therefore, some selectivity is expected.

1.2.5 Fluorescence Resonance Energy Transfer (FRET)

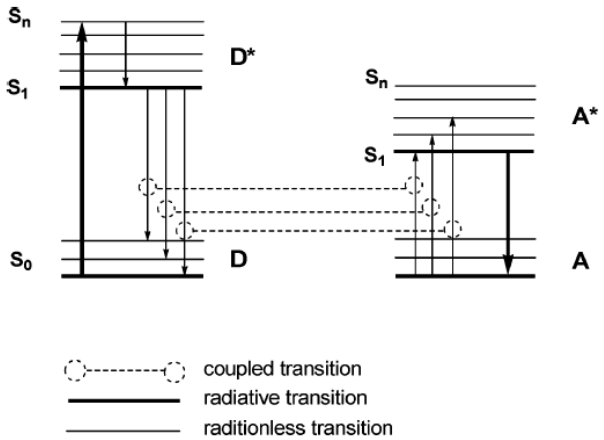

Figure 1.9. Fluorescence (Förster) resonance energy transfer system.

FRET arises from an interaction between a pair of dissimilar fluorophores in which one acts as a donor of excited-state energy to the other (acceptor). This returns the donor to its electronic ground state, and emission may then occur from the acceptor center (Figure 9). FRET is influenced by three factors: the distance between the donor and the acceptor, the extent of spectral overlap between the donor emission and acceptor absorption spectrum (Figure 10), and the relative orientation of the

donor emission dipole moment and acceptor absorption moment.[64]

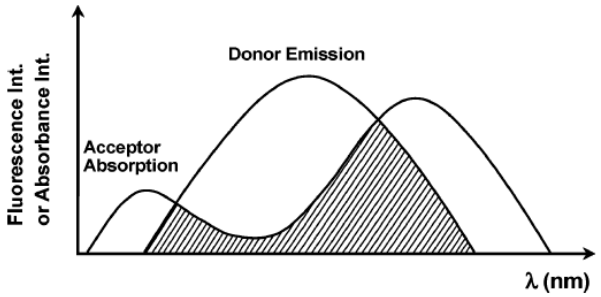

Figure 1.10. Spectral overlap for FRET.

1.3 Fluorescent probes based on calixarene

1.3.1Calixarene-derived sensors for cations

Figure 11 illustrates all the known modes of cation binding by native and functionalized calixarenes exploiting cation–π, induced dipole, or electrostatic interactions.[65]

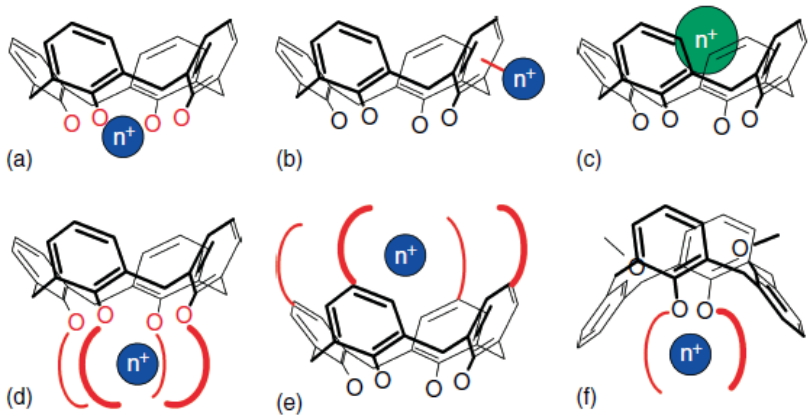

Figure 1.11. Different ways in which calixarenes interact with cations: (a) metallation at the *lower rim*; (b) *exo*-cavity (π-metallation); (c) *endo*-cavity; (d) at the *lower rim* with participation of additional binding sites; (e) at the *upper rim* by coordinating groups; (f) at the *lower rim* with participation of cation–π interactions. O atoms at the lower rim may be O−, OH or OR.

Strictly speaking, only for situations (c)–(f), we can talk of cation recognition by calixarene receptors, whereas in metallation with transition and f-element (situations (a) and (b)),[66] which are often exploited in anion complexation or catalysis, little control is experienced on selectivity.[67] Usually, the most important calixarene-based cation receptors are obtained by the introduction of chelating units at the lower rather than at the upper rim. This ensures a more convergent disposition of the chelating

units and the direct involvement of the phenolic O atom in cation binding. In the following sections, we highlight the role of the macrocycle size and conformation and the nature of binding groups on efficiency and selectivity in cation recognition and sensing.

1.3.1.1 Alkali and alkaline-earth metal ions

Ni et al. synthesized a novel ditopic receptor possessing two complexation sites and bearing 1,3-alternate conformation based on thiacalix[4]arene was prepared.[68] The binding behaviors with Na+, K+ and Ag+ ions have been examined by 1H NMR titration experiment in ($CDCl_3/CD_3CN$; 10:1, v/v) solution. The job plots prove 1:1 complexation of 1,3-alternate-**1** with Na+, K+ and Ag+ ions. Although the formation of heterogeneous dinuclear complexes was not clearly observed, the exclusive formation of mononuclear complexes of 1,3-alternate-**1** with metal cations is of particular interest with positive/negative allosteric effect in thiacalix[4]arenefamily as shown in Figure 1.12. These findings further demonstrate that preorganization, suitable conformational changes and affinity have a pronounced effect on the complexation process between the two different arms placed at the two edges of the thiacalix[4]arene cavity.

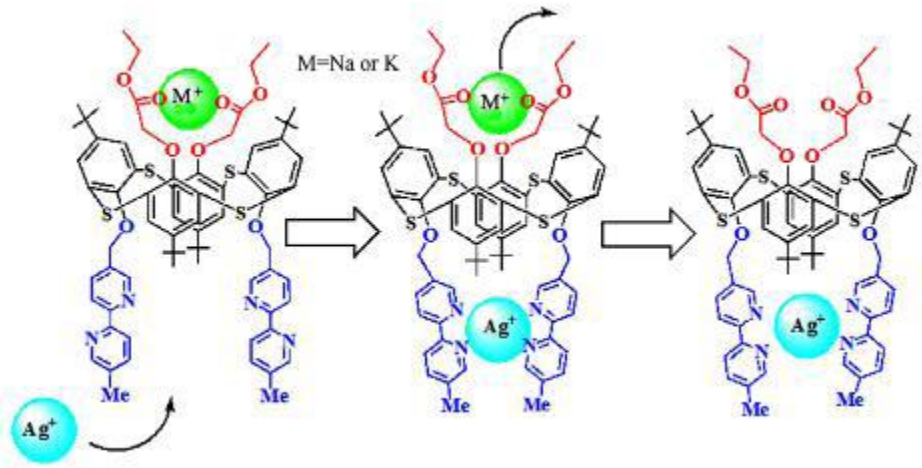

Figure 1.12. Plausible binding mode of **1** with Ag^+, Na^+ or K^+.

Chung et al. synthesized calixarene **2** containing a crown ether and triazoles, as metal ion binding sites, from 1,3-alternate calixcrown and 9-(azidomethyl) anthracene. The fluorescence of **2** was strongly quenched by Pb^{2+} ions, while the revival of emission from strongly quenched **2** • Pb^{2+} complex could be achieved by the addition of K^+ ions. The 1H NMR spectra of **2** • Pb^{2+} and **2** • K^+ complexes showed that the K^+ ion was bound to the crown-**2** ring, whereas the Pb^{2+} ion was bound to the OCH_2-triazole unit as shown in Figure 13. Thus, **2** acts as a novel fluorescent off-on

switchable chemosensor. [69]

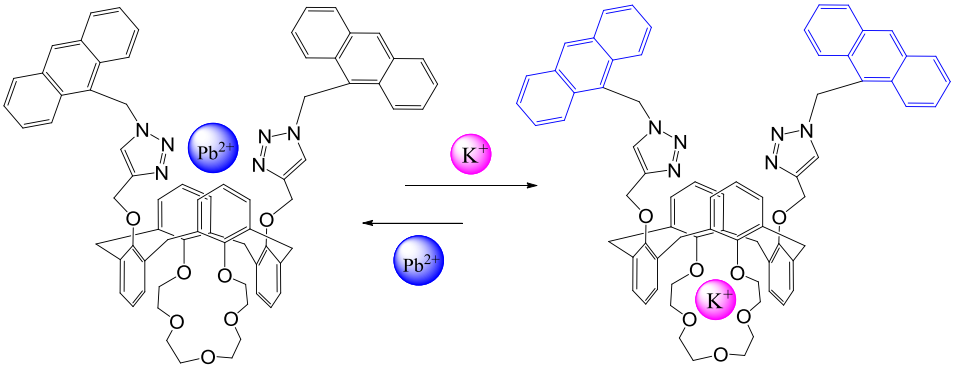

2

Figure 1.13. Structure of compound **2**.

Li groups designed and synthesized triazole-modified calixarene **3** by the 1,3-dipolar cycloaddition of azide esters with alkynylcalixarene (Figure 1.14). The cooperative complexation ability of the triazoles and ester groups towards alkali metal ions was investigated. Alkali metal ions were selectivity detected in the presence of picrate ions in the aqueous phase as shown by the UV spectra of **3**. The percentage extraction of alkali metal ions showed that **3** exhibits high selectivity towards Cs^+ ions.[70]

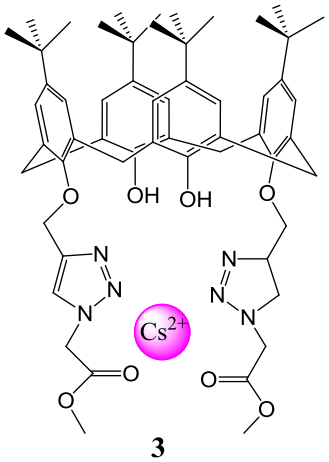

3

Figure 1.14. Structure of compound **3**.

Chung et al. synthesized a bifunctional chromogenic calixarene **4** that exhibited an INHIBIT logic gate with a YES logic function using Ca^{2+} and Fions as the chemical inputs. [71] The metal ion binding property of **4** was evaluated with perchlorate salts of Li^+, Na^+, K^+, Mg^{2+}, Ca^{2+}, Ba^{2+}, Ag^+, Zn^{2+}, Pb^{2+}, Ni^{2+}, Hg^{2+}, Mn^{2+}, and Cr^{3+} ions. From the UV-visible spectra, triazole-azophenol derivative **4**, containing triazoles as the metal-ligating groups, showed remarkable selectivity toward Ca^{2+}, Pb^{2+}, and Ba^{2+} ions. The color of the solution of **4** changed from green to bright yellow upon adding these ions. In addition to the metal ion binding properties, the sensing properties of **4**

toward anions was studied. The addition of F^-, AcO^-, and H_2PO4^- anions resulted in a red shift in the UV-visible spectra of **4**. Because of different colors produced when **4** was treated with either Ca^{2+} or F^- ion, the molecular logic gate was possible as shown in Figure 1.15.

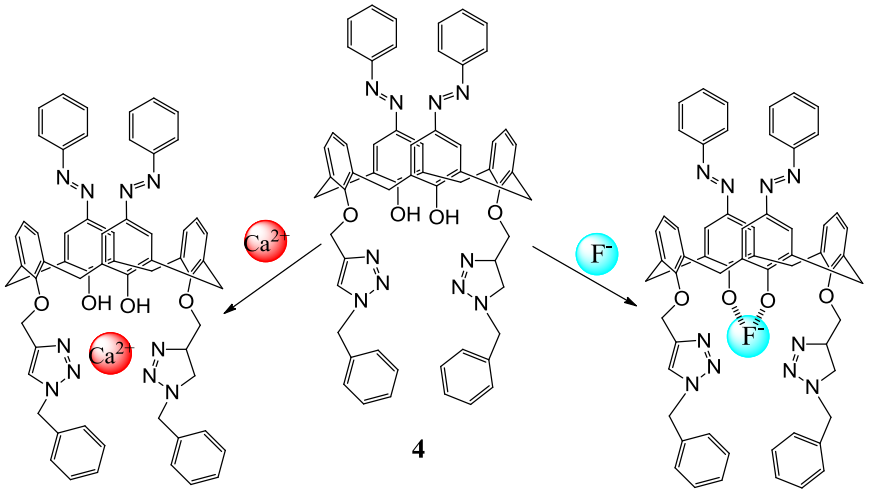

Figure 1.15. Structure of compound **4**.

1.3.1.2 Ammonium, and alkylammonium cations

Early observations by Gutsche *et al*. indicated that parent calix[4]arenes interact strongly with primary alkyl amines in polar solvents, in consequence of a proton transfer. The formation of intracavity *endo*-complexes of the resulting alkylammonium ions was proposed and a selectivity for *tert* - over *sec*- and *n*-alkyl amines was observed. Tripodal $NH^+ \ldots O$ interactions with the phenolic oxygen atoms and CH–π interactions were supposed to stabilize the complex. However, it is currently accepted that calix[4]arenes usually form *exo*-complexes with ammonium salts, while direct proofs of *endo*-complexes have been only collected for the larger calix[5]-, calix[6]-, and hexahomotrioxacalix[3]arenes. The insertion of cationbinding groups (OCH_2COX, X = OR, NR_2) at the *lower rim* of calix[6]arenes has the beneficial effect of increasing the extraction of NH_4^+ and guanidinium (Gua^+) salts from water to the organic solvents. A remarkable selectivity in the transport of Gua+ over alkali salts through SLM was obtained by us with the highly complementary and preorganized C_{3v} symmetrical triamide **5**.[72] On the other hand, rigidification of the calixarene cavity by bridging or simply by insertion of bulk alkyl chains at the *lower rim* of calix[5]- and homooxacalix[3]arenes gives receptors with a preorganized cavity and high selectivity for alkylammonium salts.

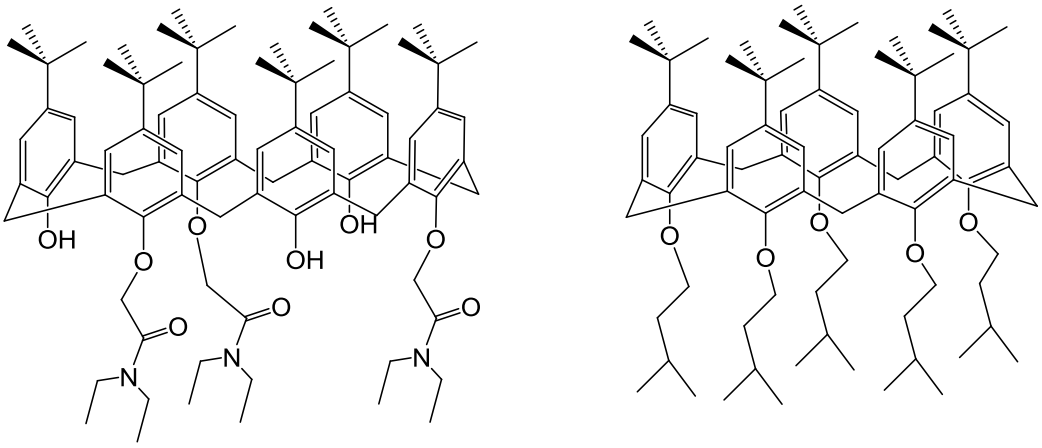

5 **6**

Figure 1.16. Structure of compound **5** and **6**.

The calix[5]arene **6**, synthesized by Parisi *et al*., for example, presents a marked shape and size selectivity even in ISEs for *n*-alkyl over *iso*-, *sec*-, and *tert*-alkylammonium salts. It was proven that linear *n*-alkyl ammonium salts form *endo*-complexes with the NH_3^+ head group interacting with the phenolic oxygen atoms and the alkyl residue with the calixarene cavity, while other branched alkyl ammonium salts generally form *exo*-complexes. [73]

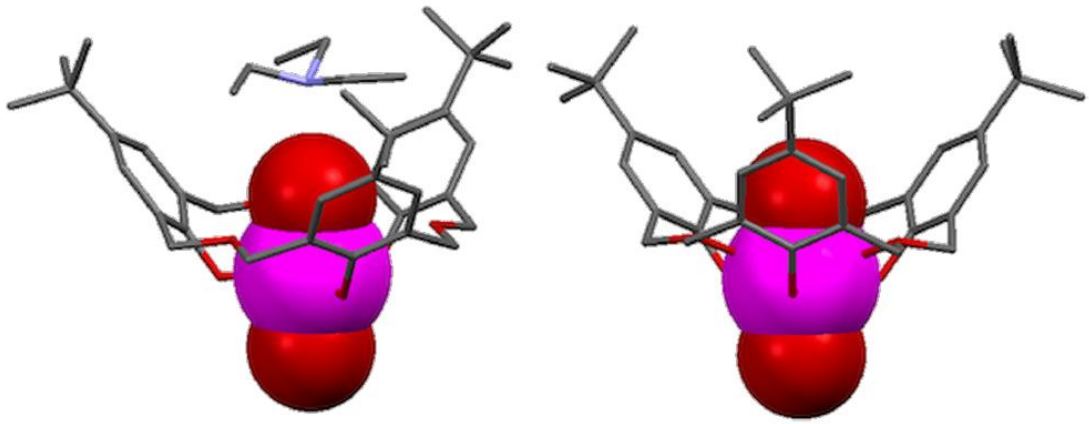

Figure 1.17. X-ray crystal structures of $[\mathbf{7}\cdot UO_2]^-$ with a cavity-bound cation and without a coordinated cation

Although the simple parent oxacalix[3]arene **7** is able to bind quaternary ammonium ions (as described above), several derivatives have also been studied with respect to these and other ammonium ions. Extrac tion studies from alkaline aqueous picrate solutions into CH_2Cl_2 indicated that the *n*-butyl ether derivative **9** showed a high affinity for *n*-$BuNH_3^+$ (82% *E*) as postulated by the authors, because both host and guest possess the same C_3-symmetry [74]. Ethyl ester **10** was more efficient at extracting *n*-$BuNH_3^+$ picrate from water into CH_2Cl_2 than its calix[4]arene analogue was, in both the *cone* (77% vs 24% *E*) and *partial-cone* (42% vs 6% *E*) conformers [75]. In a wider study, Yamato determined extraction data for **10** with *n*-BuNH3+ picrate

(98% *E cone* vs 93% *E partial-cone*), *i*$BuNH_3^+$ picrate (48% *E cone* vs 37% *E partial-cone*) and *t*-$BuNH_3^+$ picrate (35% *E cone* vs 14% *E partial-cone*). The hexaamide derivative **8** bound *n*-BuNH3+ well, and an anion dependence was determined; *K*assoc values in $CDCl_3$ were 536 ± 32 M^{-1} for Cl^- and 230 ± 17 M^{-1} for Br^-.[76]

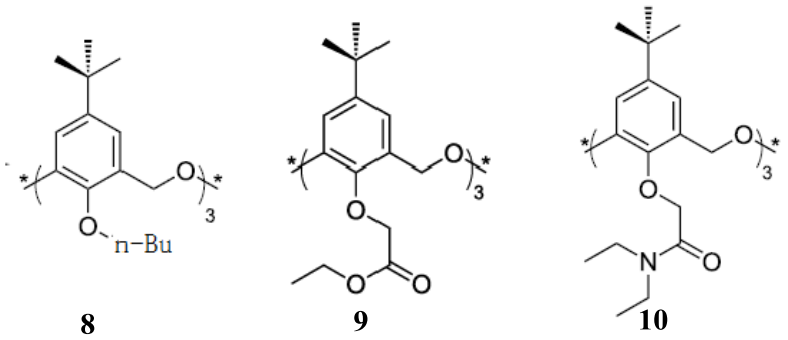

Figure 1.18. Structure of compound **8**, **9** and **10**.

Jabin et al. describes the straightforward synthesis of fluorescent calix[6]arene-based receptor **11** bearing three pyrenyl subunits and the study of their binding properties toward anions and ammonium salts using different spectroscopies. It was found that receptor **11** exhibits a remarkable selectivity for the sulfate anion in DMSO, enabling its selective sensing by fluorescence spectroscopy. In $CDCl_3$, the receptor is able to bind ammonium ions efficiently only in association with the sulfate anion. Interestingly, this cooperative binding of ammonium sulfate salts was also evidenced in a protic environment. Finally, a cavity-based selectivity in terms of size and shape of the guest was observed with receptor **11**, opening interesting perspectives on the elaboration of fluorescent cavity-based systems for the selective sensing of biologically relevant ammonium salts such as neurotransmitters.

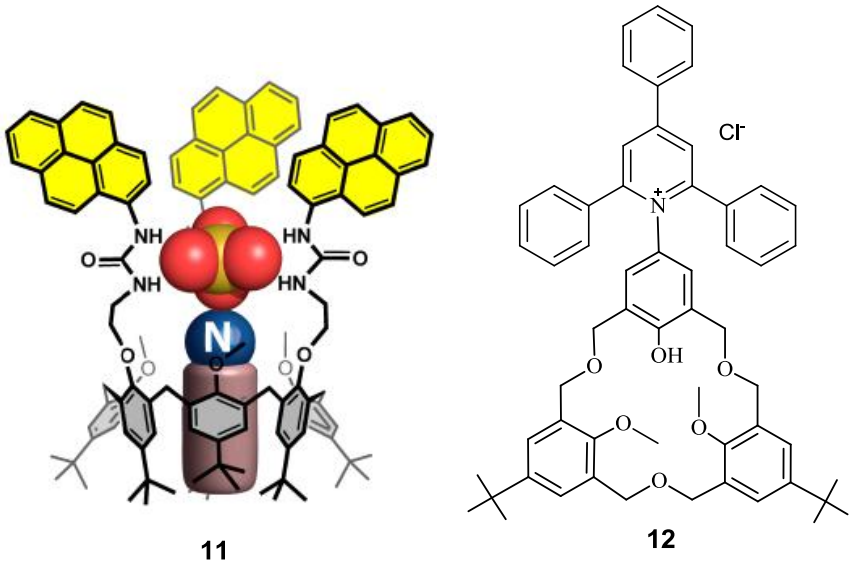

Figure 1.19. Structure of compound **11** and **12**.

One of the more unusual derivatives to have been prepared, **12**, incorporates an *N*-pyridinium dye on one of the upper-rim positions, which, in combination with the phenolic unit of the macrocycle, forms a proton-ionizable Reichardt dye, illustrated in Figure 1.19. [78] The other *p-tert*-butyl substituted phenols are blocked from ionization, as are the methyl ethers. The native oxacalix[3]arene dye is pale green and gives no response to benzylamine ($BzNH_2$) or triethylamine (Et_3N), but cyclohexylamine (*c*-$HexNH_2$) and *n*-butylamine (*n*-$BuNH_2$) bind with a concomitant colour change to blue.

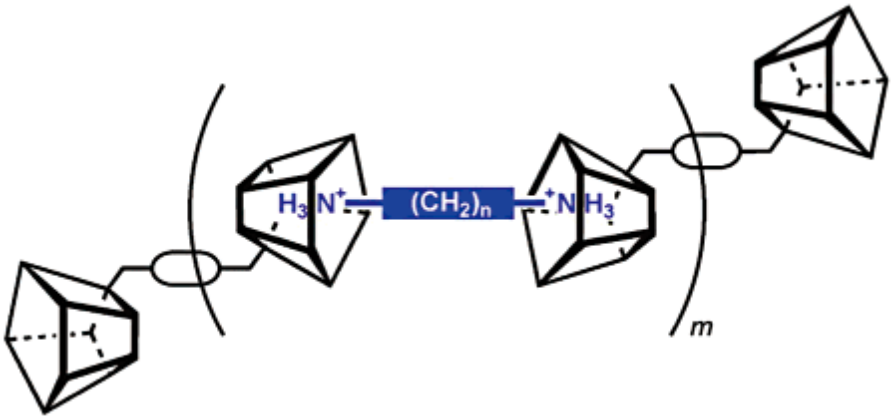

Figure 1.20. Plausible binding mode of **13** with alkyldiammonium ions.

Tail-to-tail connection of two cone calix[5]arene moieties by a rigid *p*-xylyl spacer affords the new exoditopic receptor **13** featuring two π-rich cavities (assembling cores) in a centrosymmetric divergent arrangement, as established by a single-crystal X-ray analysis. ^{1}H NMR complexation studies of **13** with alkyldiammonium ions support the formation of discrete bis-*endo*-cavity complexes and/or capsular assemblies along a polymer chain (polycaps), according to the length of the connector.[79]

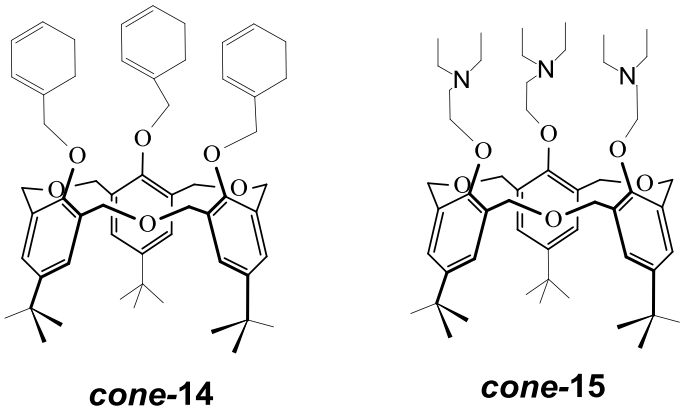

Figure 1.21. Structure of compound *cone*-**14** and *cone*-**15**.

Ni et al. synthesized the lower rim functionalized hexahomotrioxacalix[3]arene derivatives *cone*-**14** and *cone*-**15** bearing three benzyl and three N,N-diethyl-2-aminoethoxy groups.[80] Their complexation with 2-(3,4-dihydroxy-phenyl)-ethylamine (dopamine), 5-hydroxytryptamine (serotonin), and 2-phenylethylamine (phenethylamine), which have biologically important activities, has been studied by 1H-NMR spectroscopy. The chemical shifts of the aromatic protons of the host and guest molecules and the up-field shifts of the ethyl protons of the guest molecules strongly suggest the formation of inclusion complexes in solution. The formation of the host–guest complexes is assisted by a hydrogen bond and/or an electrostatic interaction between the host and ammonium ion (RNH_3^+) of the guest.

1.3.1.3 d-Block and heavy metal ions

Complexation of d-block metal ions has been exploited in the supramolecular chemistry of calixarenes for several purposes including catalysis Owing to the vastness of this field, here we briefly survey only the recognition properties of calixarene receptors for late transition and heavy metal ions designed for separation and detection. For this group of metal ions, in general, selectivity is primarily influenced by the number and type of donating atoms arranged around the cation and to a much lesser extent by the conformation of the calixarene.[81]

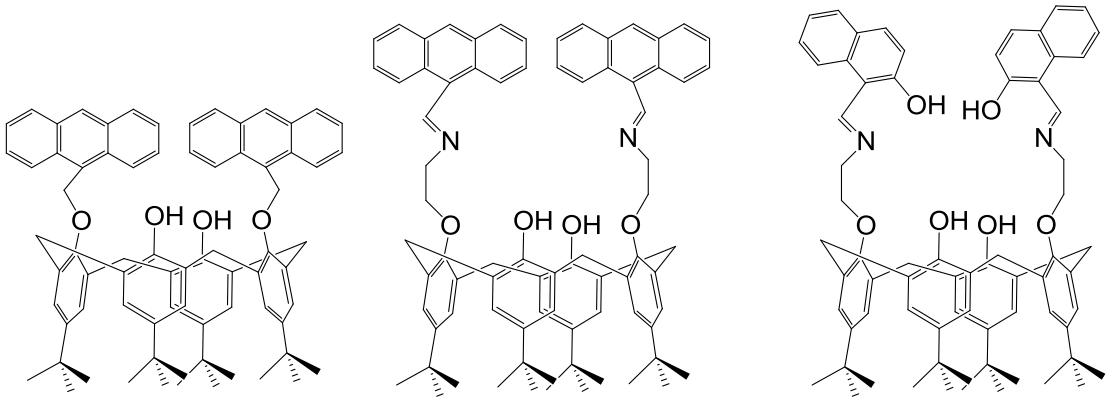

16 **17** **18**

Figure 1.22. Schematic structures of **16-18.**

Based on calixarene a simple O-methylanthracenyl derivative **16** as shown in Figure 1.22, exhibits a low fluorescence enhancement toward some transition metal ions. [82] When an imine moiety is introduced into this to result in **17**, this starts exhibiting some selectivity by showing significant fluorescence enhancement toward a few transition ions over the others in the order, $Fe^{2+} \approx Cu^{2+} > Zn^{2+} >$ other 3d ions, but the selectivity is poor. Further, when the arms were derivatized with 2-hydroxy naphthalidene moiety **18**, exhibits selectivity toward Zn^{2+} over a number of other ions

studied , by showing a large fluorescence enhancement that is sufficient enough to detect Zn^{2+} even at ≤60 ppb in methanol.[83] Fluorescence enhancement is attributable to the reversal of PET when Zn^{2+} forms a 1:1 chelate complex with **18**, its imine and phenolic-OH moieties participate in the complexation and the association constant has been found to be 2.3×10^5 M^{-1} in methanol.

Also, Rao et al, designed and synthesized a calix[4]arene derivative with a lower rim linked with triazole, which served as a fluorescence switch for sensing Zn^{2+} in blood serum milieu as shown in Figure 1.23.[84] The receptor **19** exhibits very weak fluorescence emission owing to photo electron transfer at 450nm when excited at 380nm in water-methanol mixture (v/v = 1: 4) at pH = 7.4. Titration of this by Zn^{2+}, results in the enhancement of fluorescence intensity as a function of added Zn^{2+} concentration as shown in Figure 1.24. While no significant enhancement was observed in the presence of other metal ions, thus, **19** was found to be highly selective toward Zn^{2+} ions, **20** was synthesized as reference compound, not calixarene but monomeric compound, the fluorescence enhancement was found to be very low even when the Zn^{2+} at 30 equivalents. It informed that the calixarene structure paly an important role in this system.

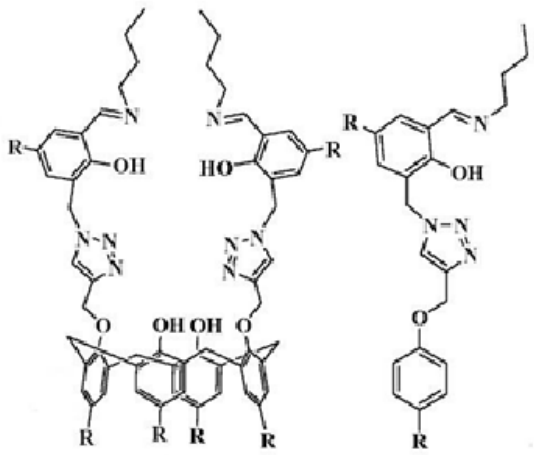

19 **20**

Figure 1.23. Fluorescent chemosensor of 19 and reference compound 20.

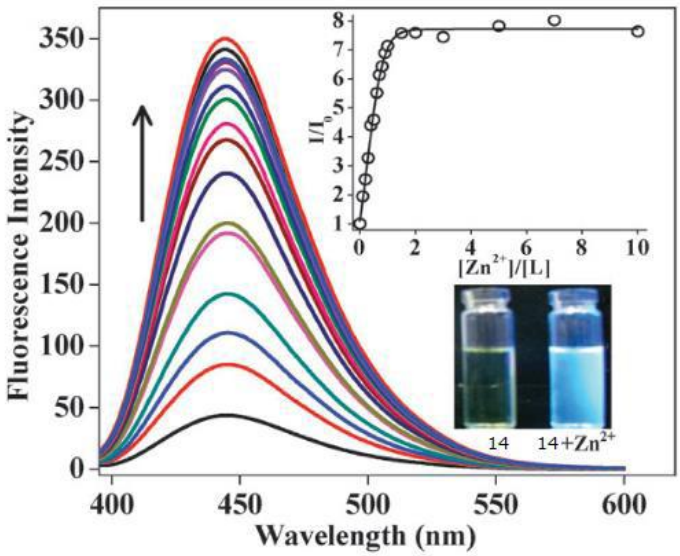

Figure 1.24. Fluorescence spectra obtained during the titration of 19 (10 mM) with Zn^{2+} in a water-methanol mixture (v/v = 1: 4) at PH = 7.4 (λ_{ex} = 380 nm). The inset shows the relative fluorescence intensity (I/I_0) as a function of $[Zn^{2+}]/[L]$ mole ratio and visual color change under UV light.

Cao et al. synthesized compound **21**, which can be used as a fluorescent chemosensor for Cu^{2+} and Zn^{2+} in CH_3OH/H_2O (9:1, v/v) with pH control. [85] When excited at 340 nm, free **21** (Figure 22) shows a weak emission at 408 nm due to the PET between the imidazoles and the fluorophore. When protonated, the PET process is suppressed to give an increased fluorescence. While Cu(II) coordination could be expected to produce a CHEF effect, in its complex with 3 there is an ET between Cu^{2+} and the excited fluorophore which dominates and leads to quenching. As expected, the ET pathway is not available for Zn(II), so the CHEF effect operates and the emission intensity is greater. Other cations tested gave negligible effects due to their weak complexation. The fluorescence changes induced by Cu^{2+} and Zn^{2+} are most apparent in a medium of pH 10.

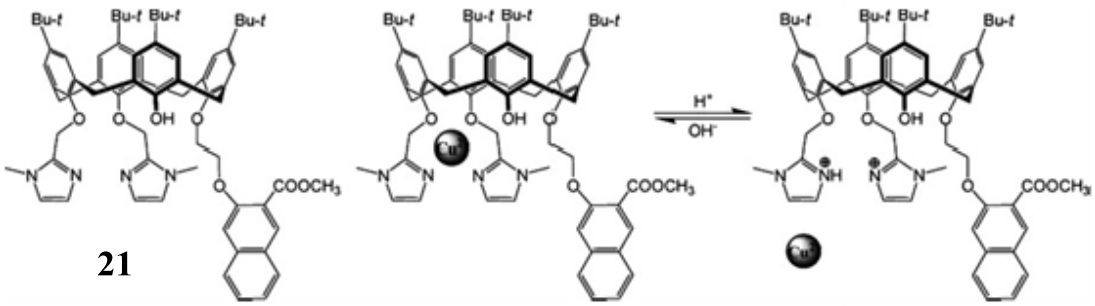

Figure 1.25. Schematic structure of **21**

Receptor compounds **22** and **23** (Figure 1.26), containing two pyrene moieties and

a pendent primary alkylamine, provide systems where both monomer and excimer emissions may be affected by PET. [86] That their weak emission is a consequence of PET is confirmed by a comparison with **23**, a calixarene having the same structure as **22** but without an attached amine group, where strong monomer and excimer emissions are seen. In the presence of Pb^{2+}, both **22** and **23** in CH_3CN exhibit an enhanced monomer emission and diminished excimer emission. This CHEF effect can be attributed to a conformational change due to the metal binding as well as to the coordination of the electron-donor N center. However, upon addition of alkali-metal ions to **22** and **23**, both monomer and excimer emissions are enhanced, suggesting that there is no conformational change involved. A competitive metal ion exchange experiment shows that the binding ability of **22** for Pb^{2+} is much greater than that for Li^+.

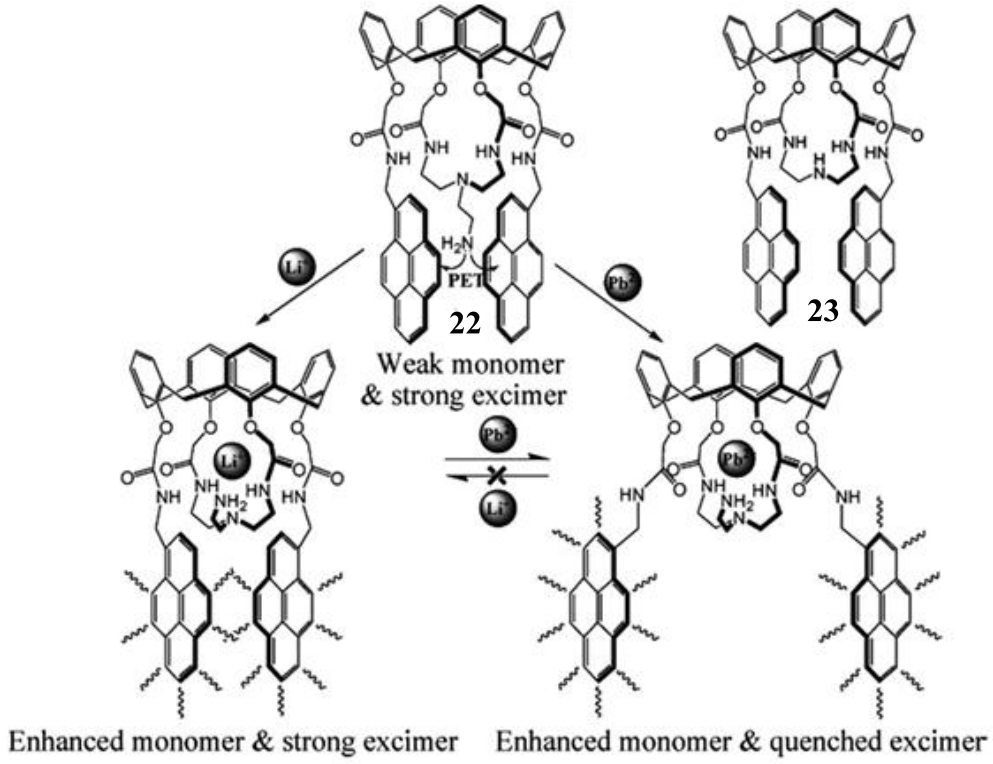

Figure 1.26. Schematic structures of **22** and **23**

1.3.1.4 f -Element metal ions

Complexation of f-element ions has been pursued in calixarene chemistry with ambitious aims, such as to separate lanthanides and actinides, [87] to obtain luminescent and paramagnetic probes, to study the reactivity of the coordinated metal ion at the metal-oxo surface, or to direct the self-assembly of calixarenes in nanostructured architectures in the solid state.

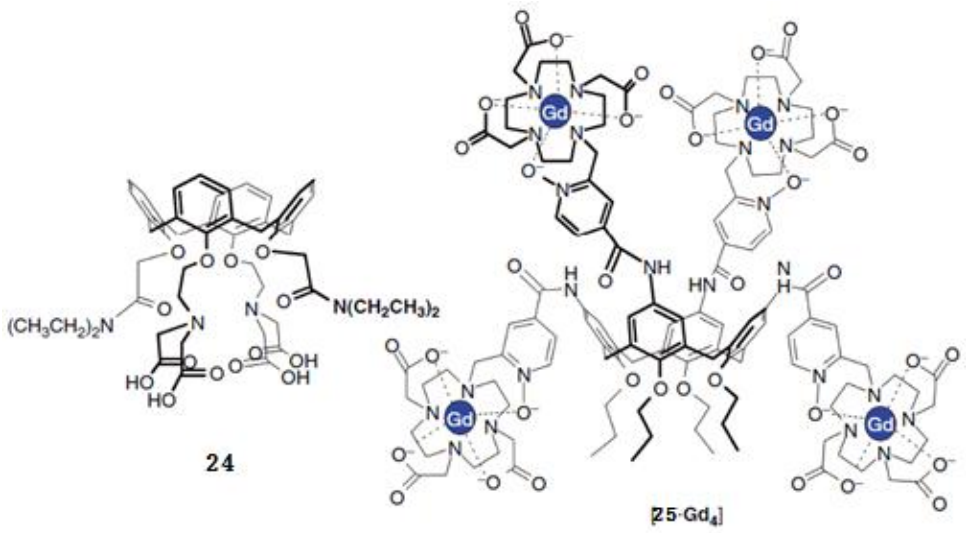

Figure 1.27. Schematic structures of **24** and **25.**

The complexation of Gd(III) ion by synthetic receptors is attracting the interest of several research groups as it will potentially allow to prepare new contrast agents for magnetic resonance imaging (MRI). A prerequisite for the use of Gd(III) complexes in vivo is an extremely high kinetic and thermodynamic stability with log values in aqueous solution much higher. The bis-iminodiacetic acid **24** shows a relaxivity 2 times higher than that of [Gd-DOTA(H_2O)]−; this is one of the best MRI contrast agents known so far, but with a stability constant as 13.22 To ensure higher stability and higher relaxivity, especially at higher magnetic field strength (>1.5 T), where traditional contrast agents do not show good performances, two densely packed Gdchelates (e.g., **25**) based on tetrapropoxycalix[4]arene were recently synthesized.[88]

Marcos investigated the lanthanide extraction by both **26** [89] and **27** [90] using the same conditions as described above (Table 1.1). Ketone **27** is a poor phase-transfer agent (% E ranges from 5 to 7), while amide 17a clearly discriminates between the light and heavy lanthanides. The lower-weight cations, such as Ce^{3+}, Pr^{3+} and Nd^{3+} (34% E) are preferred over the heavier, such as Er^{3+} and Yb^{3+} (13% E). The stability constants for the 1:1 complexes with **26** were also determined by UV absorption spectrophotometry in methanol at 25 ℃, by using chloride salts. The same positive discrimination for the light lanthanides was observed (log β = 5.5 and 3.4 for La^{3+} and Yb^{3+}, respectively).

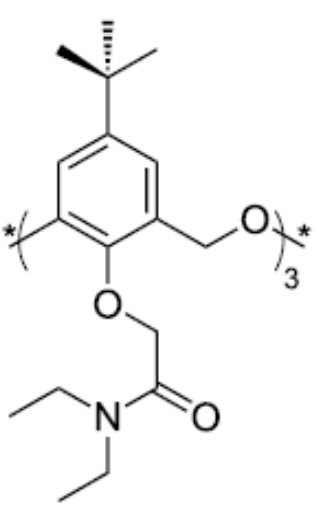

26

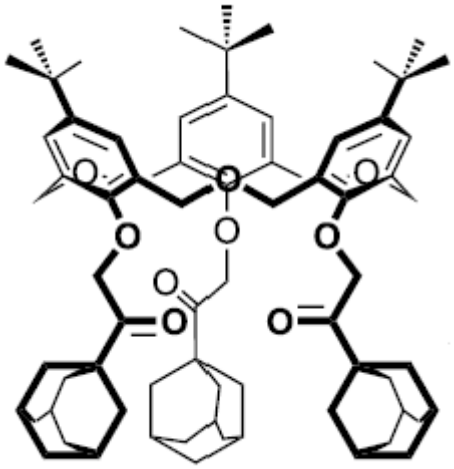

27

Figure 1.28. Schematic structures of **26** and **27.**

	La^{3+}	Ce^{3+}	Pr^{3+}	Nd^{3+}	Sm^{3+}	Eu^{3+}	Gd^{3+}	Dy^{3+}	Er^{3+}	Yb^{3+}
26	28	34	34	34	31	30	17	18	13	13
27	6	5	5	6	6	6	6	5	6	7

Table 1.1. Percentage extraction of lanthanide-metal picrates into CH_2Cl_2.

1.3.2Calixarene-derived sensors for anion

Calixarenes, resorcinarenes, and their simple ether derivatives have an electron-rich, π-basic cavity, which is able to host cations and neutral molecules but not anions, which, therefore, do not form endo-cavity inclusion complexes with these receptors. However, directπ-metallation of the exterior of the macrocycles provides a vacant cavity with altered electrostatic properties.[91]

Indeed, Sessler et al. reported A calix[4]pyrrole, which strapped by a bulky calix[4]arene diester locked in its cone conformation.[92] On the basis of ^1H NMR spectroscopic analyses carried out in $CDCl_3$, it is concluded that this hybrid system, receptor **28**, binds only the fluoride anion and does so with remarkably high affinity even in the presence of an excess of various potentially competing environmentally and biologically ubiquitous anions (studied as the tetrabutylammonium, cesium, or lithium salts). Solid state structural analyses provide support for the notion that receptor **28** interacts well with the fluoride anion in the solid state.

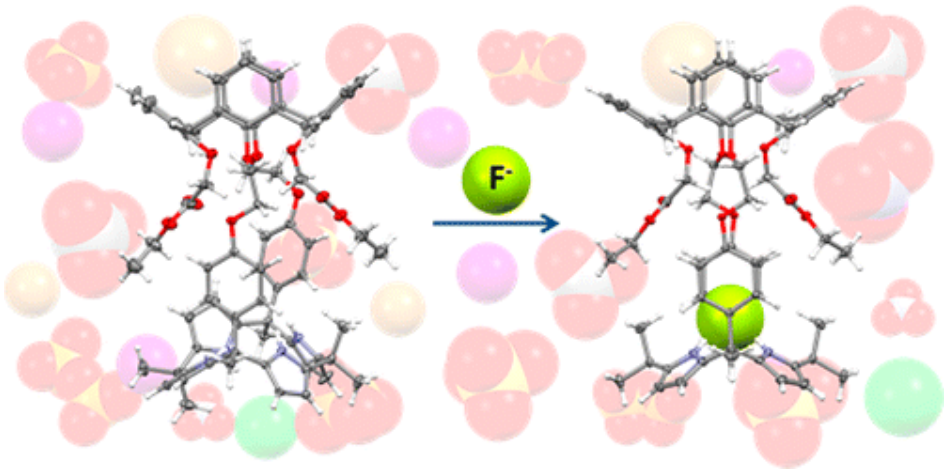

Figure 1.29. Schematic structures of **28.**

Kim et al. reported an amide-based calix[4]arene derivative bearing pyrene and nitrophenylazo moieties (**29** and **30**) exhibited F^- recognition as studied by UV_vis and fluorescence spectroscopy.[93] The interaction of F^- with **29**, **30** has been found to be through the amide and the phenolic protons, respectively, Addition of F– to **29** in CH_3CN produces a bimodal response in which initially the excimer emission is quenched but then a new species with emission bands at 385 and 460 nm appears. This behavior has been rationalized in terms of static pyrene dimer formation in the ground state influenced by H-bonding between F^- and the amide proton. The fluorescence of **30** also changes upon addition of F^- but in a different manner. In this case, the presence of a methylene spacer between the pyrene moiety and amide N probably forces the two pyrenes to be orthogonal to each other, as in a similar compound, thus preventing the interaction which might give a dynamic excimer.

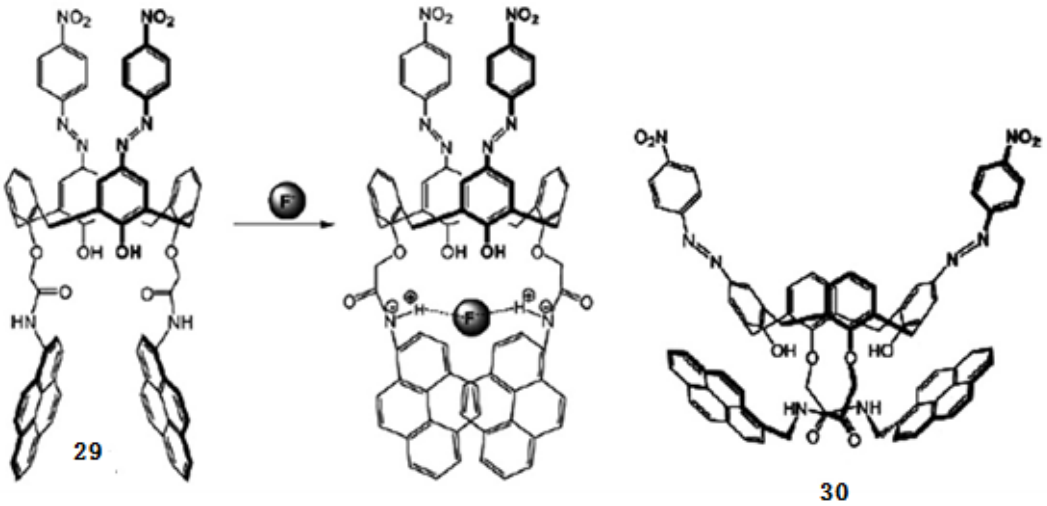

Figure 1.30. Schematic structures of **29** and **30.**

The anion-recognition properties of receptors 31-33 were found to be dependent on the structure of the upper rim of the calix[4]arene.[94] For example, in DMSO solution, the bis-cobaltocenium receptor **31** shows a greater affinity for acetate (K = 21000M^{-1}) and other carboxylate anions over dihydrogen phosphate (K = 3100M^{-1}), whereas for its isomer **32** the trend is reversed and the binding constants are lower for all anions. Interestingly, receptor **33**, in which the calix[4]arene is bridged by a single cobaltocenium moiety, displays significantly greater affinity for the above-mentioned anions (K = 41520M^{-1} for acetate) despite possessing only one positive charge. This selectivity preference was attributed to the upper rim bidentate amide hydrogen bond donor cavity of **33** being of complementary topology to bidentate anions such as carboxylates. The cobaltocene/cobaltocenium redox couple of **33** was found to undergo an anodic shift of 155mV in the presence of acetate anion, which indicates that these compounds are very promising as amperometric sensors for anions.

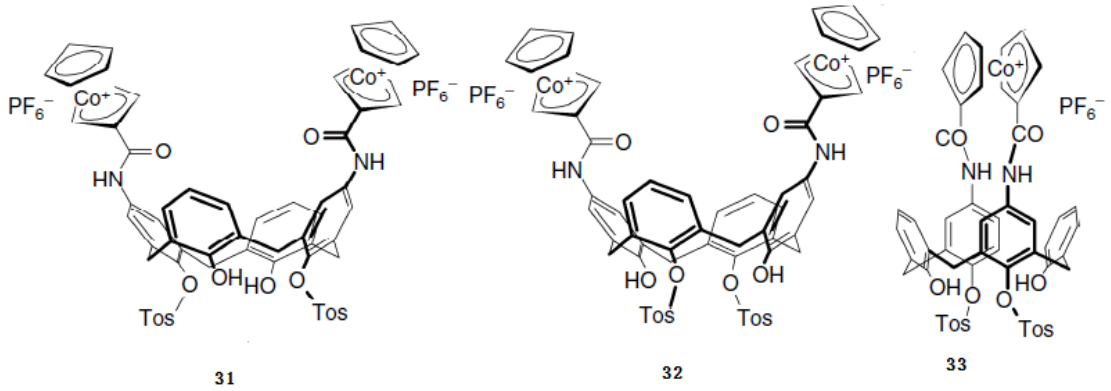

Figure 1.31. Schematic structures of **31, 32** and **33.**

In order to transform simple calixarenes into anion receptors, suitable anion-binding groups such as hydrogenbonding donor moieties, positively charged groups, or metal ions must be introduced onto the calixarene scaffold. [95-100] As for cations, if a reporter group (redox active, fluorophoric, chromophoric, etc.) of the molecular recognition event is also incorporated, then we have a useful anion-sensing device.[101-103]

1.3.3 Heteroditopic receptors for simultaneous cation–anion complexation

In the previous sections, we have discussed the strategies for obtaining efficient and selective receptors for cations or anions of a salt, which were studied as single ions eliminating the effect of the counterion by using a noncoordinating anion (perchlorate, hexafluorophosphate, tetraphenylborate, etc.) or cation (usually tetra-alkylammonium), respectively. However, the simultaneous complexation of the cation and the anion of an ion pair by bifunctional receptors is quite attractive for

several reasons. It can positively affect the extraction of salts in organic media or their transport through membranes, influence the selectivity in complexation, or disclose interesting allosteric effects. For these reasons, it has become a distinct field of investigation in supramolecular chemistry. [104-105] The simultaneous complexation of cations and anions by a heteroditopic receptor may lead to three limiting ion pair interactions (Figure 35), each having its own advantages and disadvantages in relation with the particular objective which is pursued. As calixarenes are endowed with two rims, which could, in principle, be functionalized with two different types of binding units, one for cations and one for anions, they soon appeared to be quite attractive for the design and synthesis of heteroditopic receptors.[106]

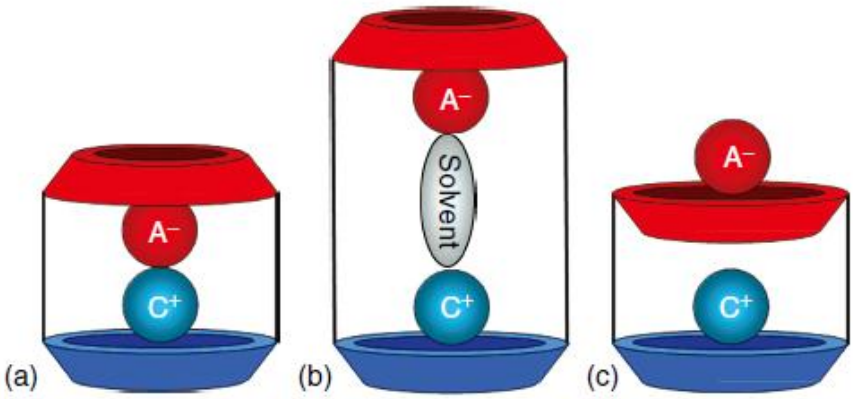

Figure 1.32. Three limiting situations for the complexation of ion pairs by a ditopic receptor: (a) contact, (b) solvent bridged, and (c) host separated.

Addition of Cu(II) to the fluorescent heteroditopic receptor **34** in CH_3CN (Figure 36) causes a reduction of the metal to Cu(I) by the phenolic groups of the calix[4]arene and a strong enhancement in fluorescence, which was attributed to a rigidification of the receptor in the cationic complex to which acetate ($K = 159000\ M^{-1}$) and fluoride ($K = 59900\ M^{-1}$) anions can be further bound through H-bonding and electrostatic interactions, inducing a further increase in fluorescence. No anion binding occurs in the absence of copper cation. Receptor **34** probably represents the only reported example of a calixarene-based heteroditopic receptor in which Cu(I) is directly involved in ion pair complexation.[107]

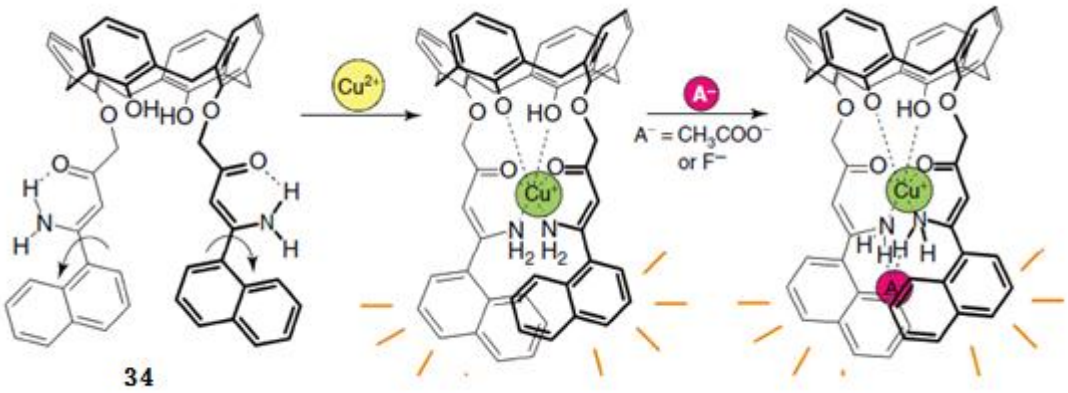

Figure 1.33. Complexation of copper salts by the heteroditopic receptor **34**.

The switching-on anion binding by the cocomplexation of alkali metal cations is even more dramatically shown by receptor **35**, reported by Reinhoudt et al. and highlighted in several review articles, which exploits urea groups at the calix[4]arene upper rim as anion-binding sites (Figure 1.34). The free receptor **35** adopts a flattened cone conformation in $CDCl_3$ due to the formation of strong intramolecular hydrogen bonding between the urea groups. In this situation, the upper rim cavity is closed, and no anion binding takes place when titration experiments are carried out using tetrabutylammonium salts. However, when sodium or potassium halides are used, the complexation is switched on and these salts are easily solubilized in $CDCl_3$. Evidently, the complexation of alkali metal ions to the ester groups at the lower rim causes the breaking of the intramolecular hydrogen bonds between the urea units and an opening of the calixarene cavity, which can now accommodate the anionic guests by hydrogen bonding with the NH groups.[108]

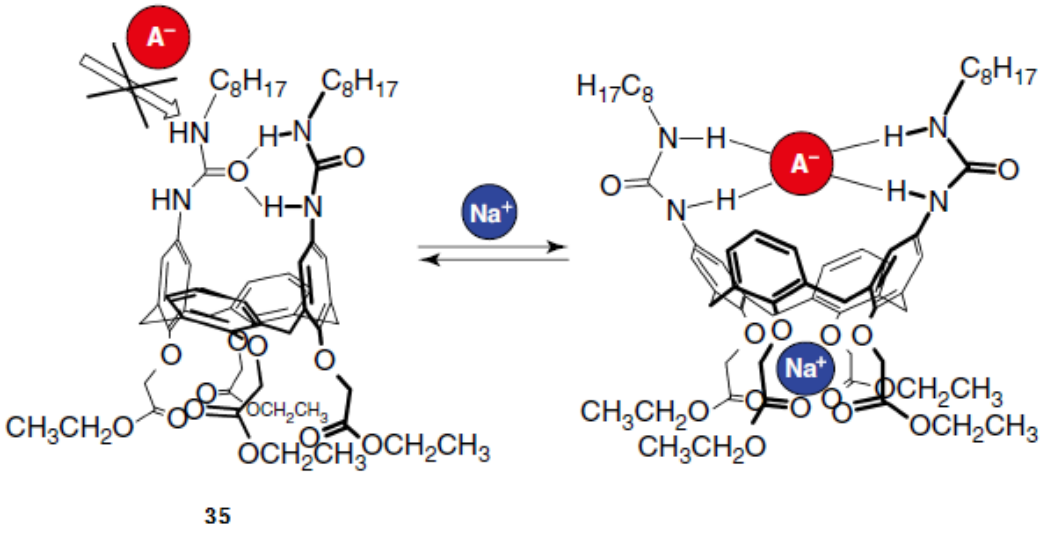

Figure 1.34. *Switching-on* anion binding by sodium complexation at the *lower rim* of heteroditopic receptor **35**.

1.4 Conclusions

According to the above review of recently development of chemosensor for cations, anions and micromolecule based on calixarene scaffold. The synthesis, characterization, and ions selectivity recognition properties of receptor focused on calixarene would exhibit further interests and challenges to the supramolecular chemists, because such scaffold not only provide requisite binding cores but also are flexible enough to accommodate various ions and molecular species. Thus, against this background, several kinds of heteropolytopic chemosensor or fluorescent chemosensors for cation and anions were designed and synthesized based on hexahomotrioxacalix[3]arene in this dissertation.

1.5 References

1. J. P. Desvergne, A W. Czarnik, Chemosensors of ion and molecule recognition. Kluwer, Dordrecht, 1997.
2. A W. Czarnik, Fluorescent chemosensors for ion and molecule recognition. American Chemical Society. Washington DC, 1993.
3. C. Bargossi, M. C. Fiorini, M. Montalti, L. Prodi, N. Zaccheroni, *Coord.Chem.Rev.*, **2000**, *208*, 17–32.
4. R. Martínez-Máñez, and F. Sancenón, *Chem.Rev.*, **2003**, *103*, 4419.
5. B. Valeur, and I. Leray, *Coord.Chem.Rev.*, **2000**, *205*, 3–40.
6. A. P. Silva, H. Q. N. Gunaratne, T. Gunnlaugsson, A. J. M. Huxley, C. P. McCoy, J. T Rademacher, and T. E. Rice, *Chem.Rev.*, **1997**, *97*, 1515–1566,
7. J. S. Kim, and D. T. Quang, *Chem. Rev.*, **2007**, *107*, 3780−3799.
8. D. Coquière, S. Le Gac, U. Darbost, O. Sénèque, I. Jabin and O. Reinaud, *Org. Biomol. Chem.*, **2009**, *7*, 2485.
9. Brodesser, G., Vögtle, F. *J. Incl. Phenom. Mol. Recognit. Chem.*, **1994,** *19*, 111–135.
10. C. D. Gutsche, and L. J. Bauer, *J. Am. Chem. Soc.* **1985,** *107*, 6052–6059.
11. K. Araki, K. Inada, H. Otsuka, and S. Shinkai, *Tetrahedron*, **1993,** *49*, 9465–9478.
12. R. A. Bissell, A. P. de Silva, H. Q. N. Gunaratne, P. L. M. Lynch, G. E. M. Maguire, and K. R. A. S. Sandanayake, *Chem. Soc. Rev.* **1992**, *187*, 105.
13. S. L. Wiskur, H. Ait-Haddou, J. J. Lavigne, and E. V. Anslyn, *Acc. Chem. Res.* **2001**, *34*, 963.
14. T. Jin, K. Ichikawa, and T. Koyama, *J. Chem. Soc., Chem. Commun.* **1992**, *27*, 499.
15. I. Aoki, H. Kawabata, K. Nakashima, and S. Shinkai, *J. Chem. Soc., Chem. Commun.* **1991**, *99*, 1771.

16. I. Aoki, T. Sakaki, and S. Shinkai, *J. Chem. Soc., Chem. Commun.* **1992**, *54*, 730.
17. H. F. Ji, R. Dabestani, G. M. Brown, and R. A. Sachleben, *Chem. Commun.* **2000**, *56*, 833.
18. H. F. Ji, R. Dabestani, G. M. Brown, and R. L. Hettich, *J. Chem. Soc., Perkin Trans. 2* **2001**, *103*, 585.
19. H. F. Ji, R. Dabestani, G. M. Brown, and R. Dabestani, *Chem. Commun.* **1999**, *55*, 609.
20. I. Leray, F. O'Reilly, J. L. H. Jiwan, J. P. Soumillion, and B. Valeur, *Chem. Commun.* **1999**, *55*, 795.
21. C. D. Gutsche, In *Calixarene: Monographs in Supramolecular Chemistry*, J. F., Ed. Stoddart, Royal Society of Chemistry:Cambridge, U.K., 1989, Vol. 1.
22. C. D. Gutsche, In *Synthesis of Macrocycles: Design of Selecti*Ve *Complexing Agents*, R. M. Izatt, J. J., Eds. Christensen, Wiley: New York, 1987, 93.
23. J. D. Van Loon, W. Verboom, D. N. Reinhoudt, *Org. Prep. Proced. Int.*, **1992**, *24*, 437.
24. Kluwer: Dordrecht, The Netherlands, 1991 V. Böhmer, M. A. McKervey, *Chem. Unserer Zeit* **1991**, 25, 195.
25. C. D. Gutsche, In *Inclusion Compounds*, J. L. Atwood, J. E. D. Davies, D. D., Eds. MacNicol, Oxford University Press: New York, 1991, Vol. 4, p 27.
26. J.D. Van Loon, W. Verboom, and D. N. Reinhoudt, *Org. Prep. Proced. Int.*, **1992**, *24*, 437.
27. R. Ungaro, and A. Pochini, In *Frontiers in Supramolecular Organic Chemistry and Photochemistry*, H.-J., Ed. Schneider, VCH: Weinheim, Germany, 1991, 57
28. Z. Asfari, V. Böhmer, J. Harrowfield, and J. Vicens, Eds. *Calixarenes2001*.
29. Kluwer Academic Publishers: Dordrecht, The Netherlands, 2001.
30. Jin, T., Ichikawa, K., Koyama, T. *J. Chem. Soc., Chem. Commun.* **1992**, 499.
31. S. Nishizawa, H. Kaneda, T. Uchida, and N. Teramae, *J. Chem. Soc., Perkin Trans. 2* **1998**, 2325.
32. M. A. Hossain, H. Mihara, and A.Ueno, *J. Am. Chem. Soc.* **2003**, *125*, 11178.
33. H. Takakusa, K. Kikuchi, Y. Urano, T. Higuchi, and T. Nagano, *Anal. Chem.* **2001**, *73*, 939
34. M. Arduini, F. Felluga, F. Mancin, P. Rossi, P. Tecilla, U. Tonellato, and N. Valentinuzzi, *Chem. Commun*. **2003**, 1606.
35. A. P. de Silva, H. Q. N. Gunaratne, T. Gunnlaugsson, A. J. M. Huxley, C. P. McCoy, J. T. Rademacher, and T. E. Rice, *Chem. Rev.* **1997**, *97*, 1515.
36. B. Valeur, and I. Leray, *Inorg. Chim. Acta*, **2007**, *360*, 765.

37. S. H. Kim, H. J. Kim, J. Yoon, and J. S. Kim, In *Calixarenes in the Nanoworld*, Vicens, J., Harrowfield, J., Eds., Springer: Dordrecht, The Netherlands, 2007, Chapter 15.
38. L. Fabbrizzi, and A. Poggi, *Chem. Soc. Rev.* **1995**, 197.
39. B. Valeur, J. Bourson, J. Pouget, A. W. Czarnik, *Fluorescent Chemosensors for Ion and Molecule Recognition*, ACS Symposium Series 538, American Chemical Society: Washington, DC, 1993, 25.
40. A. J. Dixon, and G. S. Benham, *Int. Lab*. **1988**, *4*, 38.
41. B. Valeur, *Molecular fluorescence*, Wiley-VCH: Weinheim, Germany, 2001.
42. J. R. Lakowicz, Ed. *Principles of Fluorescence Spectroscopy*, Plenum Publishers Corp.: New York, 1999.
43. J. S. Kim, K. H. Noh, S. H. Lee, S. K. Kim, J. Yoon, *J. Org. Chem.*, **2003**, *68*, 597.
44. J. S. Kim, O. J. Shon, J. A. Rim, S. K. Kim, J. Yoon, *J. Org. Chem.*, **2002**, *67*, 2348.
45. F. Unob, Z. Asfari, J. Vicens, *Tetrahedron Lett.*, **1998**, *39*, 2951.
46. L. Fabbrizzi, M. Licchelli, P. Pallavicini, A. Perotti, A. Taglietti, D. Sacchi, *Chem.Eur. J.*, **1996**, *2*, 75.
47. G. De Santis, L. Fabbrizzi, M. Licchelli, C. Mangano, D. Sacchi, *Inorg. Chem.*, **1995**, *34*, 3581.
48. G. De Santis, L. Fabbrizzi, M. Licchelli, N. Sardone, A. H. Velders, *Chem.Eur. J.*, **1996,** *2*, 1243.
49. R. Bergonzi, L. Fabbrizzi, M. Licchelli, C. Mangano, *Coord. Chem. Rev.*, **1998**, *170*, 31.
50. P. Suppan, *Chemistry and Light*, The Royal Society of Chemistry: Cambridge, U.K., 1994.
51. J. B. Birks, *Photophysics of Aromatic Molecules*, John Wiley: New York, 1970, Chapter 7.
52. W. Klopffer, *InOrganic Molecular Photophysics*, J. B. Birks, Ed., Wiley: New York, 1973, Vol. 1, Chaper 7.
53. J. B. Birks, M. D. Lumb, I. H. Munro, *Proc. R. Soc. London*, **1964**, *A280*, 289.
54. S. K. Kim, S. H. Lee, J. Y. Lee, R. A. Bartsch, J.S. Kim, *J. Am. Chem. Soc.*, **2004**, *126*, 16499.
55. F. M. Winnik, *Chem. Rev.*, **1993**, *93*, 587.
56. S. H. Lee, S. H. Kim, S. K. Kim, J. H. Jung, J. S. Kim, *J. Org. Chem.*, **2005**, *70*, 9288.
57. J. Y. Lee, S. K. Kim, J. H. Jung, J. S. Kim, *J. Org. Chem.*, **2005**, *70*, 1463.
58. M. A. Winnik, *Chem. Rev.*,**1981**, *81*, 491.
59. Y. C. Wang, H. Morawetz, *J. Am. Chem. Soc.*, **1976**, *98*, 3611.
60. H. Morawetz, *J. Lumin.*, **1989**, *43*, 59.

61. M. Goldenberg, J. Emert, H. Morawetz, *J. Am. Chem. Soc*., **1978**, *100*, 7171.
62. W. Rettig, R. Lapouyade, In *Probe design and chemical sensing*, Lakowicz, J. R., Ed., Topics in Fluorescence Spectroscopy, Plenum: New York, **1994**, 4, 109.
63. H.-G. Lohr, F. Vogtle, *Acc. Chem. Res*. **1985**, *18*, 65.
64. L. Stryer, R. P. Haugland, *Proc. Natl. Acad. Sci. U.S.A.* **1967**, *58*,719.
65. C. D. Gutsche, *Calixarenes. An Introduction*, ed. J. F. Stoddart, The Royal Society of Chemistry, Cambridge, 2008.
66. Z. Asfari, V. Böhmer, J. Harrowfield, and J. Vicens, eds., *Calixarenes 2001*, Kluwer Academic Publishers, Dordrecht, 2001.
67. A. Casnati, F. Sansone, and R. Ungaro, Calixarene receptors in ion recognition and sensing, in *Advances in Supramolecular Chemistry*, ed. G. W. Gokel, Cerberus Press Inc., South Miami, 2004, 9, 165–218.
68. X. L. Ni, H. Cong, A. Yoshizawa, S. Rahman, H. Tomiyasu, U. Rayhan, X. Zeng and T. Yamato, *J. Mol. Struct.*, **2013**, *1046*, 110–115.
69. K. C. Chang, I. H. Su, A. Senthilvelan and W. S. Chung, *Org. Lett.* **2007**, *9*, 3363–3366.
70. H. B. Li, J. Y. Zhan, M. L. Chen, D. M. Tian and Z. L. Zou, *J. Incl. Phenom. Macrocycl. Chem.* **2010**, *66*, 43–47.
71. K. C. Chang, I. H. Su, Y. Y. Wang and W. S. Chung, *Eur. J. Org. Chem.*, **2010**, *75*, 4700–4704.
72. S. Pappalardo, V. Villari, S. Slovak, Y. Cohen, G. Gattuso, A. Notti, A. Pappalardo, I. Pisagatti, and M. F. Parisi, *Chem. Eur. J.***, 2007**, *13*, 8164–8173.
73. C. Capici, G. Gattuso, A. Notti, M. F. Parisi, S. Pappalardo, G.Brancatelli, § and S. Geremia, *J. Org. Chem.*, **2012**, *77*, 9668−9675.
74. K. Araki, K. Inada, H. Otsuka, S. Shinkai, *Tetrahedron*, **1993,** *49*, 9465–9478.
75. K. Araki, N. Hashimoto, H. Otsuka, S. Shinkai, *J. Org. Chem.*, **1993,** *58*, 5958–5963.
76. T. Yamato, S. Rahman, X. Zeng, F. Kitajima, J. T. Gil, *Can. J. Chem.*, **2006,** *84*, 58–64.
77. E. Brunetti, J. F. Picron, K. Flidrova, G. Bruylants, K. Bartik, and I. Jabin, *J. Org. Chem.*, **2014**, *79*, 6179–6188.
78. K. Tsubaki, T. Morimoto, T. Otsubo, K. Fuji, *Org. Lett.*, **2002,** *4*, 2301–2304.
79. D. Garozzo, G. Gattuso, F. H. Kohnke, A. Notti, S. Pappalardo,| M. F. Parisi, I. Pisagatti, A. J. P. White, and D. J. Williams, *Org. Lett.*, **2003**, *5*, 4025–4028.
80. X. L. Ni, S. Rahman, S. Wang, C. C. Jin, X. Zeng, D. L. Hughes, C. Redshaw and T. Yamato, *Org. Biomol. Chem.*, **2012**, *10*, 4618–4626
81. D. M. Homden and C. Redshaw, *Chem. Rev.*, **2008**, *108*, 5086.
82. A. Kumar, A. Ali, C. P. Rao, *J. Photochem. Photobiol.A*, **2006**, *177*, 164.
83. J. Dessingou, R. Joseph, C. P. Rao, *Tetrahedron Lett*., **2005**, *46*, 7967.

84. R. K. Pathak, A. G. Dikundwar, T. N. G. Row and C. P. Rao. *Chem. Commun.*, **2010**, *46*, 4345–4347.

85. Cao, Y.-D., Zheng, Q.-Y., Chen, C.-F., Huang, Z.-T. *Tetrahedron Lett.* **2003**, *44*, 4751.

86. Lee, S. H., Kim, S. H., Kim, S. K., Jung, J. H., Kim, J. S. *J. Org. Chem.* **2005**, *70*, 9288.

87. H. H. Dam, D. N. Reinhoudt, and W. Verboom, *Chem. Soc. Rev.*, **2007**, *36*, 367.

88. D. T. Schuehle, M. Polasek, I. Lukes, *et al*., *Dalton Trans.*, **2010**, *39*, 185.

89. K. Araki, N. Hashimoto, H. Otsuka, S. Shinkai, *J. Org. Chem.*, **1993,** *58*, 5958–5963.

90. T. Yamato, F. L. Zhang, *J. Inclusion Phenom. Macrocyclic Chem.*,**2001,** *39*, 55–64.

91. P. Lhotak, Anion receptors based on calixarenes, in *Topics in Current Chemistry 255: Anion Sensing*, ed. I. Stibor, Springer, Berlin, 2005, 65–95.

92. S. K. Kim, V. M. Lynch, and J. L. Sessler, *Org. Lett.*, **2014**, *16*, 6128–6131

93. Kim, H. J., Kim, S. K., Lee, J. Y., Kim, J. S. *J. Org. Chem*. **2006**, *71*, 6611.

94. P. Blondeau, M. Segura, R. Perez-Fernandez, and J. de Mendoza, *Chem. Soc. Rev.*, **2007**, *36*, 198.

95. S. H. Lee, H. J. Kim, Y. O. Lee, J. Vicens, J. S. Kim, *Tetrahedron Lett*., **2006**, *47*, 4373.

96. B. Schazmann, N. Alhashimy, D. Diamond, *J. Am. Chem. Soc.*, **2006**, *128*, 8607.

97. J. Morales-Sanfrutos, M. Ortega-Muñoz, J. Lopez-Jaramillo, F. Hernandez-Mateo, F. Santoyo-Gonzalez, *J. Org. Chem*., **2008**, *73*, 7768.

98. Q.-Y. Chen, C.-F. Chen, *Eur. J. Org. Chem*. **2005**, *70*, 2468.

99. S.-Y. Liu, Y.-B. He, J.-L. Wu, L.-H. Wei, H.-J. Qin, L.-Z. Meng, L. Hu, *Org. Biomol. Chem*., **2004**, *2*, 1582

100. A. Nehra, D. S. Yarramala, V. K. Hinge, K. Samanta, and C. P. Rao, *Anal. Chem.*, **2015**, *87*, 9344–9351

101. I. Aoki, H. Kawabata, K. Nakashima, S. Shinkai, *J. Chem. Soc., Chem. Commun.*, **1991**, 1771.

102. S. L. Wiskur, H. Ait-Haddou, J. J. Lavigne, E. V. Anslyn, *Acc. Chem. Res.*, **2001**, *34*, 963.

103. K. Samanta and C. P. Rao, *ACS Appl. Mater. Interfaces*, **2016**, *8*, 3135–3142

104. P. M. Marcos, F. A. Teixeira, M. A. P. Segurado, J. R. Ascenso, R. J. Bernardino, S. Michel, and V. Hubscher-Bruder, *J. Org. Chem.*, **2014**, *79*, 742–751

105. G. J. Kirkovits, J. A. Shriver, P. A. Gale, and J. L. Sessler, *J. Incl. Phenom. Macr. Chem.*, **2001**, *41*, 69.

106. J. L. Sessler, P. A. Gale, and W. S. Cho, *Anion Receptor Chemistry*, ed. J. F. Stoddart, Royal Society of Chemistry, Cambridge, 2006.

107. S. K. Kim, J. L. Sessler, D. E. Gross, *et al*., *J. Am. Chem. Soc*., **2010**, *132*, 5827.
108. A. Senthilvelan, I. T. Ho, K. C. Chang, *et al*., *Chem. Eur. J.*, **2009**, *15*, 6152.

Chapter 2

Synthesis and structures of *O*-anthrylmethyl substituted hexahomotrioxacalix[3]arenes

This chapter focused on the synthesized of lower rim functionalized substituted hexahomotrioxacalix[3]arenes (compound ***2****H_2An, compound* ***3****HAn_2, cone-****4****An_3 and partial-cone-****4****An_3). It is known that the introduction of compound* ***1****H_3 was achieved through selective alkylation with different equiv. of 9-chloromethyl-anthracene* ***5*** *in the acetone system to give different compound (compound* ***2****H_2An, compound* ***3****HAn_2 and partial-cone-****4****An_3). On the other hand, the success for synthesizing the cone-****4****An_3 in a acetone /benzene (1: 1 v/ v) mixed solvent system; it suggests that the solvent also can control the conformation due to hydrogen bonding between the hydroxyl of calixarene. Respectively, the possible reaction routes of cone and partial-cone were discussed.*

2.1 Introduction

In the field of supramolecular chemistry, calixarenes and related macrocycles have been receiving considerable attention as useful hosts for cations, anions and neutral molecules.[1–7] The increasing interest in these compounds is stimulated by the availability of simple large-scale syntheses and the different ways in which they can be selectively functionalized either at the narrow (phenolic, lower) rim or at the wide (upper) rim. Molecular recognition is a fundamental phenomenon in biology, and tuning the affinity of a receptor for a ligand by the environment is key to the regulation of biological processes. This has inspired many chemists to design artificial receptors. [8–11]

Hexahomotrioxacalixarenes, a class of synthetic macrocycles having phenolic units linked by CH_2OCH_2 bridges and their trimer, has been widely used as a platform to generate versatile hosts for metal cations [12–19], ammonium cations [20–22], and fullerene derivatives [23–25]. In most cases, the functionalization of hexahomotrioxacalix[3]arene has been achieved by *O*-alkylation of the OH groups at the lower rim. Recently, we reported in detail on the influence of *O*-substituents on the conformational isomerism of hexahomotrioxacalix[3]arenes, which selectively recognize primary ammonium ions and heavy metal ions [26–30].

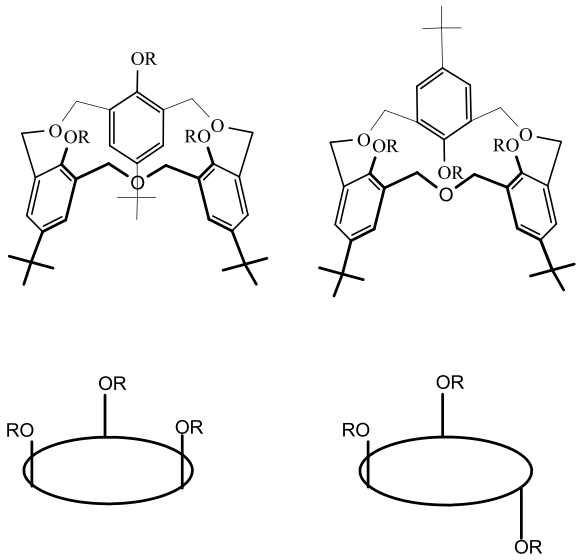

Figure 2.1 Two possible conformers of *O*-alkylated hexahomotrioxacalix[3]arenes

Introduction of larger alkyl groups on the phenolic oxygens of calix[4]arenes led to a situation where the OR groups within a cyclophane ring cannot pass each other by oxygen-through-the-annulus rotation [3]. Although there exists four possible conformational isomers in calix[4]arenes; i.e. *cone*, *partial-cone*, 1,2-*alternate* and

1,3-*alternate*, only two different conformational isomers, "*cone*" and "*partial-cone*" can be clearly obtained in hexahomotrioxacalix[3]arene.

Shinkai and co-workers have reported the influence of *O*-substituents on the conformational isomerism of hexahomotrioxacalix[3]arenes in detail [22,31,32]. They have established that interconversion between conformers occurring under oxygen-through-the-annulus rotation and it is sterically allowed for methyl, ethyl, and propyl groups whereas inhibited for butyl groups. More recently, we found that the interconversion is also facile for the propargyl moiety [30].

In their studies on the conformer distribution of hexahomotrioxacalix[3]arenes, Shinkai co-workers reported that the partial-cone is sterically less crowded than the cone and therefore formed preferentially, regardless of the *O*-alkylation conditions. On the other hand, the cone results only when a template metal is present in the reaction system [32,33]; the metal ion interacts strongly with phenolic oxygen atoms substituted with groups such as ethoxycarbonylmethyl or *N*, *N*-diethylaminocarbonylmethyl groups. However, the selective introduction of alkyl groups on the lower-rim has not yet been reported.

In this paper, we describe the selective synthesis of tris(anthrylmethyloxy)hexahomo- trioxacalix[3]arenes **4**An_3, with cone and partial-cone conformations, by *O*-alkylation of hexahomotrioxacalix[3]arene **1**H_3 in the different solvent system and the possible reaction routes of the final products, *cone*-**4**An_3 and *partial-cone*-**4**An_3 in detail.

2.2 Results and discussion

2.2.1 Synthesis

Hexahomotrioxacalix[3]arene **1**H_3 was *O*-alkylated with 9-chloromethylanthracene **5** (3.3 equiv.) using acetone as solvent in presence of Cs_2CO_3 or K_2CO_3 as base, exclusively afforded conformational isomer, *partial-cone*-**4**An_3 in 95 % yield, while the other possible isomer *cone*-**4**An_3 was not observed. On the other hand, when Na_2CO_3 or NaH are employed, only the hexahomotrioxacalix[3]arene **1**H_3 was recovered in 92 %, even when a large excess of Na_2CO_3 or NaH were used. Interestingly, hexahomotrioxacalix[3]arene **1**H_3 using a acetone/benzene (1:1 v/v) mixed solvent system in presence of Cs_2CO_3, to yield one pure conformational isomer, *cone*-**4**An_3 as a major product (Scheme 2.1). The conformer distribution for the reaction of **1**H_3 and 9-chloromethyl-anthracene **5** are summarized in Table 2.1. *Cone*-**4**An_3 and *partial-cone*-**4**An_3 were identified by ^{1}H NMR.

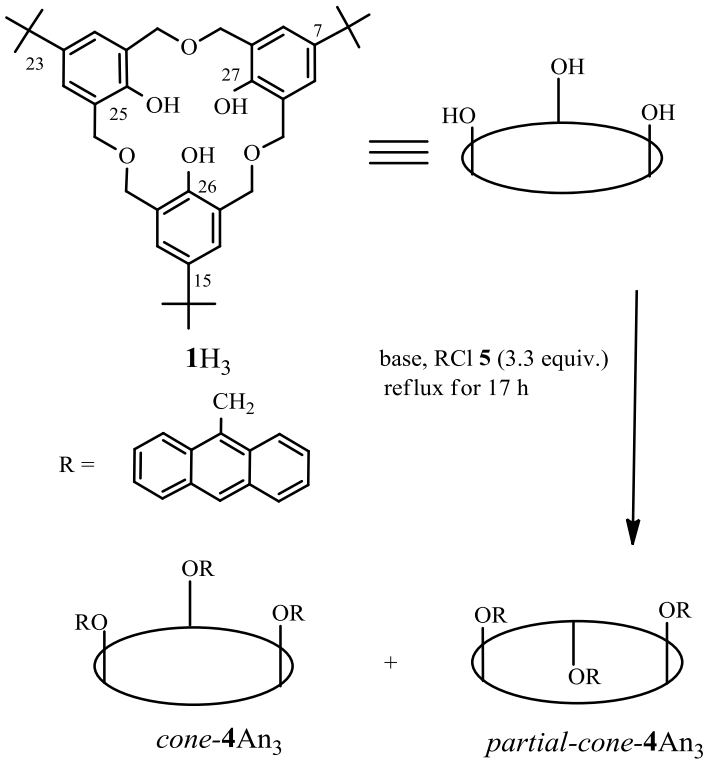

Scheme 2.1. *O*-Substitution reaction of hexahomotrioxaocalix[3]arene **1**H_3 with 9-chloromethylanthracene **5** (3.3 equiv.).

Table 2.1 *O*-Substitution reaction of hexahomotrioxaocalix[3]arene **1** with 9-chloromethylanthracene **5** (3.3equiv.).

Run	Base	Solvemt	Distribution(%) [a, b]		Recovery [c]
			cone-**4**An_3	*partial-cone*-**4**An_3	
1	NaH	THF	0	0	100
2	Na_2CO_3	Acetone	0	0	100
3	K_2CO_3	Acetone	0	95 (75)	5
4	Cs_2CO_3	Acetone	0	95(72)	5
5	Cs_2CO_3	Acetone/ Benzene (1:1)	90 (69)	5	5

[a]Relative yields determined by ^{1}H NMR. [b]Isolated yields are shown in parentheses. [c]Starting compound **1** was recovered in quantitative yield.

Interestingly, we have succeeded in synthesizing both mono-*O*-alkylated product **2**H_2An and di-*O*-alkylated product **3**HAn_2. The synthetic pathway of compounds **2**H_2An and **3**HAn_2 was shown in Scheme 2.2. Selective *O*-alkylation reaction of hexahomotrioxaocalix[3]arene **1**H_3 with 1 equiv. of 9-chloromethylanthracene **5** was

carried out in presence of K_2CO_3 to afford calixarene **2**H_2An in 66 % yield. When 2.1 equiv. of 9-chloromethylanthracene **5** was used, the desired di-substituted product *partial-cone*-**3**HAn_2 was obtained in 71 % yield.

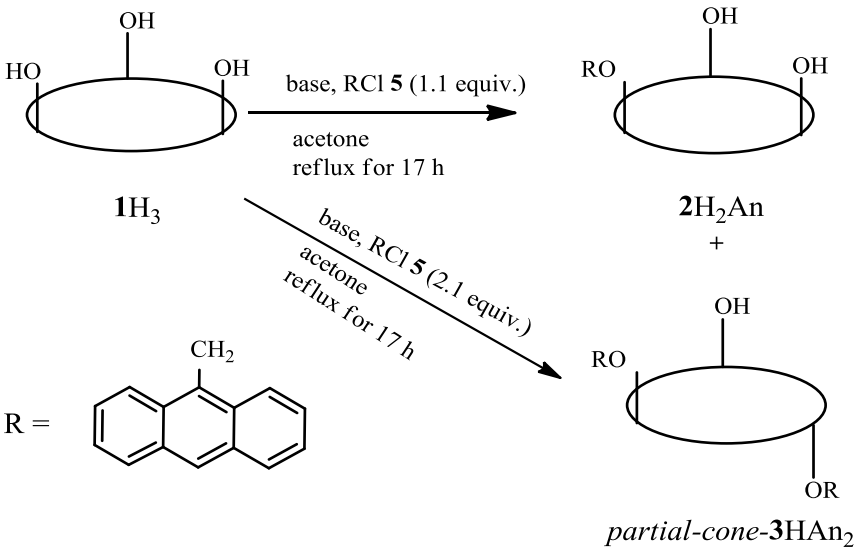

Scheme 2.2. *O*-Substitution reaction of hexahomotrioxaocalix[3]arene **1** with different amount of 9-chloromethylanthracene **5** (1.1 equiv., 2.1 equiv) in the presence of K_2CO_3.

2.2.2 Structure Assignment

In the ^{1}H NMR spectrum ($CDCl_3$, 300 MHz) of compound **2**H_2An, the signals for the aromatic protons are supposed to appear as two pairs of singlet at δ 7.04 and 7.06 ppm and those for the *tert*-butyl groups as two singlets at δ 1.31, 1.22 ppm. ^{13}C NMR spectrum ($CDCl_3$, 400 MHz) of **3**H_2An exhibits four peaks for *tert*-butyl carbon at δ 31.48, 31.52, 33.88 and 34.29 ppm. On the other hand, there are six pairs of doublets for bridge protons (ArO*C*H_2O) which show the existence of the intramolecular hydrogen bonding between the hydroxyl groups and 9-anthryl groups of cyclic structure, which may fix the "*cone*" conformation. Compound **2**H_2An is expected to have a plane of chirality, because it has two types of substituents which are fixed and the C_1 symmetrical conformer does not show conformational change at room temperature.

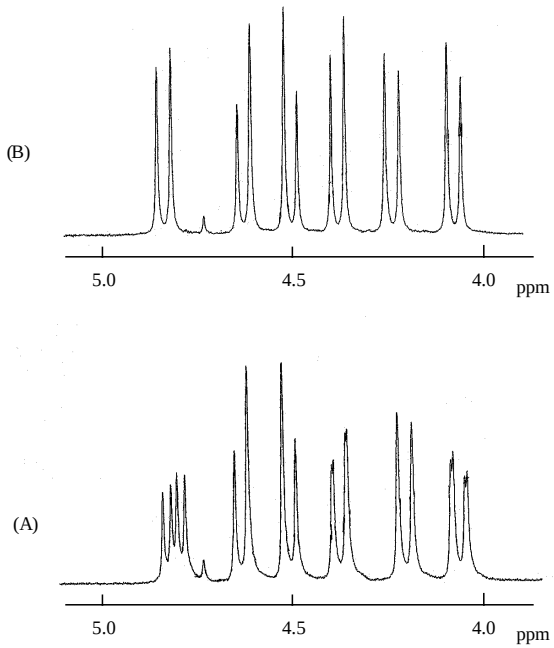

Figure 2.2. Partial ^{1}H NMR spectra for bridge proton in compound **2**H_2An in CD_3Cl, 300 MHz. (A) in the absence of Pirkle's reagent ([**2**] = 1.5×10^{-3} M) and (B) in the present of Pirkle' reagent (1.2 times of [**2**]).

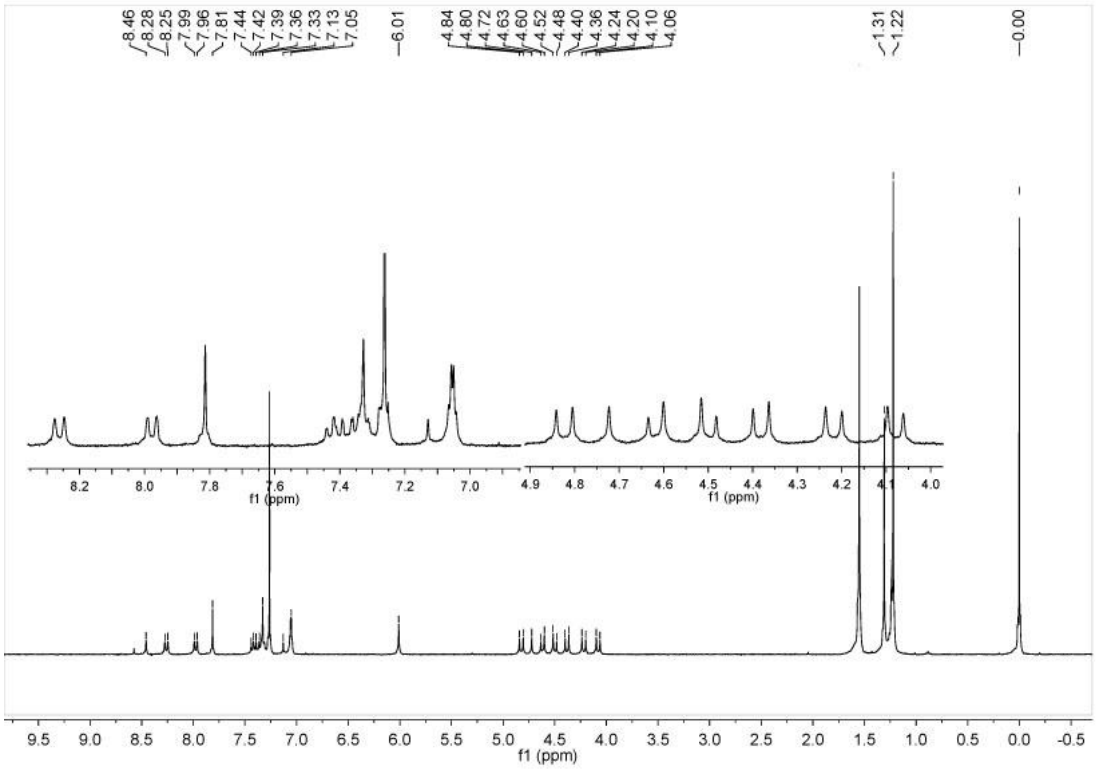

Figure 2.3. (a) ^{1}H NMR spectrum of compound **2**H_2An in $CDCl_3$ at 25 ℃, 300 MHz.

The ^{1}H NMR spectra in the presence of chiral shift reagents was measured to

confirm that the compound **2**H_2An consists of one pair of enantiomers [35]. The ^{1}H NMR spectra of the compound **2**H_2An in the presence of Pirkle's reagent [(*S*)-2,2,2-trifluoro-1-(9-anthryl)ethanol] are shown in Figure 2.2. It is reported [21] that hydroxyl groups which do not participate in the intramolecular hydrogen bonding are necessary for an effective interaction between chiral calix[4]arenes and Pirkle's reagent. In the spectrum of compound **2**H_2An, all peaks of the bridged protons are splitted on addition of Pirkle's reagent due to the formation of two diastereomeric complexes (Figure 2.2). These findings suggest that one oxygen atom and a hydroxyl group of **2**H_2An play an important role to coordinate with Pirkle's reagent.

The ^{1}H NMR spectrum ($CDCl_3$, 300 MHz) of compound **3**HAn_2 presents two singlets for the *tert*-butyl protons at δ 1.15 and 1.21 ppm (relative intensity 2:1). Furthermore, the resonance for the ArO*CH*$_2$Ph methylene protons appeared as a pair of doublets at δ 5.54 and 5.77 (J_{AB} = 11.7 Hz) ppm. The rotation of unmodified OH group is still allowed, so that two 9-anthryl groups are regarded to be equivalent both in a *cone* and a *partial-cone* conformation. Therefore, we cannot specify the conformation from ^{1}H NMR. ^{13}C NMR spectrum ($CDCl_3$, 400 MHz) of **3**HAn_2 exhibits four peaks for *tert*-butyl carbon at δ 31.36, 31.56, 33.84, 34.14.

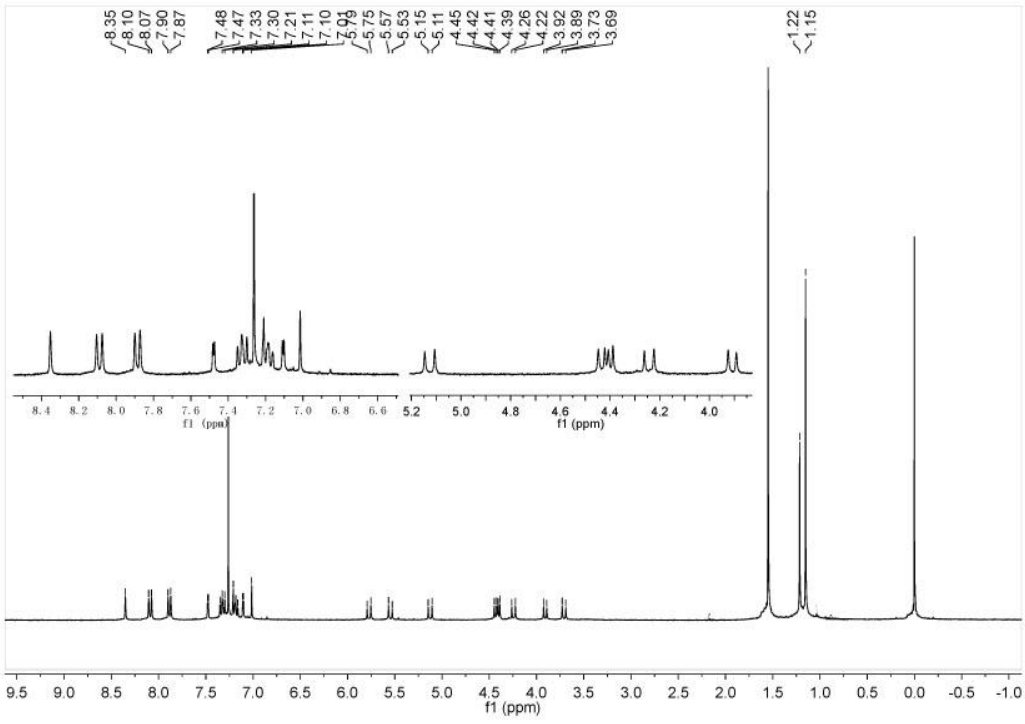

Figure 2.4. ^{1}H NMR spectrum of compound *partial-cone*-**3**HAn_2 in $CDCl_3$ at 25 ℃, 300 MHz.

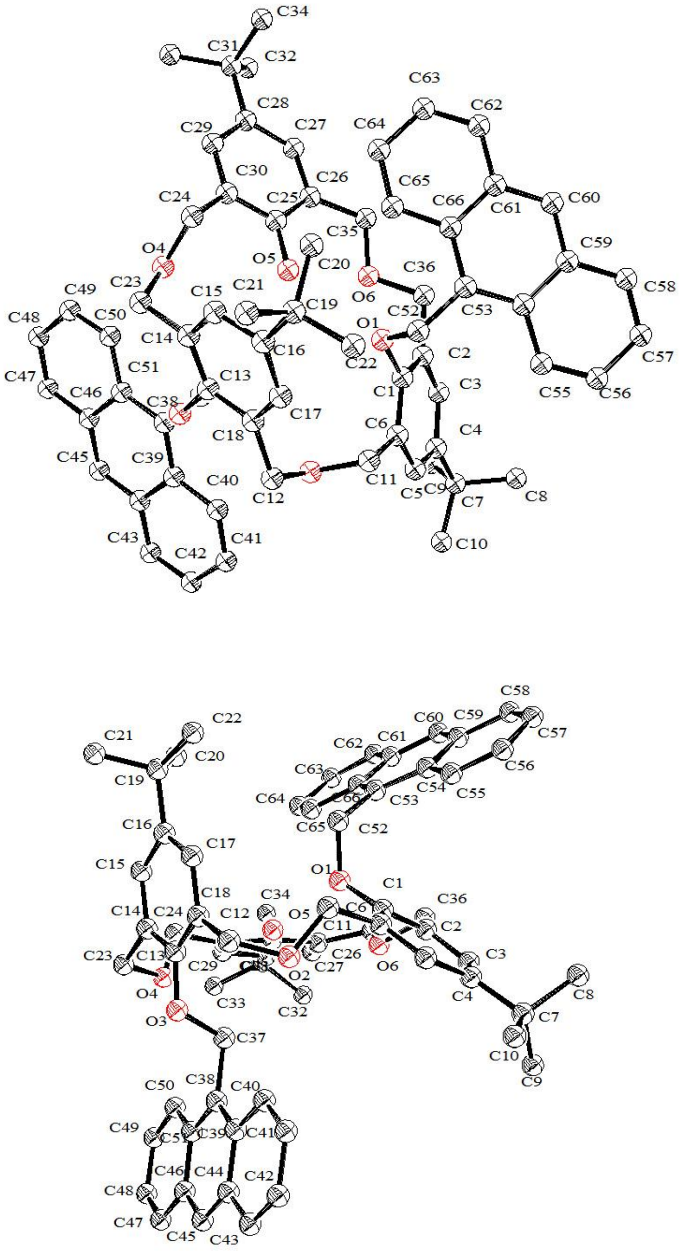

Figure 2.5. Top-view and side-view of X-ray structure of *partial-cone*-**3**HAn$_2$.

Fortunately, we get the crystal structure of *partial-cone*-**3**HAn$_2$ (Figure 2.5). Thus, the two 9-anthryl groups in the compound point up and down between the calixarene ring. Single crystals of **3**HAn$_2$ was grown from a mixture of hexane and chloroform (1:10), and the structure was investigated by X-ray crystallography to justify the conformation. The crystal structure was found to belong to the monoclinic crystal system with the space group l 2/a. The crystal structure of **3**HAn$_2$ is shown in Figure 2.5. The X-ray structure also supports the ^{1}H NMR spectrum. It is clear that one 9-anthryl group is present upper side of calixarene ring and the other 9-anthryl group is in the lower side. In contrast, both the ^{1}H NMR spectrum and the single crystal

analysis confirmed the *partial-cone* conformation of **3**HAn$_2$.

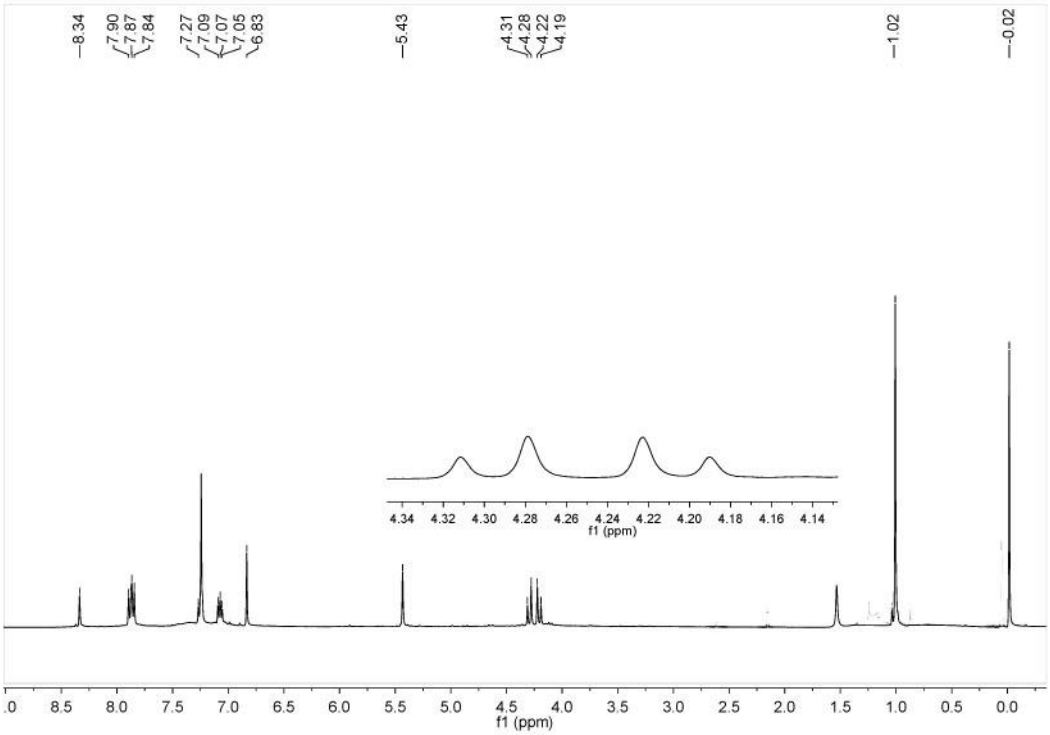

Figure 2.6. ^{1}H NMR spectrum of *cone*-**4**An$_3$ in $CDCl_3$ at 25 ℃, 300 MHz.

The ^{1}H NMR spectrum of *cone*-**4**An$_3$ shows a singlet for the *tert*-butyl protons at δ 1.01 ppm and a singlet for ArO*CH*$_2$Ph and the aromatic protons at δ 5.45 and 6.85 ppm, respectively indicating a C_3-symmetric structure of *cone*-**4**An$_3$. The X-ray structure of *cone*-**2**An$_3$ was shown in Figure 2.8. Within each calixarene is H-bond between the chloroform molecules and bridge oxygen atom, another H-bond between the chloroform molecules and *t*-Bu-H. The calixarene molecule adopts a collapsed, or squashed conformation to facilitate this H-bond and a π···π interaction between arene rings. In the lower rim, the three anthryl rings are close to parallel and overlapping. This is achieved by considerable distortion from the potential C_3 symmetry and a very irregular 18-membered ring, through O, around the center of the calixarene system. ^{13}C NMR spectrum ($CDCl_3$, 400 MHz) of *cone*-**4**An$_3$ exhibits two peaks for *tert*-butyl carbon at δ 28.98 and 30.14 ppm. In contrast, both the NMR spectrum and single crystal analysis confirmed the *cone* conformation of *cone*-**4**An$_3$.center of the calixarene system. The intermolecular bonds aren't found in this unit.

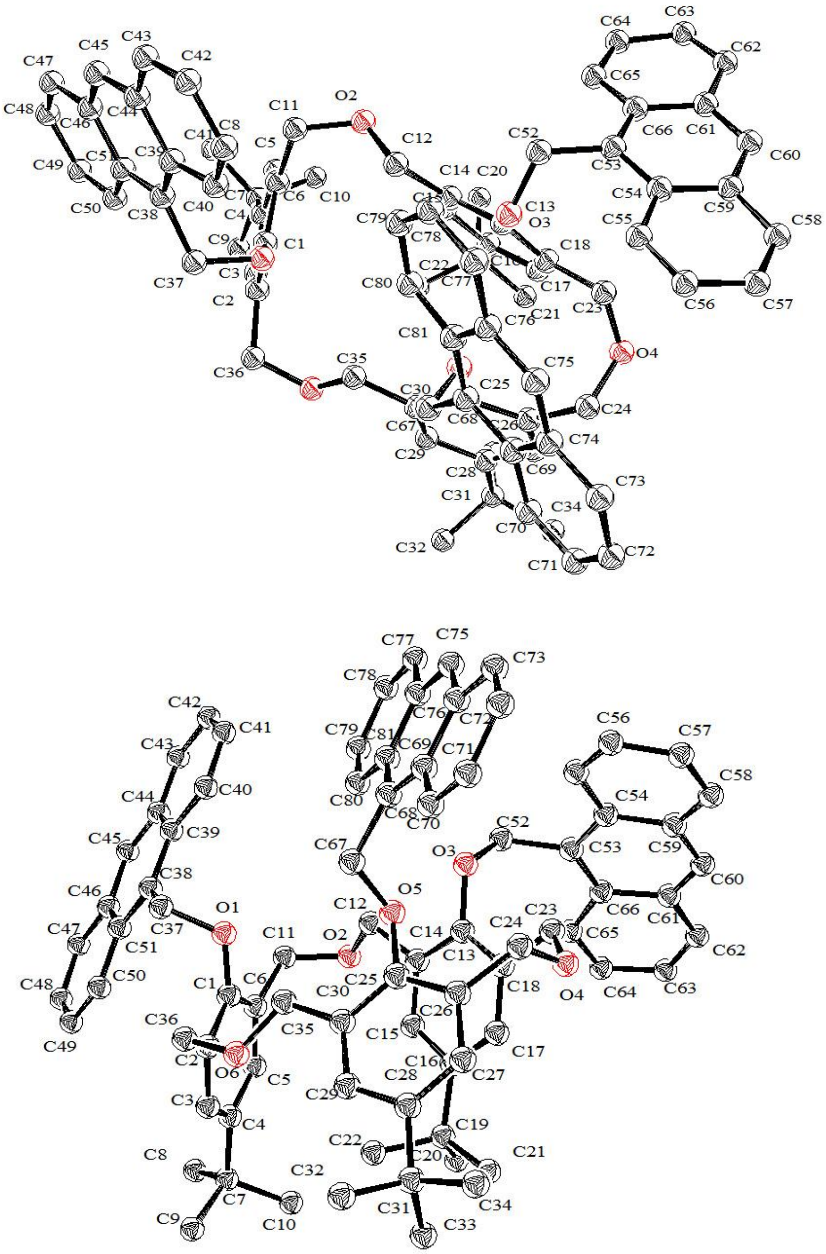

Figure 2.7. Top-view and side-view of X-ray structure of *cone*-**4**An$_3$.

^{1}H NMR spectrum ($CDCl_3$, 300 MHz) of *partial-cone*-**4**An$_3$ exhibits two group peaks for anthryl protons at δ 8.37, 7.91 and 8.35, 7.89 (relative intensity 2:1), two singlets for the *tert*-butyl protons at δ 0.83, 1.05 ppm (relative intensity 2:1). Furthermore, the resonance for the ArO*CH*$_2$Ph methylene protons appeared as a singlet at δ 5.25 ppm and a pair of doublets at δ 5.36, 5.54 ppm (J_{AB} = 12.7 Hz). Upfield shifts for the inverted 9-anthryl ring protons were observed. ^{13}C NMR spectrum ($CDCl_3$, 400 MHz) of *partial-cone*-**4**An$_3$ exhibits four peaks for *tert*-butyl carbon at δ 31.12, 31.33, 33.88, 33.97 ppm. These signals correspond to C_S-sym-

metric structure.

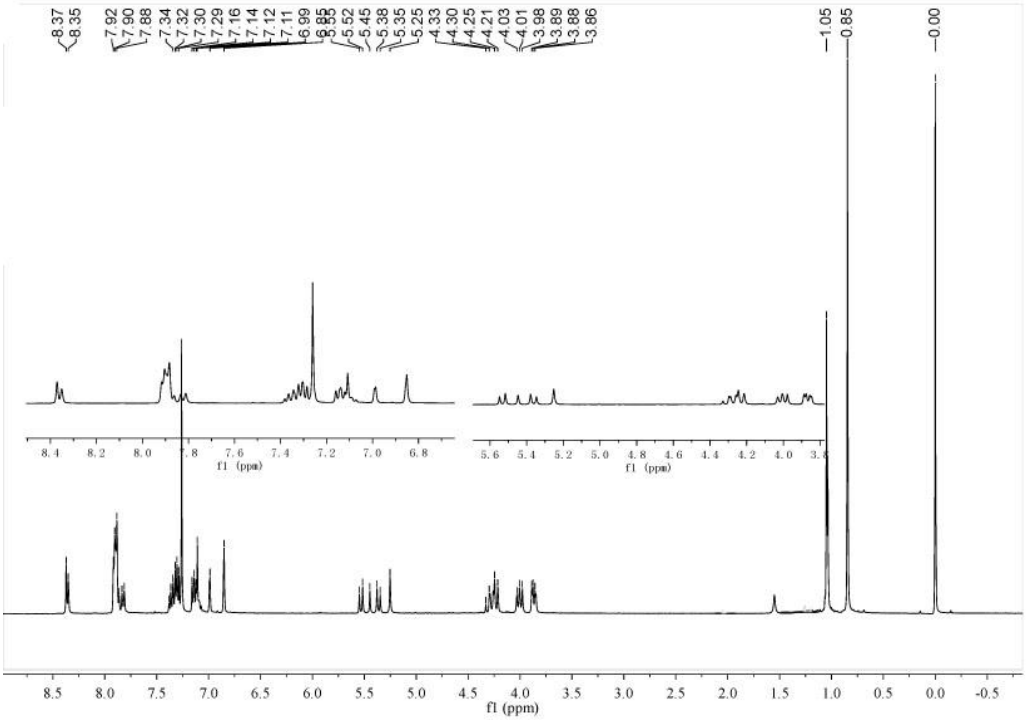

Figure 2.8 ^{1}H NMR spectrum of *partial-cone*-**4**An$_3$ in $CDCl_3$ at 25 ℃, 300 MHz.

2.2.3 Partial-cone and cone conformation

Shinkai et. al. reported that conformer distribution of calixarene can be affected by metal cation in base. [19] It is shown that template metal cations such as Na^+ which strongly interacts with calix[4]arenes, suppressing the rotation of phenyl units and giving rise to less-rotated conformers (such as *cone* and *partial-cone*) whereas nontemplate metal cations such as Cs^+ which scarcely interact with calix[4]arenes cannot suppress the rotation of phenyl units, giving rise to rotated conformer (such as 1,2- and 1, 3-*alternate*). Here, we can use this result in the used base on the conformer distribution of *partial-cone*-**4**An$_3$.

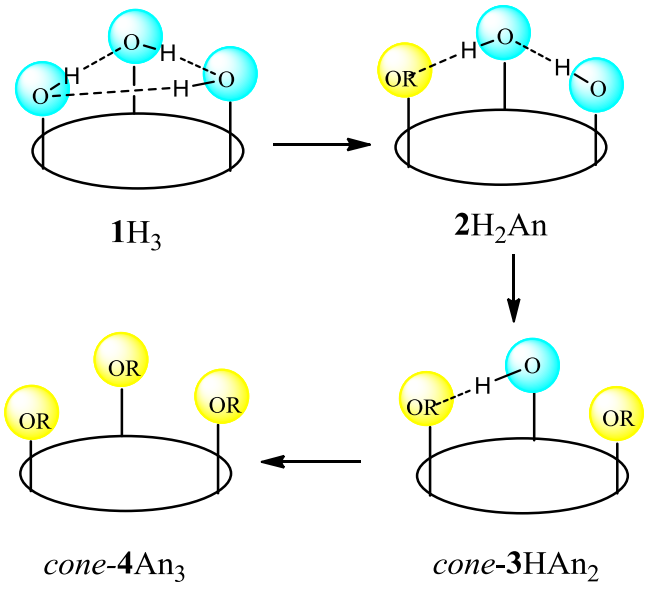

Figure 2.9. Possible reaction pathway of *cone*-**4**An$_3$.

Table 2.2 *O*-Substitution reaction of hexahomotrioxaocalix[3]arene 1 with 9-chloromethylanthracene **5** (3.3equiv.) in different ratio of acetone and benzene.

Run	Ratio (acetone: benzene)	Reaction time (h)	Distribution(%) [a, b]	
			cone-**4**An$_3$	*partial-cone*-**4**An$_3$
1	100:0	17	0	95 (72)
2	90:10	30	16	79 (52)
3	80:20	35	33 (14)	62 (38)
4	70:30	35	47 (23)	48 (31)
5	60:40	35	64 (42)	31 (12)
6	50:50	40	90 (69)	5

[a]Relative yields determined by ^{1}H NMR. [b]Isolated yields are shown in parentheses. [c]Starting compound **1** was recovered in quantitative yield.

On the other hand, the possible reaction route from **1**H$_3$ to *cone*-**4**An$_3$ can be illustrated as in Figure 2.9. Table 2.2 reveals that the success for synthesizing the *cone*-**4**An$_3$ in the presence of Cs_2CO_3 in a acetone /benzene (1: 1 v/ v) mixed solvent system gives *cone*-**4**An$_3$ in 95% selectivity. shinkai et. al. reported that template metal cations could strongly interact with calixarenes, suppressing the rotation of phenyl units and giving rise to *cone* conformer. [20] But, in this solvent system, it can suppose that there are hydrogen bonding between the hydroxyl of calixarene. Hydrogen bonds

can have different lengths, strengths, and geometries. A strong hydrogen bond can resemble a covalent bond with respect to the energy required to break the interaction, while the energy of a weak hydrogen bond will be closer to a van der Waals force. [21] The influencing factor of hydrogen bonds contain solvent polarity; some significant cooperative effect can enhance the strength of hydrogen bonds. The acetone is an polar solvent. The hydrogen bond between solvent and hexahomotrioxacalix[3]arene forms more easily which can destroy intramolecular hydrogen bond in the molecule. But in presence of benzene which is non-polar solvent, strong intramolecular hydrogen bonds are observed for the molecule in which hydrogen bond formation is very difficult. Strong hydrogen bond favorably forms between three phenolic oxygens arranged in the same side in the presence of benzene whereas weak hydrogen bond favorably form three phenolic oxygens across the ring in the presence of acetone.

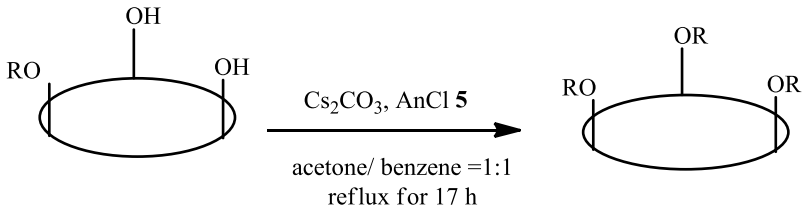

2H_2An *cone*-**4**An_3

Scheme 2.3. *O*-Substitution reaction of compound **2**H_2An with 9-chloromethyl anthracene **5** in the presence of Cs_2CO_3.

To confirm the reaction path of *cone*-**4**An_3, mono-substituted compound **2**H_2An was *O*-alkylated with 9-chloromethylanthracene **5** (2.3 equiv.) in a acetone /benzene (1: 1 v/ v) mixed solvent system which was showed in Scheme **2.3** in the presence of Cs_2CO_3 in the solvent of acetone/ benzene (v/ v = 1:1). The product was separated by column; ^{1}H NMR spectroscopy established that there are the *cone*-**4**An_3 derivatives. Respectively, it can be used to prove the reaction path of *cone*-**4**An_3 as from compound **2**H_2An to *cone*-**4**An_3.

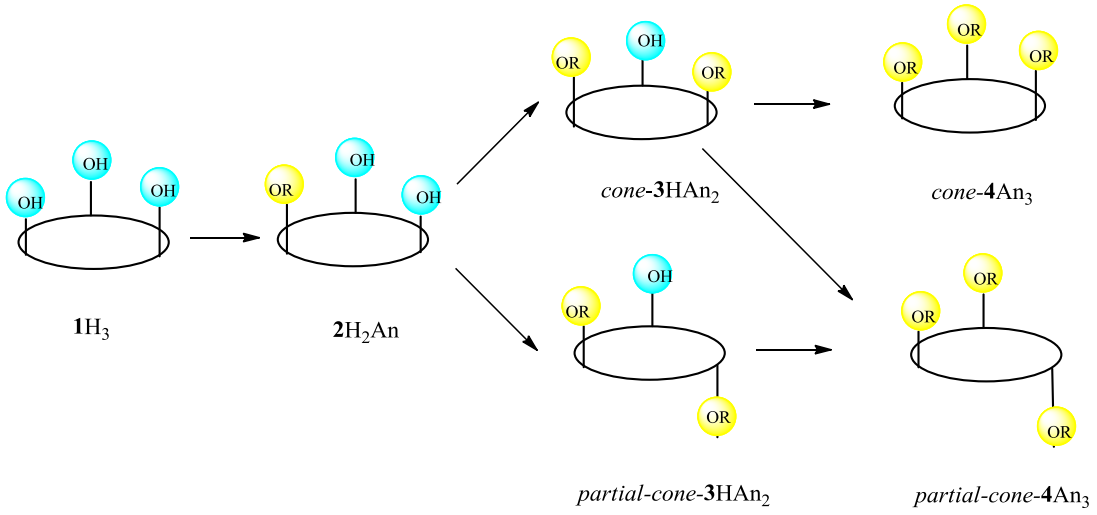

Figure 2.10. Reaction pathway from compound **1**H_3 to compound **4**An_3**.**

From what I have mentioned above, the isolable conformational isomer exists in compound **2**H_2An, compound **3**HAn_2, *cone*-**4**An_3 and *partial-cone*-**4**An_3. The reaction route from **l**H_3 to **4**An_3 can be illustrated as in Figure 2.10. In compound **3**HAn_2, in contrast, *cone*-**3**HAn_2 and *partial-cone*-**3**HAn_2 can exist and *cone*-**4**An_3 results only from *cone*-**3**HAn_2 whereas *partial-cone*-**3**HAn_2 results from both *cone*-**3**HAn_2 and *partial-cone*-**3**HAn_2. In other words, *cone*-**4**An_3 can't be found unless compound **3** contains the cone conformer.The ^{1}H NMR analysis of **3**HAn_2 indicated that in the reaction mixture obrained in acetone system or acetone /benzene (1: 1 v/ v) mixed solvent system a peak for *partial-cone*-**3**HAn_2 is detectable but a peak for *cone*-**3**HAn_2 is not. The result indicates that the conformation to yield *partial-cone*-**4**An_3 already determined when the second 9-anthryl groups enters and the path from compound **2**H_2An to *cone*-**3**HAn_2, then, *partial-cone*-**4**An_3 scarcely contributes to the formation of *partial-cone*-**4**An_3. In the reaction mixture obtained in the acetone system or acetone /benzene (1: 1 v/ v) mixed solvent system, we could detect a small peak attributable to *cone*-**3**HAn_2, this suggests that the formation of *cone*-**4**An_3 be rationalized in relation to the role of benzene in the step from compound **2**H_2An to compound *cone*-**3**HAn_2. These conformational preferences well explain the final conformer distribution in **4**An_3.

2.3 Conclusions

In conclusion, We have succeeded to synthesize the lower rim functionalized hexahomotrioxacalix[3]arene (compound **2**H_2An, compound **3**HAn_2, *cone*-**4**An_3 and

partial-cone-**4**An_3.), and these were confirmed by ^1H NMR, ^{13}C NMR, IR, MS spectroscopy and X-ray analysis. It is known that The introduction of compound **1** was achieved through selective alkylation with different equiv. of 9-chloromethyl-anthracene **5** in the acetone system to give different compound (compound **2**H_2An, compound **3**HAn_2 and *partial-cone*-**4**An_3). Fortunately, mono-substituted hexahomotrioxacalix[3]arene compound **2**H_2An was isolated for the first time. On the other hand, the success for synthesizing the *cone*-**4**An_3 in a acetone /benzene (1: 1 v/ v) mixed solvent system, it suggests that the solvent also can control the conformation due to hydrogen bonding between the hydroxyl of calixarene. Respectively, the possible reaction routes, the relative stability of the final products, interconversion between *cone* and *partial-cone*, etc. in detail.

2.4 Experimental Section

General

All melting points (Yanagimoto MP-S1) are uncorrected.^1H NMR and ^{13}C NMR spectra were recorded on a Nippon Denshi JEOL FT-300 NMR spectrometer and Varian-400MR-vnmrs400 with $SiMe_4$ as an internal reference: J-values are given in Hz. IR spectra were measured for samples as KBr pellets on a Nippon Denshi JIR-AQ2OM spectrophotometer. Mass spectra were obtained with a Nippon Denshi JMS-HX110A Ultrahigh Performance mass spectrometer at 75 eV by using a direct-inlet system. UV-vis spectra were recorded using a Shimadzu UV-3150UV-vis-NIR spectrophotometer. Elemental analyses were performed by a Yanaco MT-5.

*2.4.1. Synthesis of mono- substituted hexahomotrioxacalix[3]arenes (**2**H_2An)*

A mixture of **1**H_3 (700 mg, 1.22 mmol) and potassium carbonate (3.55 g, 10.9 mmol) in dry acetone (20 ml) was heated at reflux for 1 h under N_2. Then 9-chloromethylanthracene **5** (310 mg, 1.35 mmol) was added and the mixture heated at reflux for an additional 17 h. After cooling to room temperature, the mixture was filtered. The filtrate was concentrated to give a yellow oil, which was chromatographer over silica gel (Wako, C-300; 100 g) with hexane as eluent to give a colourless solid of which ^1H NMR analyses was accord with its being compound **2**H_2An. This solid was washed with methanol (20 ml) to give 845 mg (66%) of

2H_2An as a pale yellow solid. Recrystallization from hexane afforded *cone*-7,15,23-Tri-*tert*-butyl-25-(9-anthrylmethyl)-26,27-dihydroxy-2,3,10,11,18,19-hexahomo-3,11,19-trioxacalix[3]-arene (**2**) as a pale yellow prisms. Pale yellow prisms, m.p. 208 °C. IR (KBr): υ_{max} = 3415, 2951, 2904, 2865, 1481, 1362, 1195, 1070, 883 cm^{-1}. ^{1}H NMR ($CDCl_3$): δ = 1.22 (18H, s, t-Bu), 1.31 (9H, s, t-Bu), 4.08 (2H, d, *J* = 10.5 Hz, Ar*CH*$_2$O*CH*$_2$Ar), 4.21 (2H, d, *J* = 10.5 Hz, Ar*CH*$_2$O*CH*$_2$Ar), 4.38 (2H, d, J =10.5 Hz, Ar*CH*$_2$O*CH*$_2$Ar), 4.50 (2H, d, *J* = 10.5 Hz, Ar*CH*$_2$O*CH*$_2$Ar), 4.61 (2H, d, *J* = 10.5 Hz, ArC*H*$_2$OC*H*$_2$Ar), 4.82 (2H, d, *J* = 10.5 Hz, Ar*CH*$_2$O*CH*$_2$Ar), 6.00 (2H, s, ArO*CH*$_2$An), 7.04 (2H, d, *J* = 2.4 Hz, Ar-*H*), 7.06 (2H, d, *J* =2. 4 Hz, Ar-*H*), 7.24–7.43 (4H, m, An-*H*), 7.81(2H, s, *OH*), 7.97 (2H, d, *J* = 10.0 Hz, Ar-*H*), 8.26 (2H, d, *J* = 9.0 Hz, An-*H*), 8.45 (1H, s, An-H). ^{13}C NMR (400 MHz, CDCl3, 25 °C): δ = 31.48, 31.52, 33.88, 34.29, 68.24, 68.83, 69.20, 71.53, 123.49, 123.67, 124.62, 124.91, 126.15, 126.50, 126.90, 127.75, 128.82, 130.24, 131.10, 141.48, 146.33, 153.69, 155.78 ppm; EI-MS: *m/z*: = 766.28 [M^+]. $C_{66}H_{67}O_6$ (767.00): calcd. C 82.90, H 7.06; found C 82.75, H 7.13.

2.4.2 Synthesis of di-anthrylmethyl substituted hexahomotrioxacalix[3]arenes (**3**HAn_2)

A mixture of **1**H_3 (700 mg, 1.22 mmol) and potassium carbonate (3.55 g, 10.9 mmol) in dry acetone (70 mL) was heated at reflux for 1 h under N_2. Then 9-chloromethylanthracene **5** (690 mg, 2.55 mmol) was added and the mixture heated at reflux for an additional 17 h. After cooling to room temperature, the mixture was filtered. The filtrate was concentrated to give a yellow oil, which was chromatographer over silica gel (Wako, C-300; 100 g) with hexane as eluent to give a colourless solid of which ^{1}H NMR analyses was accord with its being a mixture of the starting compound **1**H_3 and *partial-cone*-**3**HAn_2 in the ratio of 5:95. This solid was washed with methanol (20 ml) to give 845 mg (71%) of *partial-cone*-**3**HAn_2 as a pale yellow solid. Recrystallization from hexane afforded *partial-cone*-7,15,23-tri-tert-butyl-25,26-bis(9-anthrylmethyl)-27-hydroxy-2,3,10,11,18,19-hexahomo-3,11,19- tri-oxacalix[3]arene (*partial-cone*-**3**) as a pale yellow prisms, m.p. 126–127 °C; IR (KBr): υ_{max} = 3415, 2951, 2904, 2865, 1481, 1362, 1195, 1070, 883 cm^{-1}. ^{1}H NMR ($CDCl_3$): δ = 1.15 (18H, s, t-Bu), 1.22 (9H, s, t-Bu), 3.71 (2H, d, *J* = 11.7 Hz, Ar*CH*$_2$O*CH*$_2$Ar), 3.90 (2H, d, *J* = 10.5 Hz, Ar*CH*$_2$O*CH*$_2$Ar), 4.24 (2H, d,

J =11.5 Hz, Ar*CH*$_2$O*CH*$_2$Ar), 4.40 (2H, d, *J* = 9.2 Hz, Ar*CH*$_2$O*CH*$_2$Ar), 4.44 (2H, d, *J* = 10.5 Hz, Ar*CH*$_2$O*CH*$_2$Ar), 5.14 (2H, d, J = 11.7 Hz, ArC*H*$_2$OC*H*$_2$Ar), 5.54 (2 H, d, J = 11.7 Hz, ArO*CH*$_2$An), 5.77 (2 H, d, J = 11.7 Hz, ArO*CH*$_2$An), 7.01 (4 H, s, Ar-*H*), 7.10 (2 H, d, J =2. 4 Hz, Ar-*H*), 7.15–7.32 (8 H, m, An-*H*), 7.48 (1 H, s, *OH*), 7.88 (4 H, d, J = 8.25 Hz, Ar-*H*), 8.09 (4H, d, *J* = 9.0 Hz, An-*H*), 8.35 (1H, s, An-H). ^{13}C NMR (400 MHz, CDCl3, 25 °C): δ = 31.36, 31.56, 33.84, 34.14, 65.58, 67.29, 68.24, 68.85, 123.54, 124.72, 124.88, 125.73, 126.68, 127.62, 128.47, 128.64, 130.43, 130.74, 131.21, 140.99, 146.10, 153.77, 155.36. ppm; EI-MS: *m/z*: = 955.28 [M$^+$]; C66H67O6 (956.27): calcd. C 82.90, H 7.06; found C 82.75, H 7.13.

*2.4.3 Synthesis of tri-anthrylmethyl substituted hexahomotrioxacalix[3]arenes (**4**An$_3$)*

*2.4.3.1 Synthesis of cone-**4**An$_3$*

A mixture of **1**H$_3$ (200 mg, 0.347 mmol) and potassium carbonate (2.27 g, 6.94 mmol) in dry acetone/ benzene (1:1) (15 ml) was heated at reflux for 1 h under N_2. Then 9-chloromethylanthracene **5** (310 mg, 1.15 mmol) was added and the mixture heated at reflux for an additional 40 h. After cooling to room temperature, the mixture was filtered. The filtrate was concentrated to give a yellow oil, which ^{1}H NMR spectrum was accord with being *cone*-**4**An$_3$. The residue was chromatographed over silica gel (Wako, C-300; 100 g) with hexane as eluent to give a yellow solid. This solid was washed with hexane to give 108 mg (69%) of *cone*-**4**An$_3$ as a pale yellow solid. Recrystallization from hexane afforded *cone*-**4**An$_3$, 15,23-tri-tert-butyl-25,26,27-tris(9-anthrylmethyl)-2,3,10,11,18,19-hexahomo-3,11,19-trioxacalix[3]arene (*cone*-**4**An$_3$) as a yellow prisms. m.p.: 257–258 °C; IR (KBr): υ_{max} = 3410, 3058, 2988, 2920, 2897, 1760, 1480, 1455, 1377, 1200, 1199, 1094, 1058 cm^{-1}; ^{1}H NMR (300 MHz, $CDCl_3$, 25 °C): δ = 1.02 (s, 27 H, *t*Bu), 4.21 (6H, d, *J* = 13.4 Hz, Ar*CH*$_2$O*CH*$_2$Ar), 4.30 (6H, d, *J* = 13.4 Hz, Ar*CH*$_2$O*CH*$_2$Ar), 5.43 (6H, s, ArO*CH*$_2$An), 6.83 (6H, s, Ar-*H*), 7.10–7.15 (6H, m, An-*H*), 7.20–7.28 (6H, m, Ar-*H*), 7.85 (6H, d, *J* = 8.3 Hz, An-*H*), 7.89 (6H, d, *J* = 8.3 Hz, An-*H*), 8.34 (3H, s, An-*H*) ppm; ^{13}C NMR (400 MHz, $CDCl_3$, 25 °C): δ = 28.98, 30.14, 64.79, 67.05, 68.48, 122.40, 123.47, 124.00, 125.06, 126.28, 126.73, 127.82, 128.26, 129.57, 144.34, 152.54. ppm; EI-MS: *m/z*: 1146.65 [M$^+$]; Elemental analysis calcd (%) for C55H48O5 (1147.52): (1147.52): C 84.78, H 6.85; found C 84.92, H 7.05.

*2.4.3.2 Synthesis of partial-cone-**4**An$_3$*

A mixture of **1**H_3 (200 mg, 0.347 mmol) and potassium carbonate (2.63 g, 6.94 mmol) in dry acetone (20 ml) was heated at reflux for 1 h under N_2. Then 9-chloromethylanthracene **5** (310 mg, 1.15 mmol) was added and the mixture heated at reflux for an additional 17 h. After cooling to room temperature, the mixture was filtered. The filtrate was concentrated to give a yellow oil, which ^{1}H NMR spectrum was accord with being only *partial-cone*-**4**An_3. The residue was chromatographer over silica gel (Wako, C-300; 100 g) with hexane as eluent to give a yellow solid. This solid was washed with hexane to give 126 mg (75%) of *partial-cone*-**4**An_3 as a pale yellow solid. Recrystallization from hexane afforded *partial-cone*-7,15,23-tri-*tert*-butyl-25,26,27-tris(9-anthrylmethyl)-2,3,10,11,18,19-hexahomo-3,11,19-trioxacalix[3]arene (*partial-cone*-**4**An_3) as a yellow prisms. m.p.: 257–258 °C; IR (KBr): υ_{max}= 3400, 2975, 2915, 2867, 1758, 1483, 1456, 1363, 1234, 1199, 1094, 1058 cm^{-1}; ^{1}H NMR (300 MHz, $CDCl_3$, 25 °C): δ = 0.85 (18H, s, *t*Bu), 1.05 (9H, s, *t*Bu), 3.87 (2H, d, *J* = 11.7 Hz, Ar*CH*$_2$O*CH*$_2$Ar), 3.89 (2H, d, *J* = 11.2 Hz, Ar*CH*$_2$O*CH*$_2$Ar), 3.99 (2H, d, *J* = 11.7 Hz, Ar*CH*$_2$O*CH*$_2$Ar), 4.00 (2H, d, *J* = 11.2 Hz, Ar*CH*$_2$O*CH*$_2$Ar), 4.23 (2H, d, *J* = 11.7 Hz, Ar*CH*$_2$O*CH*$_2$Ar), 4.31 (2H, d, *J* = 11.2 Hz, Ar*CH*$_2$O*CH*$_2$Ar), 5.25 (2H, s, ArO*CH*$_2$An), 5.36 (2H, d, *J* = 12.7 Hz, ArO*CH*$_2$An), 5.54 (2H, d, J = 12.7 Hz, ArO*CH*$_2$An), 6.86 (2H, d, *J* = 2.4 Hz, Ar-*H*), 6.99 (2H, d, *J* = 2.4 Hz, Ar-*H*), 7.10 (2H, s, Ar-*H*), 7.14–7.40 (12H, m, Ar-*H*), 7.82 (2H, d, *J* = 8.3 Hz, An-*H*), 7.89 (4H, d, *J* = 8.3 Hz, An-*H*), 7.91 (6H, m, An-*H*), 8.35 (1 H, s, An-*H*), 8.37 (2H, s, An-*H*) ppm; ^{13}C NMR (400 MHz, $CDCl_3$, 25 °C): δ = 31.12, 31.33, 33.88, 33.97, 64.71, 66.59, 67.97, 68.48, 69.63, 68.81, 124.46, 124.69, 124.72, 124.76, 125.78, 125.84, 125.91, 128.30, 128.38, 128.41, 128.57, 128.86, 129.68, 129.84, 130.90, 131.00, 131.15, 145.86, 152.96, 154.14, 157.34 ppm; EI-MS: *m/z*: 1146.72 [M$^+$]; Elemental analysis calcd (%) for C55H48O5 (1147.52): C 84.78, H 6.96; found C 84.99, H 7.06.

2.4.4 Crystallographic analysis of partial-cone-**3**HAn_2 and cone-**4**An_3.

Data were processed using the CrysAlisPro-CCD and –RED16 programs. The structure was determined by the direct methods routines in the SHELXS program17 and refined by full-matrix least-squares methods, on F2's, in SHELXL21. The non-hydrogen atoms were refined with anisotropic thermal parameters (but from a rather limited data-set, some thermal parameters appeared barely acceptable).

Hydrogen atoms were included in idealised positions and their Uiso values were set to ride on the Ueq values of the parent carbon atoms.

Table 2.4 Summary of crystal data for *partial-cone*-**3**HAn_2 and *cone*-**4**An_3.[a,b]

parameter	*cone*-**4**An_3	*partial-cone*-**3**HAn_2
Formula	C_{81} H_{78} O_6	C_{70} H_{75} O_6
Formula weight	1266.80	957.20
Space group	*P*2(1)/n	*I*2/a
a [Å]	17.8903(4)	30.303(2)
b [Å]	16.8621(4)	14.1499(10)
c [Å]	21.6293(5)	30.774(2)
α [°]	90	90
β [°]	90.561(12)	115.729(2)
γ [°]	90	90
Volume ($Å^3$)	6524.6 (3)	11887.2 (14)
Z	4	8
D(calc) [$g.m^{-3}$]	1.290	1.167
Temperature [K]	120 K	150 K
Unique reflns	11466	10449
Obsd reflns	2680.0	4472.0
Parameters	866	656
R_{int} [mm^{-1}]	0.197	0.075
R[I>2σ(I)][a]	0.0845	0.0596
wR[I>2σ(I)][b]	0.2216	0.1687
GOF on F^2	1.036	1.085

[a] Conventional *R* on F_{hkl}: $\Sigma ||Fo| - |Fc||/\sigma|Fo|$.
[b] Weighted *R* on $|F_{hkl}|^2$: $\Sigma [w(F_o^2 - F_c^2)^2]/ \Sigma [w(F_o^2)^2]^{1/2}$

2.5 References

1. Calixarenes 2001, ed. Z. Asfari, V. Böhmer, J. Harrowfield, J. Vicens, Kluwer Academic Publishers, Dordrecht, 2001

2. C. D. Gutsche, Calixarenes, An Introduction, Royal Society of Chemistry, Cambridge, U.K., 2008.

3. A. Ikeda, S. Shinkai, *Chem. Rev.*, **1997**, *97*, 1713–1734.

4. L. Mutihac, J. H. Lee, J. S. Kim, J. Vicens, *Chem. Soc. Rev.*, **2001**, *40*, 2777–2796.

5. L. Baldini, A. Casnati, F. Sansone, R. Ungaro, *Chem. Soc. Rev.*, **2007**, *36*, 254–266.

6. J. S. Kim, D. T. Quang, *Chem. Rev.*, **2007**, *107*, 3780–3799.

7. R. Joseph, C. P. Rao, *Chem. Rev.*, **2011**, 111, 4658–4702.

8. J. W. Steed, J. L. Atwood, Supramolecular Chemistry, John Wiley and Sons, Chichester, 2000.

9. F. P. Schmidtchen, M. Berger, *Chem. Rev.*, **1997**, *97*, 1609–1646.

10. P. D. Beer, P. A. Gale, *Angew. Chem., Int. Ed.*, **2001**, *40*, 486–516.

11. J. Yoon, S. K. Kim, N. J. Singh, K. S. Kim, *Chem. Soc. Rev.*, 2006, *35*, 355–360.

12. X.-L. Ni, M. Takimoto, X. Zeng, T. Yamato, *J. Inclusion Phenom. Macrocyclic Chem.*, **2011**, *71*, 231–237.

13. X.-L. Ni, J. Tahara, S. Rahman, X. Zeng, D. L. Hughes, C. Redshaw, T. Yamato, *Chem.–Asian J.*, **2012**, *7*, 519–527.

14. M. Bocheńska, P. J. Cragg, M. Guziński, A. Jasiński, J. Kulesza, P. M. Marcos, R. Pomećko, *Supramol. Chem.*, **2009**, *21*, 732–737.

15. P. M. Marcos, J. R. Ascenso, P. J. Cragg, *Supramol. Chem.*, **2007**, *19*, 199–206.

16. P. M. Marcos, J. R. Ascenso, M. A. P. Seguradu, R. J. Bernardino, P. J. Cragg, *Tetrahedron*, **2009**, *65*, 496–503.

17. P. J. Cragg, M. Miah, J. W. Steed, *Supramol. Chem.*, **2002**, *14*, 75–78.

18. K. Araki, H. Hayashida, *Tetrahedron Lett.*, **2000**, *41*, 1807–1810.

19. P. J. Cragg, M. G. B. Drew, J. W. Steed, *Supramol. Chem.*, **1999**, *11*, 5–15.

20. K. Tsubaki, T. Otsubo, T. Morimoto, H. Maruoka, M. Furukawa, Y. Momose, M. H. Shang, K. Fuji, *J. Org. Chem.*, **2002**, *67*, 8151–8156.

21. A. Ikeda, H. Udzu, Z. Zhong, S. Shinkai, S. Sakamoto, K. Yamaguchi, *J. Am. Chem. Soc.*, **2001**, *123*, 3872–3877.

23. K. Araki, K. Inada, S. Shinkai, *Angew. Chem., Int. Ed. Engl.*, **1996**, *35*, 72–74.

24. A. Ikeda, T. Hatano, S. Shinkai, T. Akiyama, S. Yamada, *J. Am. Chem. Soc.*, **2001**, *123*, 4855–4856.

25. A. Ikeda, S. Nobukuni, H. Udzu, Z. Zhong, S. Shinkai, *Eur. J. Org. Chem.*, **2000**, *65*, 3287–3293.

26. A. Ikeda, M. Yoshimura, H. Udzu, C. Fukuhara, S. Shinkai, *J. Am. Chem. Soc.*, **1999**, *121*, 4296–4297.

27. X.-L. Ni, S. Rahman, S. Wang, C.-C. Jin, X. Zeng, D. L. Hughes, C. Redshaw, T. Yamato, *Org. Biomol. Chem.*, **2012**, *10*, 4618–4626.

28. X.-L. Ni, S. Rahman, X. Zeng, D. L. Hughes, C. Redshaw, T. Yamato, *Org. Biomol. Chem.*, **2011**, *9*, 6535–6541.

29. T. Yamato, S. Rahman, F. Kitajima, X. Zeng, J. T. Gil, *J. Chem. Res.*, **2006**, 496–498.

30. T. Yamato, S. Rahman, F. Kitajima, X. Zeng, J. T. Gil, *Can. J. Chem.*, **2006**, *84*, 58–64.

31. X.-L. Ni, S. Wang, X. Zeng, Z. Tao, T. Yamato, *Org. Lett.*, **2011**, *13*, 552–555.

32. A. R. Harifi-Mood, M. Rahmati, M. R. Gholami, *Int. J. Chem. Kinet.*, **2011**, *43*, 185–190.

33. H. Matsumoto, S. Nishlo, M. Takeshita, S. Shinkai, *Tetrahedron*, **1995**, *51*, 4647–4654.

34. K. Araki, N. Hashimoto, H. Otsuka, S. Shinkai, *J. Org. Chem.*, **1993**, *58*, 5958–5963.

35. H. Ninagawa, H. Matsuda, Makromol. Chem., *Rapid Commun.*, **1982**, *3*, 65.

36. J. V. Prata, A. I. Costa, G. Pescitelli, C. M. Teixeira, *Tetrahedron: Asymmetry*, **2014**, *25*, 547–553.

37. J. L. Cook, C. A. Hunter, C. M. R. Low, A. Perez-Velasco, J. G. Vinter, Angew. *Chem. Int. Ed.*, **2007**, *46*, 3706–3709.

Chapter 3

Synthesis and evaluation of a novel fluorescent sensors based on hexahomotrioxacalix[3]arene for Zn^{2+} and Cd^{2+}

*This chapter focused on a novel type of selective and sensitive fluorescent sensor having triazole rings as the binding sites on the lower rim of a hexahomotrioxacalix[3]arene scaffold in a cone conformation. This sensor has desirable properties for practical applications, including selectivity for detecting Zn^{2+} and Cd^{2+} in the presence of excess competing metal ions at low ion concentration or as a fluorescence enhancement type chemosensor due to the cavity of calixarene changed from a "flattened-cone" to a more-upright form and inhibition of PET. In contrast, the results suggested that receptor **1** is highly sensitive and selective for Cu^{2+} and Fe^{3+} as a fluorescence quenching type chemosensor due to the photoinduced electron transfer (PET) or heavy atom effect*

3.1 Introduction

Owing to their simplicity, high sensitivity, and low detection limits for trace chemicals in chemistry, biology, and the environment,[1,2] fluorescent chemosensors have received much attention in the field of supramolecular chemistry. Generally, an effective fluorescent chemosensor consists of an ion recognition unit and a fluorogenic unit, which converts the actuating signal from the ionophore unit into a light signal. Amongst the different fluorogenic units, anthracene derivatives are key species in the design of fluorescent chemosensors materials, which have found wide utilization in lasers, phosphors, and light-emitting devices.[3] Although a tremendous number of anthracene-based organic materials have been investigated with the aim of potential applications as photoluminescence (PL) and/or electroluminescence (EL) devices in films and the solid state, the practical development of PL and EL devices is in fact restricted, usually owing to their poor stability. In contrast, strongly luminescent anthracene-based inorganic–organic hybrid materials with higher stability could be a class of promising candidates for light-emitting as well as EL applications.[4]

Calixarenes and their derivatives are attractive compounds for use in host–guest and supramolecular chemistry. In particular, hexahomotrioxacalix[3]arene derivatives with C_3-symmetry can selectively bind ammonium ions which play important roles in both chemistry and biology.[5,6] Furthermore, the incorporation of two types of recognition sites via the introduction of different ionophores on the hexahomotrioxacalix[3]arene will create potential hetero-ditopic receptors with the capability of binding cations and anions, *e.g.* ammonium ions and halides. Therefore, many fluorescent chemosensors based on calixarenes, which show highly selective recognition of metal cations,[7] ammonium cations,[8] and fullerene derivatives, have been reported.[9]

Additionally, the use of Click chemistry[10] has seen a significant growth in the derivatization of calixarenes owing to its reliability, specificity, biocompatibility, and efficiency. It has been proven to be a promising strategy for the chemical modification of calixarenes. In 2005, Zhao and co-workers[11] applied Click chemistry to the synthesis of water soluble calixarenes, which laid a solid foundation for this methodology. Click chemistry has also been used to synthesize calixarene conjugates of chromophores and bioactive molecules such as glycosides,[12] sialoclusters,[13] and amino acids.[14] Because of the highly selective nature of the alkyne-azide cycloaddition, the Click reaction is a general method to introduce various functional groups/moieties at the upper or lower rim of calixarenes. Therefore, we hypothesized that suitably arranged functionalized groups containing nitrogen atoms attached to a

hexahomotrioxacalix[3]arene should be a good receptor candidate for cations. Therefore, with this in mind, we have synthesized chemosensor **L** and studied its cation-binding affinity.

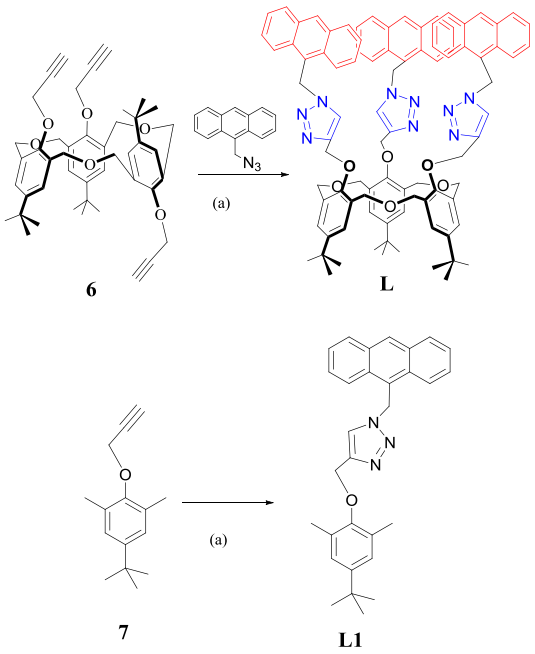

Scheme 3.1. Synthetic pathway for compounds **L** and **L1**. (a) CuI in THF and water, reflux, 20 h.

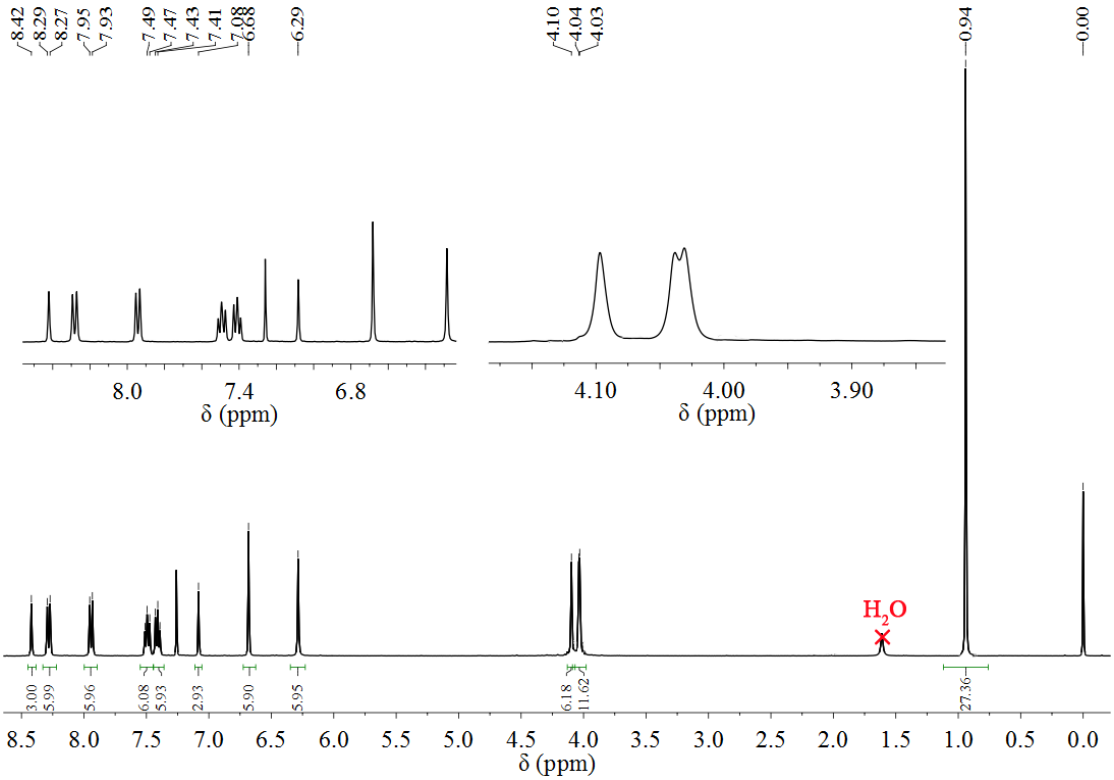

Fig. 3.1 (a) ^{1}H NMR spectrum of compound **L** in $CDCl_3$ at 25°C on a 400 MHz spectrometer.

3.2. Results and discussion

The synthesis of **L** was carried out as shown in Scheme 1. We first synthesized **6** in 55 % yield by the reaction of hexahomotri-oxacalix[3]arene and propargyl bromide in the presence of Cs_2CO_3 in dry acetone solution. The ^{1}H NMR spectroscopic results suggested that **6** adopts a *partial-cone* structure.[15] Accordingly, fluorescent compound **L** can be obtained from the reaction of **6** with 9-azidomethylanthracene under standard conditions for Click chemistry. The coupling of **6** with 9-azidomethyl-anthracene afforded *cone* conformation compound **L** in 75 % yield. ^{1}H NMR spectrum of **L** shows a singlet for the *tert*-butyl protons at δ 0.94 ppm, and a doublet at δ 4.03 ppm for the bridge protons, and ^{13}C NMR spectrum of **L** exhibits two peaks for the methyl and the quaternary carbon atoms of the *t*-Bu groups at δ 31.32, 34.04 ppm, three peaks for methylene carbon at 45.51, 66.94, 68.87 ppm and 14 peaks for aromatic carbon. respectively, indicating a C_3–symmetric structure for sensor **L**. The same procedure was also employed in the synthesis of **L1** from 4-*tert*-butyl-2,6-dimethylphenol (Scheme 3.1). Compound **L** contains both the calixarene and the triazole groups as metal ion binding sites, whereas **L1** contains only a triazole for metal ion binding. Compare to compound **L**, ^{1}H NMR spectrum of the reference compound **L1** shows that the protons on the anthracene ring appeared at the lower magnetic fields at around δ 7.52–8.60 ppm ($\Delta\delta$ 0.05–0.2 ppm), and the proton on the triazole ring also appeared at the lower magnetic field at δ 7.08 ppm ($\Delta\delta$ 0.11ppm) (Figure 3.2). These findings strongly indicate the anthracene moieties appended on **L** were sterically-fixed to be in close proximity to allow the formation of π–π stacking between the anthracene moieties.

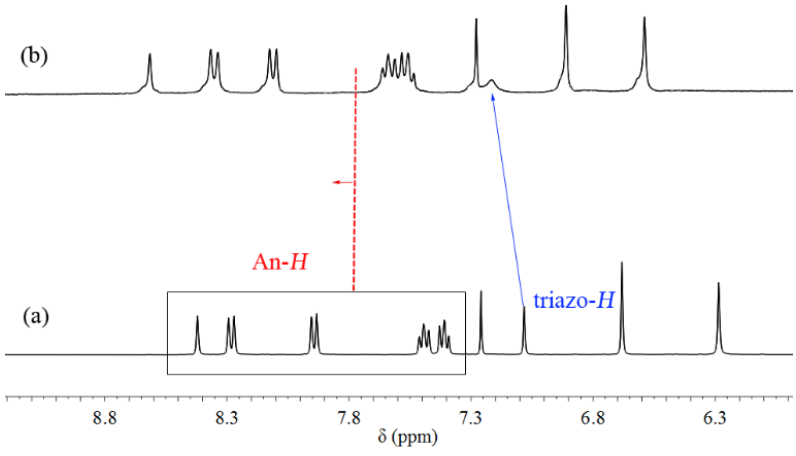

Figure 3.2. Partial ^{1}H NMR spectra of **L** (4.0 mM) and **L1** (4.0 mM) in $CDCl_3$: CD_3CN (10:1, v/v). (a) Compound **L**; (b) Compound **L1**.

3.2.1 Fluorescent spectroscopy studies

Solutions giving concentrations of **L** (10 μM) in CH_3CN were prepared as follows. Test solutions were prepared by taking 70 mL of the calixarene stock solution in a 10 mL volumetric flask, adding 0, 0.2, 0.4, 0.6, 0.8 and 1.0 mL of stock solution, and making up to the volume with CH_3CN. The fluorescence spectrum of **L** (10 μM) in CH_3CN exhibits a characteristic monomer emission of anthracene. The fluorescence emission of the solutions was measured at an excitation wavelength of 365 nm, and the emission intensities were measured at 418 nm. Measurements were repeated a minimum of three times for each addition. At high concentrations, emission quenching was observed, suggesting the formation of intermolecular associates of **L**.

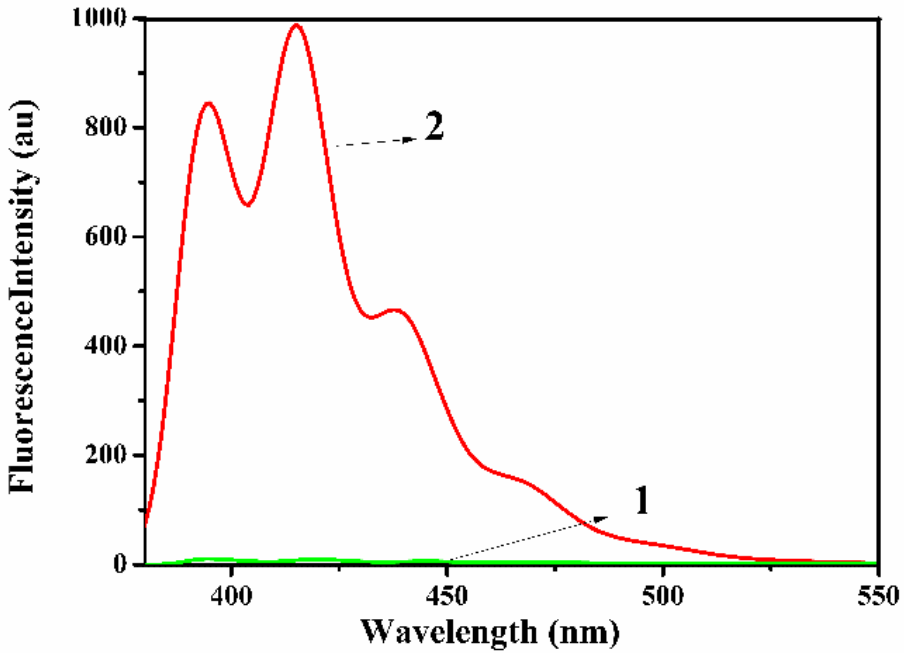

Figure 3.3. Fluorescence spectra of **L** (10 μM) and **L1** (30 μM) in CH_3CN.

However, under dilute conditions, emission quenching was not observed. The critical association concentration value determined from the concentration-variable emission spectra was determined to be 10 μM. To remove effects of the inter-molecular associates, absorption and fluorescence measurements were carried out under critical association concentration. A similar procedure for the fluorescence measurements of **L1** was conducted. The fluorescence emission of the solutions was measured at an excitation wavelength of 365 nm, and the emission intensities were measured at 418 nm. More interestingly, compared to **L1**, the fluorescence intensity of **L** is obviously different from reference compound **L1** at the concentration (30 μM). The fluorescence spectra of **L** and **L1** under the same solutions are shown in Figure 3.3. When **L1** was excited at 365 nm, strong emission peaks near 400–500 nm were observed, which were assigned as emission from single anthracene moiety,

respectively. In contrast, when **L** was excited at 365 nm, the emission peaks were weak. These observations indicated that the formation of π–π stacking between the anthracene moieties appended on **L** can quench the fluorescence.

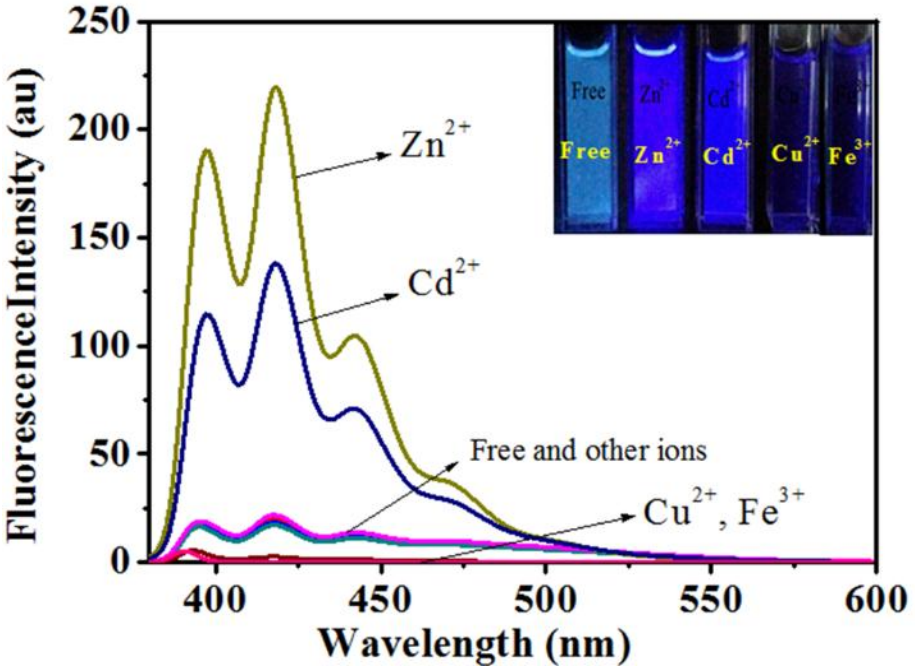

Figure 3.4. Fluorescence spectra of **L** (10 μM) in CH_3CN in the presence of different metal ions (10 equiv.). Metal ions include K^+, Na^+, Li^+, Ca^{2+}, Cr^{3+}, Ni^{2+}, Cu^{2+}, Zn^{2+}, Ag^+, Cd^{2+}, Hg^{2+}, Fe^{3+}, Fe^{2+} and Pb^{2+}. Excitation was performed at 365 nm.

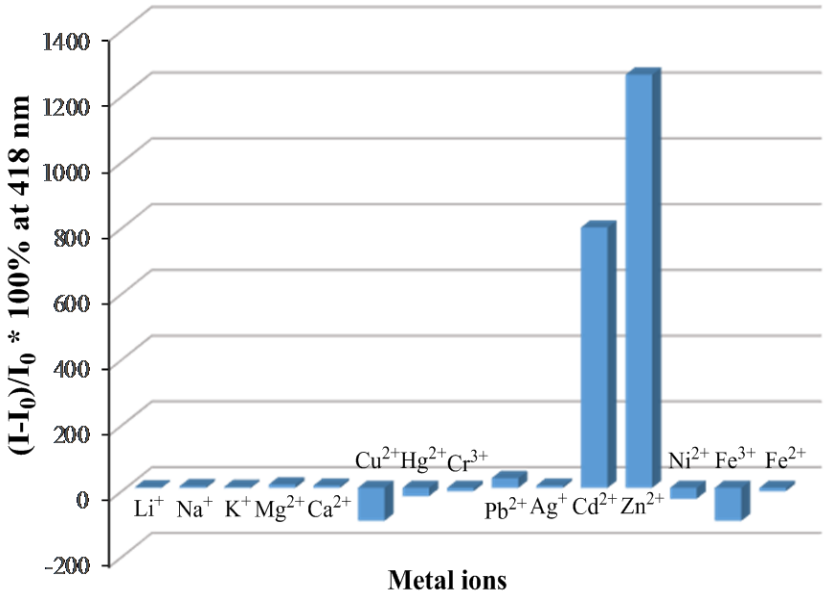

Figure 3.5. Fluorescence responses of receptor **L** (10 μM) to 100 μM various tested ions in CH_3CN. I_0 is the fluorescence emission intensity at 418 nm for free receptor **L**, and I is the fluorescent intensity after adding ions at 298 K. λ_{ex} = 365 nm.

To get an insight into the binding properties of chemosensor **L** toward metal cations, we first investigated the fluorescence changes upon addition of a wide range of metal cations including K^+, Na^+, Mg^{2+}, Ca^{2+}, Mn^{2+}, Cr^{3+}, Fe^{2+}, Ni^{2+}, Sr^{2+}, Ag^+, Hg^{2+}, Pb^{2+}, Cu^{2+}, Fe^{3+}, Zn^{2+} and Cd^{2+}. The fluorescence changes are depicted in Figure 3.4 and Figure 3.5. Addition of Zn^{2+} and Cd^{2+} to the solution of **L** induced obvious ratiometric changes, where the emission increases. By contrast, no significant spectral changes were observed upon addition of most of the other metal cations apart from Cu^{2+} and Fe^{3+} where quenching was observed. These results suggest that complexations between **L** and Cu^{2+}, Fe^{3+}, Zn^{2+} and Cd^{2+} ions through intermolecular interaction might be proposed.

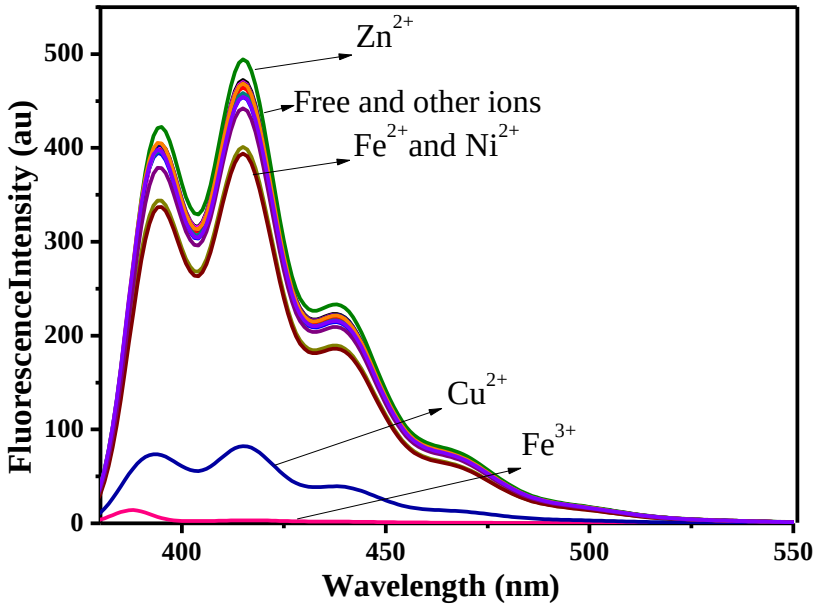

Figure 3.6. Fluorescence spectra of **L1** (0.01 mM) in CH_3CN in the presence of different metal ions (10 equiv.). Metal ions include K^+, Na^+, Li^+, Ca^{2+}, Cr^{3+}, Ni^{2+}, Cu^{2+}, Zn^{2+}, Ag^+, Cd^{2+}, Hg^{2+}, Fe^{3+}, Fe^{2+} and Pb^{2+}. Excitation was performed at 365 nm.

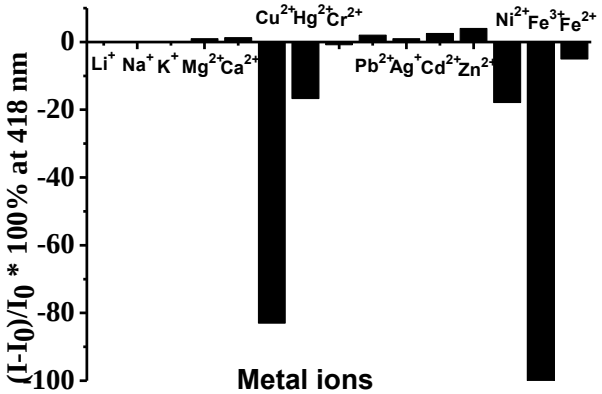

Figure 3.7 Percentage fluorescence intensity of **L1** (0.01 mM) by the addition of 10 equiv. of various metal perchlorates (K^+, Na^+, Li^+, Ca^{2+}, Co^{2+}, Ni^{2+}, Cu^{2+}, Zn^{2+}, Ag^+, Cd^{2+}, Hg^{2+}, Fe^{3+}, Fe^{2+} and Pb^{2+}) in CH_3CN. Excitation wavelength was 365 nm.

In contrast to chemosensor **L**, chemosensor **L1** exhibited a strong emission at 418 nm, and similar experiment was carried out. The fluorescence intensity changes of **2** upon addition of different metal ions are shown in Figure 3.6 and Figure 3.7. Addition of Cu^{2+} and Fe^{3+} caused a strong and medium fluorescence quenching, respectively.

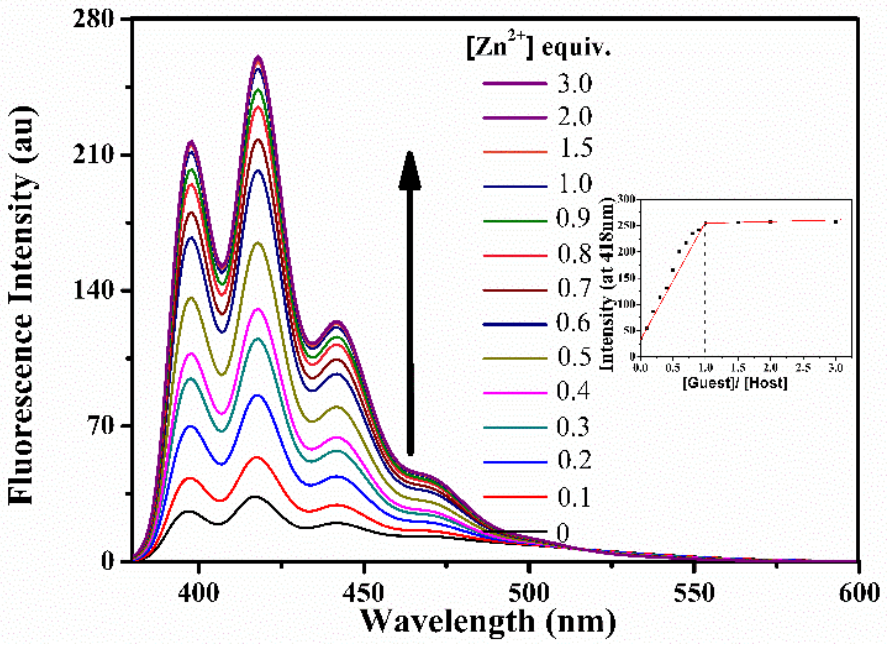

Figure 3.8. Changes in fluorescence emission spectra of **L** (10 μM) upon titration by Zn^{2+} (from 0 – 30 μM) in CH_3CN (excitation at 365 nm). Inset is molar ratio plot.

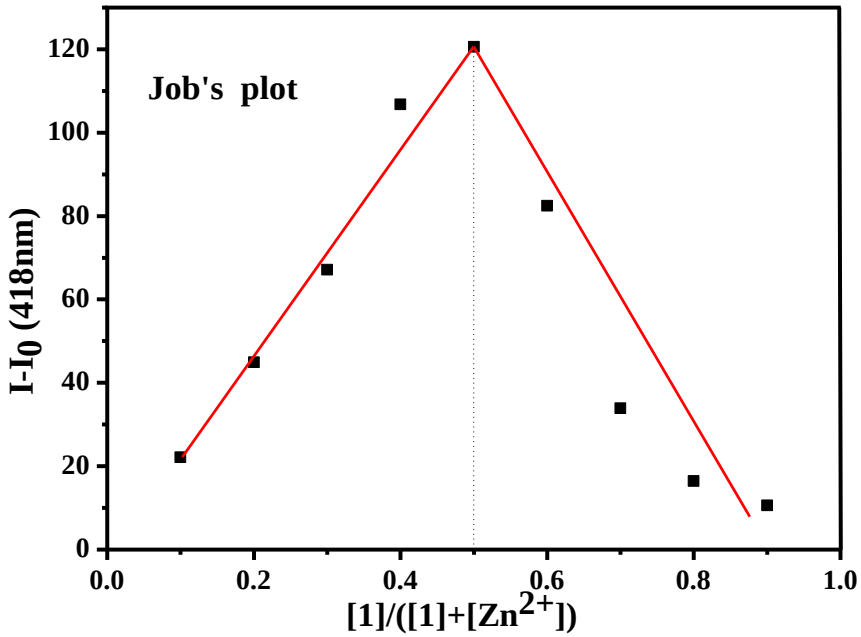

Figure 3.9. Job's plot showing the 1:1 binding of **L** to Zn^{2+} ion.

Upon addition of Zn^{2+}, the fluorescence intensity of solution **L** increased gradually (Figure 3.6). The saturation behavior of the fluorescence intensity after adding 2 equivalents of Zn^{2+} reveals that a 1:1 stoichiometry best describes the binding mode

of Zn^{2+} and **L**, which is also supported by the Job's plot data (Figure 3.9). According to the 1:1 model, the association constant of Zn^{2+}, calculated from the Benesi-Hildebrand equation,[16] was found to be 1.44×10^4 M^{-1}. As a result, **1** can be regarded as being highly sensitive to the Zn^{2+} ion, especially given the large fluorescence dynamic range and the low detection limit of 3.79×10^{-7} M. The quantum yield of **L** is $\Phi = 0.11$.

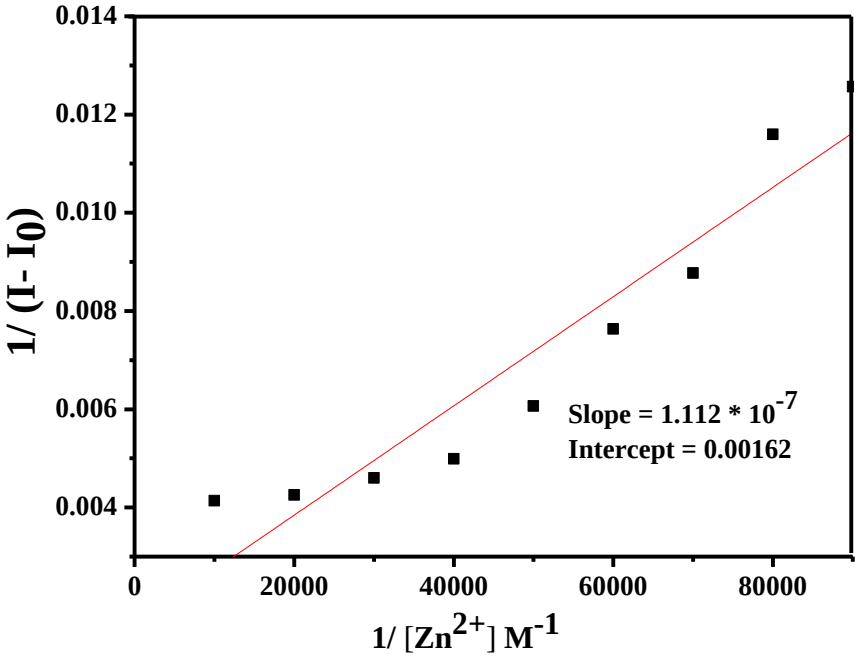

Figure 3.10. The binding constants of **L** with Zn^{2+} in different concentrations. The K_a of Zn^{2+} was calculated to be 1.44×10^4.

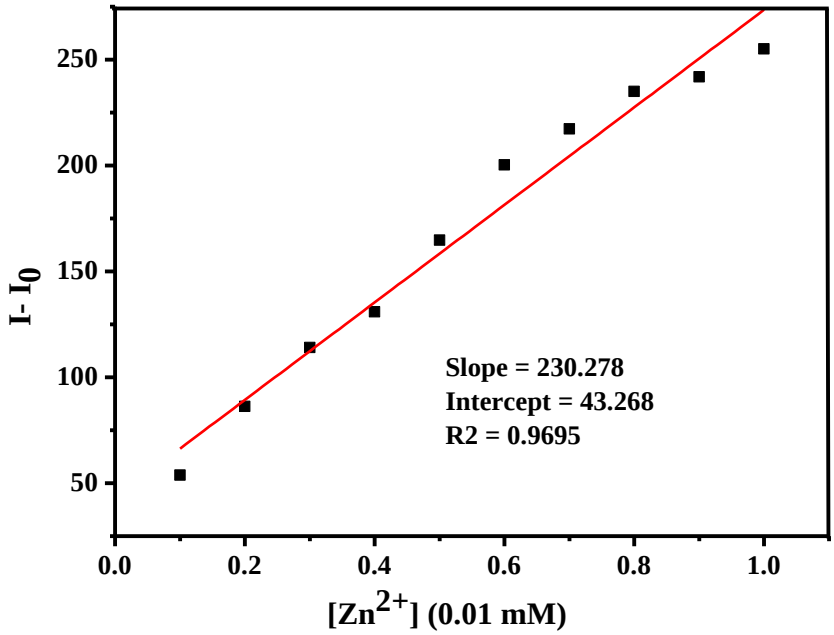

Figure 3.11 Linear concentration range of Zn^{2+} with **L**. The detection limit of Zn^{2+} was calculated to be 3.79×10^{-7} M by the formula ($3\sigma/K$).

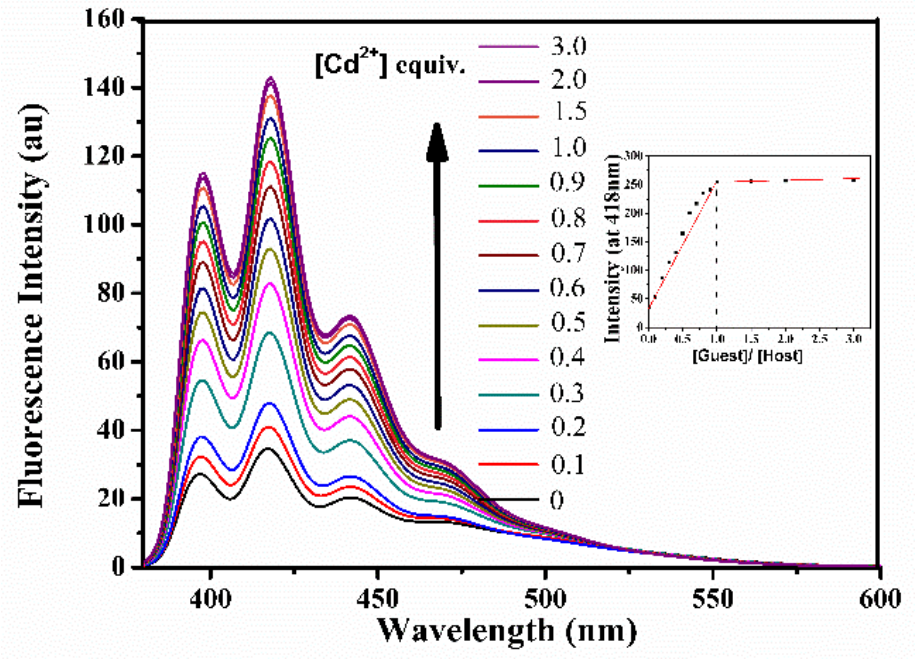

Figure 3.12. Changes in fluorescence emission spectra of **L** (10 μM) upon titration by Cd^{2+} (from 0 – 30 μM) in CH_3CN (excitation at 365 nm). Inset is molar ratio plot.

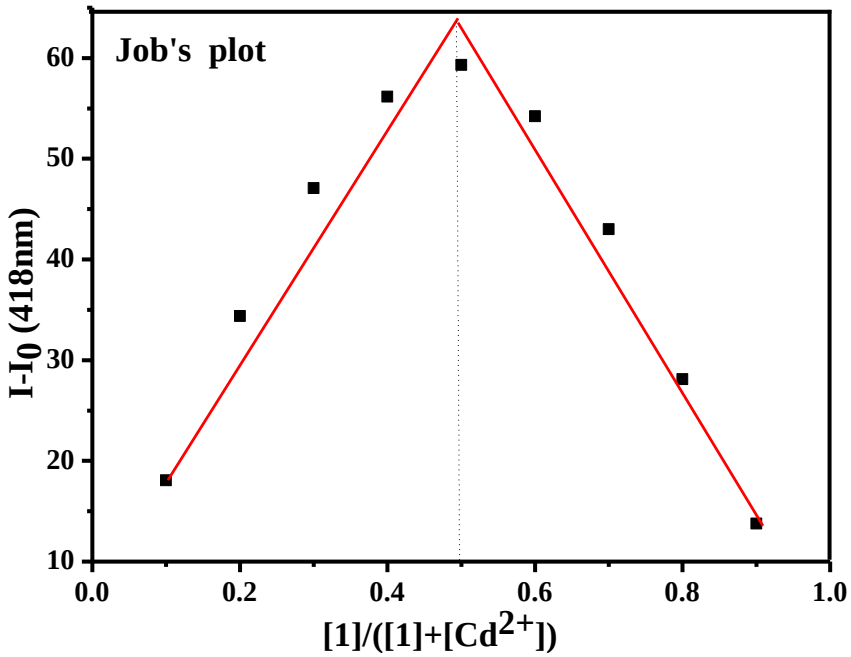

Figure 3.13. Job's plot showing the 1:1 binding of **L** to Cd^{2+} ion.

To further study the sensitivity of **L** toward Cd^{2+}, fluorescence titration experiments were carried out (Figure 3.12). Upon addition of Cd^{2+}, the fluorescence intensity of solution **L** increased gradually. A Job's plot binding between **L** and Cd^{2+} ion reveals a 1:1 stoichiometry (Figure 3.13), while the association constant (K_a value) for the complexation with Cd^{2+} ion by **L** was determined to be 4.06×10^4 M^{-1} as observed by the fluorescence titration experiments in CH_3CN.

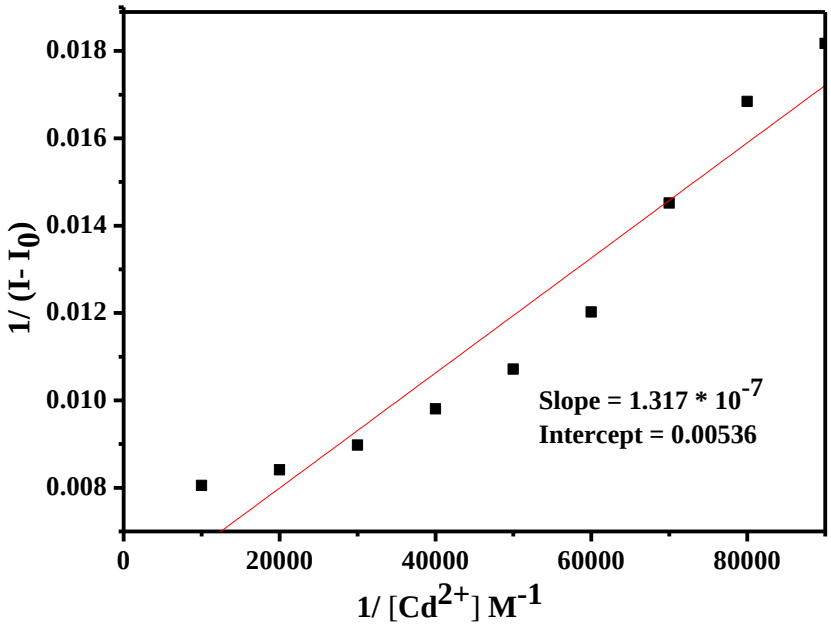

Figure 3.14 The binding constants of **L** with Cd^{2+} in different concentrations. The K_a of Cd^{2+} was calculated to be 4.06×10^4.

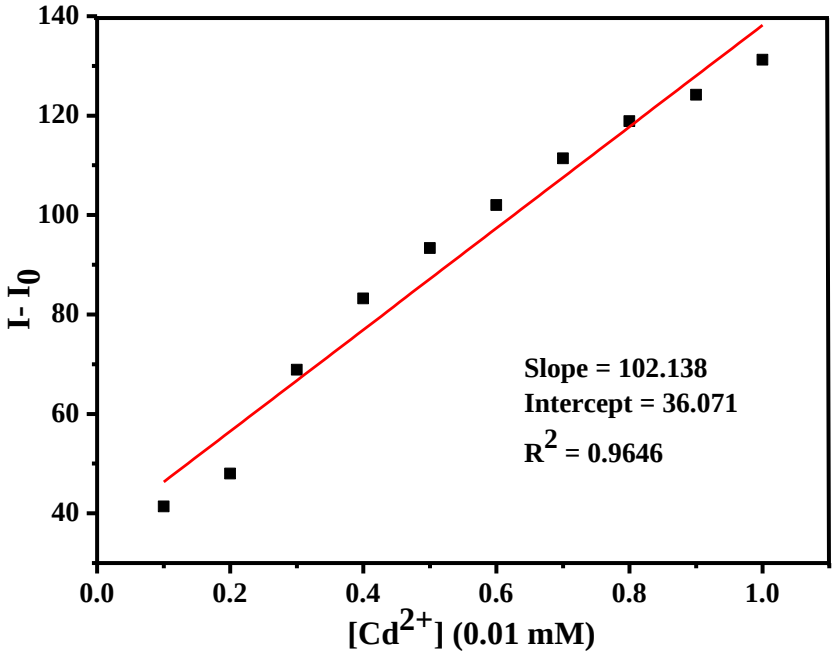

Figure 3.15 Linear concentration range of Cd^{2+} with **1**. The detection limit of Cd^{2+} was calculated to be 1.28×10^{-7} M by the formula (3σ/K).

Upon addition of Cu^{2+}, the fluorescence intensity of solution **L** quenching gradually (Figure 3.16). The saturation behavior of the fluorescence intensity after adding 2 equivalents of Cu^{2+} reveals that a 1:1 stoichiometry best describes the binding mode of Cu^{2+} and **L**, which is also supported by the Job's plot data (Figure 3.17). while the association constant of Cu^{2+}, calculated from the Benesi-Hildebrand equation,[16] was found to be $5.79 \times 10^5\ M^{-1}$.

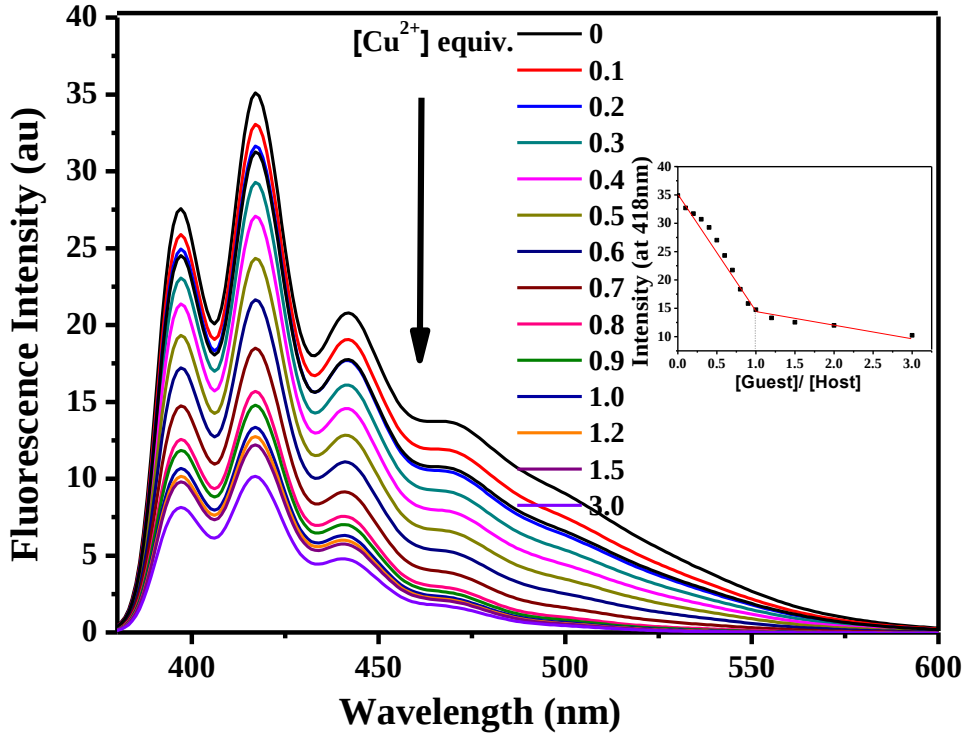

Figure 3.16 Changes in fluorescence emission spectra of **L** (0.01 mM) upon titration by Cu^{2+} (from 0- 0.03 mM) in CH_3CN (excitation at 365 nm).

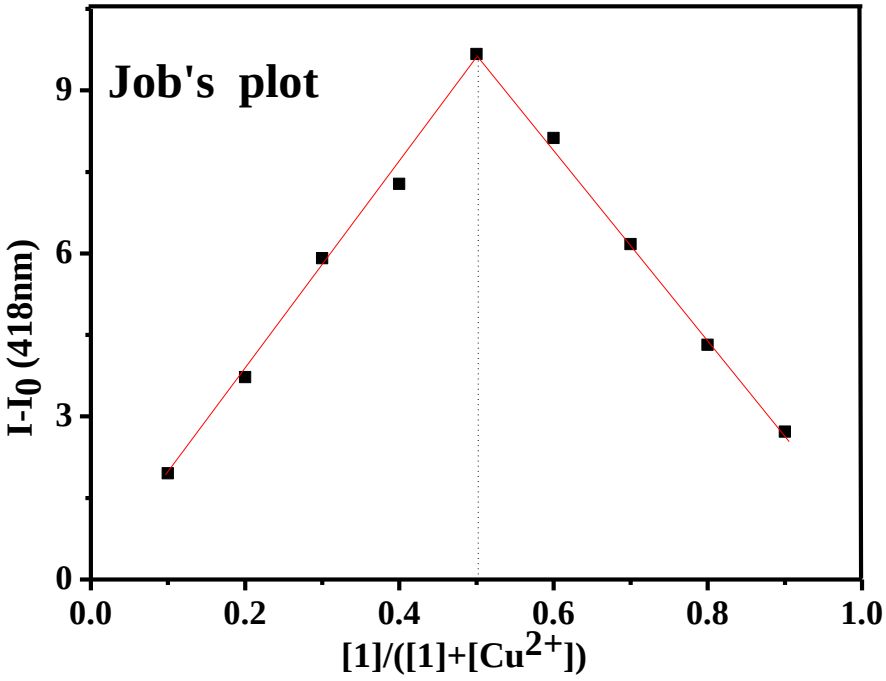

Figure 3.17. Job's plot showing the 1:1 binding of **L** to Cu^{2+} ion.

On the other hand, Upon addition of Cu^{2+} and Fe^{3+}, the fluorescence intensity of solution **L1** quenching gradually (Figure 3.18 and Figure 3.19). The saturation behavior of the fluorescence intensity after adding 2 equivalents of Cu^{2+} and Fe^{3+}

reveal that a 1:1 stoichiometry best describes the binding mode of Cu^{2+} and Fe^{3+} and **L1**, which is also supported by the Job's plot data.

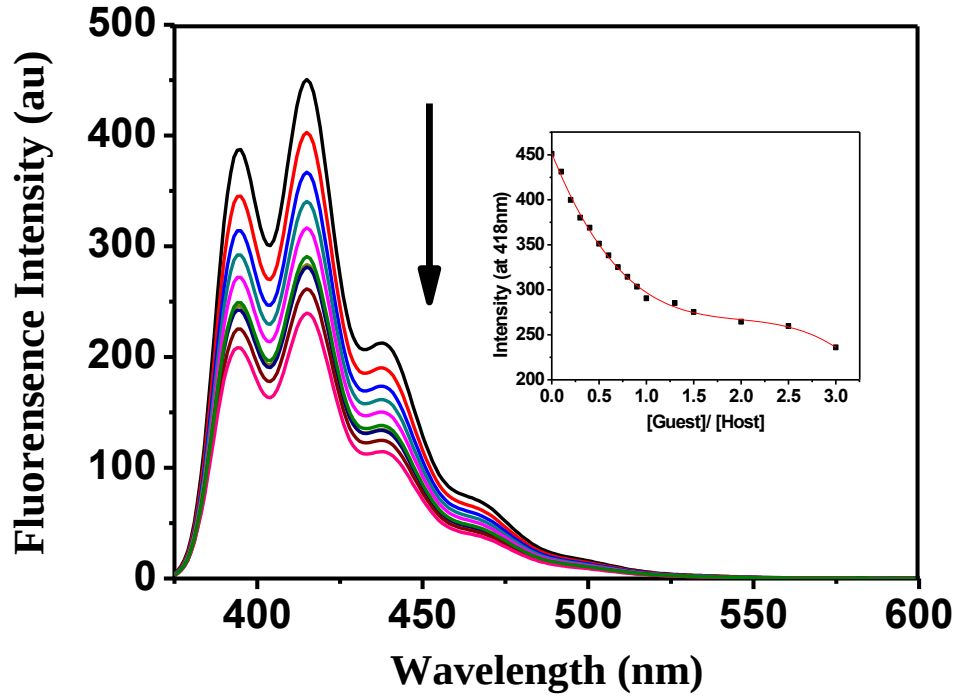

Figure 3.18 Changes in fluorescence emission spectra of **L1** (0.01 mM) upon titration by Cu^{2+} (from 0- 0.03 mM) in CH_3CN (excitation at 365 nm). Inset is molar ratio plot.

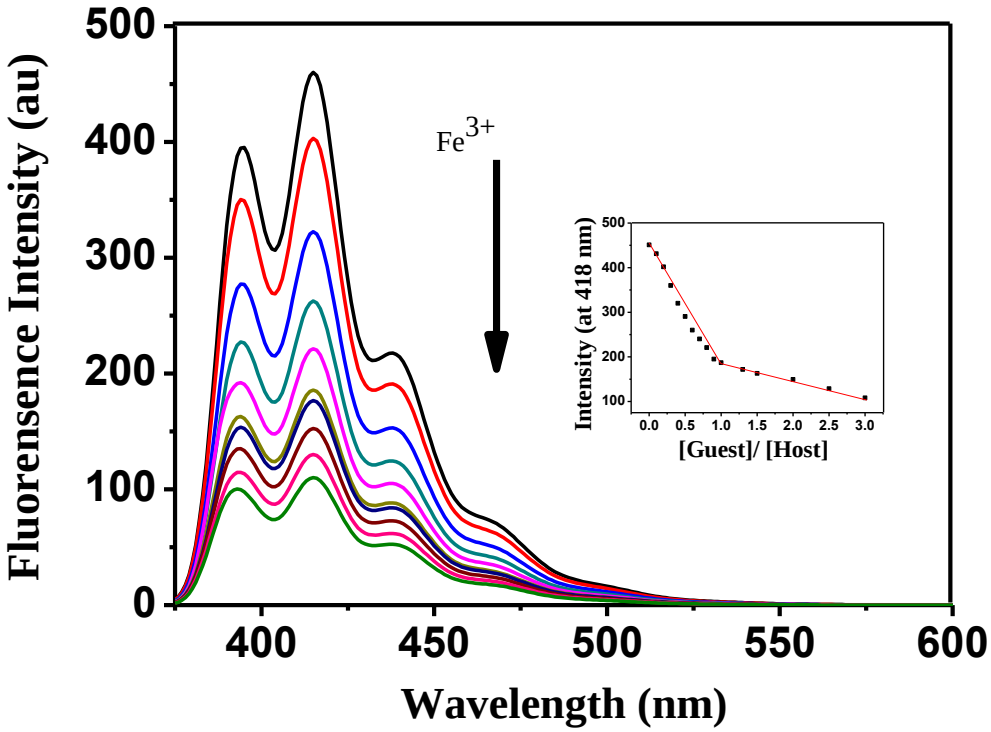

Figure 3.19. Changes in fluorescence emission spectra of **L1** (0.01 mM) upon titration by Fe^{3+} (from 0- 0.03 mM) in CH_3CN (excitation at 365 nm). Inset is molar ratio plot.

3.2.3 HPLC spectroscopy studies

The compound **L**, **L** •Cu^{2+} and **L** •Zn^{2+} mixtures were also analyzed by HPLC (Figure 3.20). A chromatographic peak of derivative **L** appeared at 8.40 min. After the addition of $Cu^{2+}$and Zn^{2+}, the intensity of the peak at 8.40 min decreased, accompanied by the emergence of a new peaks at 6.30 min and 14.50 min, respectively; these results demonstrate clearly the formation of new products (**L** •Cu^{2+} and **L** •Zn^{2} complexes).

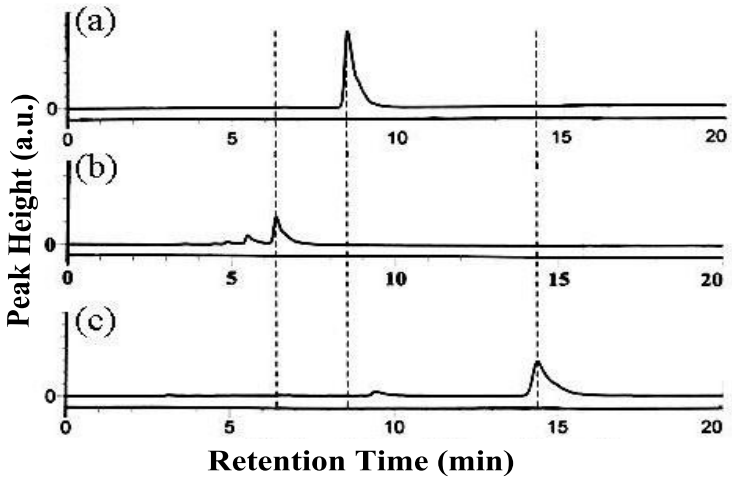

Figure 3.20. HPLC chromatograms of derivative **L** and complex (a) 0.3 mM of **L**; (b) 0.3 mM of **L** with 6 mM of Cu^{2+} is added; (c) 0.3 mM of **L** with 6 mM of Zn^{2+} is added.

3.2.4 ^{1}H NMR titration studies

To confirm the binding mechanism, ^{1}H NMR spectra of the **L** and **L** •Zn^{2+} complex were measured in a mixture of $CDCl_3$ /CD_3CN (10:1, v/v). As shown in Figure 3.21B, upon gradual addition of Zn^{2+} salt (0.5 equiv.) to a solution of **L**, the resonances corresponding to the protons of receptor **L** were split into two sets of signals. After addition of 1 equiv. Zn^{2+} in receptor **L** the original proton signals disappeared. This result suggests the presence of the complexed form between **L** ⊂ Zn^{2+} and the uncomplexed form of free **L**. The signal for proton H_a on the triazole ring undergoes a downfield shift from δ 7.16 ppm to 7.70 ppm ($\Delta\delta_H$ = 0.64 ppm), and the O*CH*$_2$-triazole linked proton of H_d is shifted from δ 4.06 ppm to 5.13 ppm (Figure 3.21B). These spectral changes suggested that the Zn^{2+} ion is selectively bound by the nitrogen atoms on the triazole rings. Moreover, the signal for the proton on the anthracene moiety revealed a down-field shift, which indicated that the anthracene moieties appended on **L** were alienated by Zn^{2+} to prohibit the formation of π–π stacking between the anthracene moiety. On the other hand, it is noted that the proton

H_b on the phenyl of hexahomotrioxacalix[3]arene also experienced a downfield shift from δ 6.60 to 6.81 ppm, and the $\Delta\delta_H$ value for H_{ax} and H_{eq} of the ArCH_2O methylene protons changed to 0.58 ppm (Figure 3.21B), respectively. The large $\Delta\delta_H$ value for H_{ax} and H_{eq} indicated that the phenol groups in the complex are positioned in a more-upright form, the calix cavity changed from a "flattened-cone" to a more-upright form that is similar to the previously reported examples.[17,18]

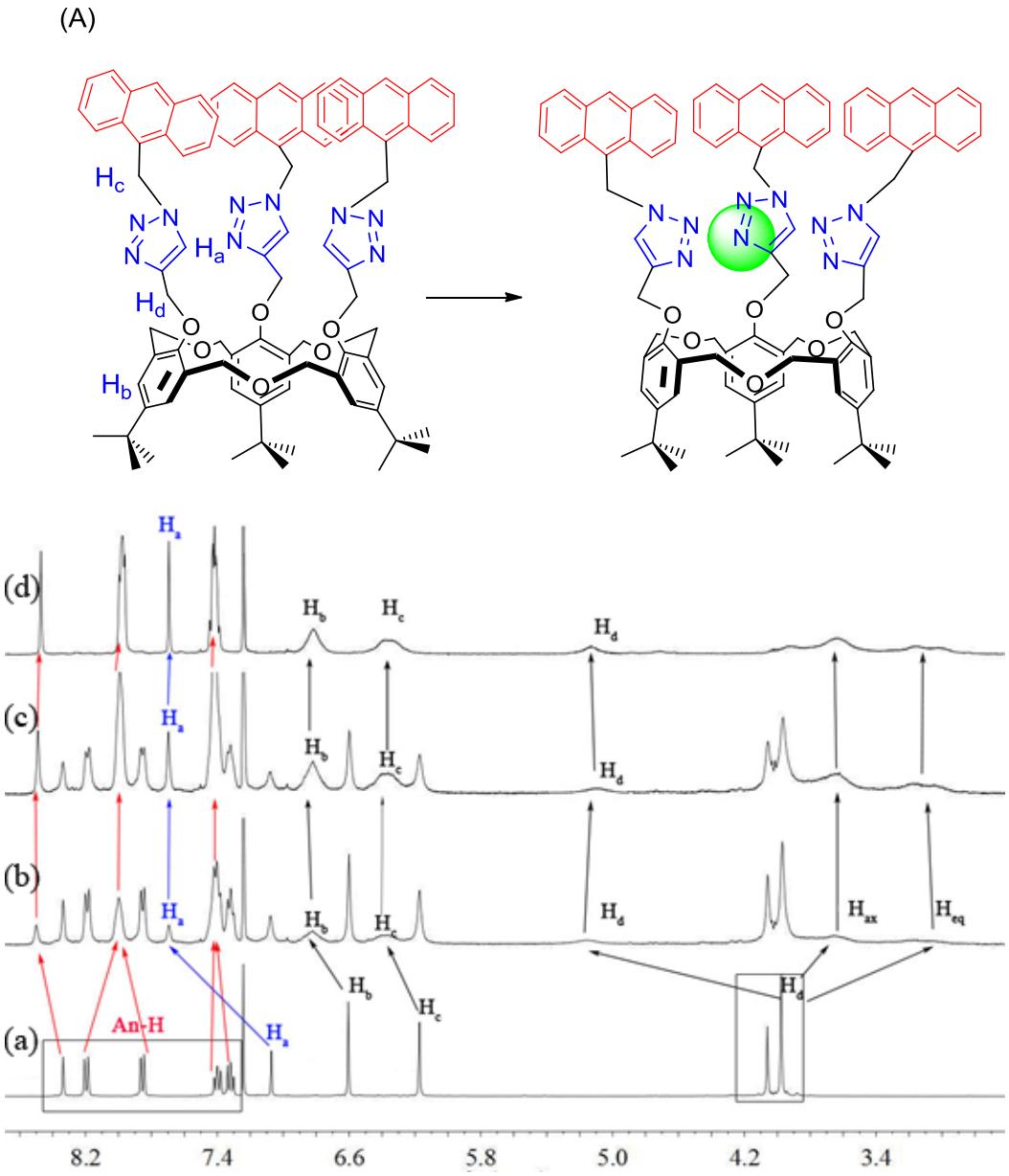

Figure 3.21. (A) Binding mode of **L** upon complexation with Zn^{2+} ion as perchlorate salt. (B) Partial ^1H NMR spectra of **L** (4.0 mM) in $CDCl_3$: CD_3CN (10:1, v/v) upon addition of Zn^{2+} ion at 298 K. (a) Free **L**, (b) **L** $\subset$ Zn^{2+} (0.5 equiv.), and (c) **L** $\subset$ Zn^{2+} (1.0 equiv.).

The concept of Zn^{2+} complexation by the host chemosensor **L** is shown in Figure 3.21A. From this above discussion, the binding mode of **L**•Zn^{2+} explore that the phenol groups in the complex are situated as an upright form and also the anthracene moieties are far apart from each other to reduce the π–π stacking in presence of Zn^{2+} which results the fluorescence enhancement.

On the other hand, the peaks of H_a, H_b, H_c and H_d completely disappeared and the signals of the anthracene ring protons and benzyl protons were blurred, which attributed to both the conformation changes and the paramagnetic effect of the Cu^{2+}. Once the Cu^{2+} was captured by the nitrogen, the protons adjacent to Cu^{2+} were strongly affected by the Cu^{2+} due to inherent paramagnetism of Cu^{2+}. Thus, the complexation between the heavy metal ions and sensor **L** led to the quenching of the fluorescence emission through the heavy metal ion effect, and/or the reversed PET that is similar to the previously reported examples.[19]

3.3. Conclusions

In summary, we have synthesized a new type of selective and sensitive fluorescent sensor having triazole rings as the binding sites at the lower rim of a hexahomotrioxacalix[3]arene scaffold in a *cone* conformation. The selective binding behaviour of chemosensor **L** has been evaluated by fluorescence spectra and ^{1}H NMR spectroscopic analysis. This sensor has desirable properties for practical applications, including selectivity for detecting Zn^{2+} and Cd^{2+} in the presence of excess competing metal ions at low ion concentration or as a fluorescence enhancement type chemosensor due to the cavity of calixarene changed from a "flattened-cone" to a more-upright form and inhibition of photoinduced electron transfer (PET). In contrast, the results suggested that receptor **L** is highly sensitive and selective for Cu^{2+} and Fe^{3+} as a fluorescence quenching type chemosensor due to the photoinduced electron transfer (PET) or heavy atom effect.

Further studies on the synthesis of tritopic receptors based on the hexahomotrioxacalix[3]arene are also underway in our laboratory.

3.4. Experimental section

3.4.1. General

All melting points (Yanagimoto MP-S1) are uncorrected. ^{1}H NMR and ^{13}C NMR spectra were recorded on a Nippon Denshi JEOL FT-300 NMR spectrometer and Varian-400MR-vnmrs400 with $SiMe_4$ as AQ2OM spectrophotometer. Mass spectra were obtained with a Nippon Denshi JMS-HX110A Ultrahigh Performance mass spectrometer at 75 eV by using a direct-inlet system. UV-vis spectra were recorded

using a Shimadzu UV-3150 UV-vis-NIR spectrophotometer. Elemental analyses were performed by a Yanaco MT-5. Fluorescence quantum yields were recorded in solution (Hamamatsu Photonics K. K. Quantaurus-QY A10094) using the integrated sphere absolute PL quantum yield measurement method.

3.4.2. Materials

Compounds **6** and **7** were synthesized according to our previous report.[15]

*3.4.2.1. Synthesis of receptor **L**.* Copper iodide (20 mg) was added to a solution of compound **6** (200 mg, 0.28 mmol) and 9-azidomethylanthracene (210 mg, 0.90 mmol) in 20 mL THF/H_2O (4:1) and the mixture was heated at 65 ℃ for 24 h. The resulting solution was cooled and diluted with water and extracted thrice with CH_2Cl_2. The organic layer was separated and dried ($MgSO_4$) and evaporated to give the solid crude product. The residue was eluted from a column chromatography of silica gel with hexane/ethyl acetate (v/v = 4:1) to give the desired product *cone*- **L** (290 mg, 75 %) as colorless prisms. Mp 154–156 ℃. ^{1}H NMR (400 MHz, $CDCl_3$): δ 0.94 (27H, s, C(*CH*$_3$)$_3$), 4.03 (12H, d, O*CH*$_2$O, *J* = 4.0 Hz), 4.10 (6H, s, –O*CH*$_2$), 6.29 (6H, s, An–*CH*$_2$), 6.68 (6H, s, Ar–*H*), 7.08 (3H, s, triazole–*H*), 7.39−7.43 (6H, m, An–*H*), 7.47−7.51 (6H, m, An–*H*), 7.94 (6H, d, *J* = 8.4 Hz, An–*H*), 8.28 (6H, d, *J* = 8.4 Hz, An–*H*) and 8.42 (3H, s, An–*H*) ppm. ^{13}C NMR (75 MHz, $CDCl_3$): δ 31.32, 34.12, 45.51, 66.94, 68.87, 122.71, 123.29, 124.42, 125.45, 125.77, 127.64, 129.42, 129.74, 130.77, 130.86, 131.43, 144.27, 146.23 and 151.78 ppm. IR: ν_{max} (KBr)/cm^{-1}: 3310, 2960, 1575, 1436, 1367, 1268, 1090 and 1002. FABMS: *m/z*: 1389.58 (M^+). Anal. Calcd for $C_{90}H_{87}O_6N_9$ (1389.12): C, 77.73; H, 6.31. Found: C, 77.90; H, 6.37.

*3.4.2.2. Synthesis of receptor **L1**.* Copper iodide (20 mg) was added to a solution of compound **7** (100 mg, 0.47 mmol) and 9-azidomethylanthracene (340 mg, 1.45 mmol) in 20 mL THF/H_2O (4:1) and the mixture was heated at 65 ℃ for 24 h. The resulting solution was cooled and diluted with water and extracted thrice with CH_2Cl_2. The organic layer was separated and dried ($MgSO_4$) and evaporated to give the solid crude product. The residue was eluted from a column chromatography of silica gel with hexane/ethyl acetate (v/v = 4:1) to give the desired product **L1** (170 mg, 81 %) as colorless prisms. Mp 194–196 ºC. ^{1}H NMR (300 MHz, $CDCl_3$) δ 1.22 (s, 9H, C(*CH*$_3$)$_3$), 2.10 (s, 6H, Ar–*CH*$_3$), 4.78 (s, 2H, –O*CH*$_2$), 6.57 (s, 2H, An–*CH*$_2$), 6.89 (s, 2H, Ar–*H*), 7.19 (s, 1H, trizole–*H*), 7.52−7.64 (m, 4H, An–*H*), 8.09 (d, 2H, *J* = 6.0 Hz, An–*H*), 8.33 (d, 2H, *J* = 6.0 Hz, An–*H*), 8.60 (s, 1H, An–*H*). ^{13}C NMR ($CDCl_3$, 75 MHz, $CDCl_3$): δ 31.6, 34.2, 37.4, 46.7, 49.85, 62.2, 114.3, 122.5, 123.1,123.8, 125.6, 126.3, 127.9, 129.7, 130.1, 130.9, 131.6, 144.0, 144.5, 156.0. IR: ν_{max} (KBr)/cm^{-1}:

3019, 1966. FABMS: *m/z*: 449.78 (M^+). Anal. Calcd for $C_{30}H_{31}ON_3$ (449.25): C, 80.14; H, 6.95. Found: C, 80.38; H, 7.03.

3.5 References and notes

1. (a) M. J. Jakubowski, K. J. Beltis, P. M. Drennana, B. A. Pindzola, *Analyst*, **2013**, *138*, 6398–6403; (b) J. P. Desvergne and A. W. Czarnik, *Chemosensors of Ion and Molecular Recognition*; Kluwer: Dordrecht, The Netherlands, 1997.
2. (a) C. Bargossi, M. C. Fiorini, M. Montalti, L. Prodi and N. Zaccheroni, *Coord. Chem. Rev.*, **2000**, *208*, 17–32; (b) B. Valeur and I. Leray, *Coord. Chem. Rev.*, **2000**, *205*, 3–40; (c) S. Q Cui, S. Z. Pu and Y. F. Dai, *Anal. Methods*, **2015**, *7*, 3593–3599.
3. R. C. Ropp, N. J. Warren, *Luminescence and the Solid State*, Elsevier, Amsterdam, 1991.
4. (a) R. S. Sundaram, M. Engel, A. Lombardo, R. Krupke, A. C. Ferrari, P. Avouris and M. Steiner, *Nano Lett.*, **2013**, *13*, 1416–1421; (b) M. Kato, A. Omura, A. Toshikawa, S. Kishi, Y. Sugumoto, *Angew. Chem.*, **2002**, *114*, 3315–3317; (c) X. H. Ouyang, X. L Li, Y. Q. Bai, D. B. Mi, Z. Y. Ge, S. J Su, *RSC Adv.*, **2015**, *5*, 32298–32306. (d) J. Seo, S. Kim, S. Y. Park, *J. Am. Chem. Soc.*, **2004**, *126*, 11154–11155.
5. (a) C. D. Gutsche, Calixarenes, *An Introduction, Royal Society of Chemistry*, Cambridge, U.K., 2008; (b) A. Ikeda, S. Shinkai, *Chem. Rev.*, **1997**, *97*, 1713–1734; (c) J. S. Kim, D. T. Quang, *Chem. Rev.*, **2007**, *107*, 3780–3799; (d) D. Coquière, S. Le Gac, U. Darbost, O. Sénèque, I. Jabin, O. Reinaud, *Org. Biomol. Chem.*, **2009**, *7*, 2485–2500; (e) K. Cottet, P. M. Marcos, P. J. Cragg, *Beilstein J. Org. Chem.*, **2012**, *8*, 201–226.
6. (a) C. C. Jin, H. Cong, X. L. Ni, X. Zeng, C. Redshaw, T. Yamato, *RSC Adv.*, **2014**, *4*, 31469–31475; (b) H. Matsumoto, S. Nishio, M. Takeshita, S. Shinkai, *Tetrahedron*, **1995**, *51*, 4647–4654. (c) X. L. Ni, C. C. Jin, X. K. Jiang, M. Takimoto, S. Rahman, X. Zeng, D. L. Hughes, C. Redshaw, T. Yamato, *Org. Biomol. Chem.*, **2013**, *11*, 5435–5442.
7. (a) T. Yamato, M. Haraguchi, J. Nishikawa, S. Ide, H. Tsuzuki, *Can. J. Chem.*, **1998**, *76*, 989–996; (b) X. L. Ni, H. Cong, A. Yoshizawa, S. Rahman, H. Tomiyasu, U. Rayhan, X. Zeng, T. Yamato, *J. Mol. Struct.*, **2013**, *1046*, 110–115; (c) R. K. Pathak, A. G. Dikundwar, T. N. G. Row, C. P. Rao. *Chem. Commun.*, **2010**, *46*, 4345–4347; (d) K. Tsubaki, T, Morimoto, T. Otsubo, K. Fuji, *Org. Lett.*, **2002**, **4**, 2301–2304.

8. (a) G. Gattuso, A. Notti, M. F. Parisi, I. Pisagatti, M. E. Amato, A. Pappalardo, S. Pappalardo, *Chem. Eur. J.*, **2010**, *16*, 2381–2385; (b) A Ikeda, H. Udzu, Z. Zhong, S. Shinkai, S. Sakamoto, K. Yamaguchi, *J. Am. Chem. Soc.*, **2001**, *123*, 3872–3877; (c) N. L. Strutt, R. S. Forgan, J. M. Spruell, Y. Y. Botros, J. F. Stoddart, *J. Am. Chem. Soc.*, **2011**, *133*, 5668–5671.
9. (a) X. L. Ni, S. Rahman, X. Zeng, D. L. Hughes, C. Redshaw, T. Yamato, *Org. Biomol. Chem.*, **2011**, *9*, 6535–6541; (b) J. L. Atwood, L. J. Barbour, P. J. Nichols, C. L. Raston, C. A. Sandoval, *Chem. Eur. J.*, **1999**, *5*, 990–996; (c) A. Ikeda, T. Hatano, S. Shinkai, T. Akiyama, S. Yamada, *J. Am. Chem. Soc.*, **2001**, *123*, 4855–4856.
10. (a) D. Wang, C. C Ge, L. Wang, X. R. Xing, L. W. Zeng, *RSC Adv.*, **2015**, *5*, 75722–75727; (b) C. Plenk, J. Krause, M. Beck, E. Rentschler, *Chem. Commun.*, **2015**, *51*, 6524–6527; (c) X. L. Ni, X. Zeng, C. Redshaw, T. Yamato, *J. Org. Chem.*, **2011**, *76*, 5696–5702; (d) J. L. Zhao, H. Tomiyasu, C. Wu, H. Cong, X. Zeng, S. Rahman, P. E. Georghiou, D. L. Hughes, C. Redshawe, T. Yamato, *Tetrahedron*, **2015**, *71*, 8521–8527; (e) C. Wu, Y Ikejiri, J. L. Zhao, X. K. Jiang, X. L. Ni, X. Zeng, C. Redshaw, T. Yamato, *Sensors and Actuators B*, **2016**, *228*, 480–485; (f) K. C. Chang, I. H. Su, A. Senthilvelan , W. S. Chung, *Org. Lett.*, **2007**, *9*, 3363–3366; (g) Y. H. Lau, P. J. Rutledge, M. Watkinson, M. H. Todd, *Chem. Soc. Rev.*, **2011**, *40*, 2848–2866.
11. H. R. Eui, Y. Zhao, *Org. Lett.*, **2005**, *7*, 1035–1037.
12. (a) A. Dondoni, A. Marra, *J. Org. Chem.*, **2006**, *71*, 7546–7557; (b) A. Dondoni, A. Marra, *Tetrahedron*, **2007**, *63*, 6339–6345; (c) L. Moni, G. Pourceau, J. Zhang, A. Mayer, S. Vidal, E. Souteyrand, A. Dondoni, F. Morvan, Y. Cherolot, J. J. Vasseur, A. Marra, *ChemBioChem.*, **2009**, *10*, 369–1378.
13. A. Marra, L. Moni, D. Pazi, A. Corallini, D. Bridi, A. Dondoni, *Org. Biomol. Chem.*, **2008**, *6*, 1396–1409.
14. (a) S. P. Bew, R. A. Brimage, N. L. Hermite, S. V. Sharma, *Org. Lett.*, **2007**, *9*, 3713–3716; (b) Y. H. Kim, S. H. Kim, D. Ferracane, J. A. Katzenellenbogen, C. M. Schroeder, *Bioconjugate Chem.*, **2012**, *23*, 1891–1901.
15. C. C. Jin, T. Kinoshita, H. Cong, X. L Ni, X. Zeng, D. L. Hughes, C. Redshaw, T. Yamato, *New J. Chem.*, **2012**, *36*, 2580–2586.
16. (a) H. A. Benesi, J. H. Hildebrand, *J. Am. Chem. Soc.*, **1949**, *71*, 2703–2707. (b) K. A. Connors, Binding Constants; Wiley: New York, 1987.

17. (a) M. Takeshita, F. Inokuchi, S. Shinkai, *Tetrahedron Lett.*, **1995**, *36*, 3341–3344; (b) A. Ikeda, H. Udzu, Z. Zhong, S. Shinkai, S. Sakamoto, K. Yamaguchi, *J. Am. Chem. Soc.*, **2001**, *123*, 872–3877.
18. X. L. Ni, J. Tahara, S. Rahman, X. Zeng, D. L. Hughes, C. Redshaw, T. Yamato, *Chem. Asian J.*, **2012**, *7*, 519–527.
19. (a) S. Adhikari, S. Mandal, A. Ghosh, S. Guria, D. Das, *Sensors and Actuators B: Chemical*, **2016**, *234*, 222-230. (b) J. Y. Zhao, Y. Zhao, S. Xu, N. Luo, R. Tang, *Inorganica Chimica Acta*, **2015**, *438*, 105-111; (c) E. Şenkuytu, E. T. E ğk, M. Durmuş, G. Y. Çift ğ, *Polyhedron*, **2015**, *101*, 223–229.

Chapter 4

Ratiometric fluorescent receptor for both Zn^{2+} and ammonium ions: based on a anthryl-linked triazole-modified homooxacalix[3]arene

This chapter focused on the structure and complexation behavior of chemosensor L. which displayed ratiometric selectivity for linear-chain ammonium ions and Zn^{2+} ions in neutral solution. It possesses a high affinity and selectivity for linear-chain ammonium ions and Zn^{2+} ions by enhancement of fluorescence intensity in organic solution, and L can distinguish between linear-chain and branched-chain ammonium guest ions. Interestingly, upon addition of Zn^{2+} to this system, chemosensor L can be capable of binding a metal ions and alkylammonium cations simultaneously through positive allosteric effect. The successful performance of these probes suggested chemosensing ensemble method had great advantage and should play more roles in sensor design.

4.1 Introduction

Alkylammonium and ammonium ions play an important role in nature. Ammonium ions has appreciable effect on the health of consumers, and its presence in water is an indicator of pollution. In recent years, ammonium ions concentration, in certain surface water is much higher than the permissible standard, as a large extent of industrial and municipal wastewater has been discharged into nearby aquatic sources[1]. Therefore, ammonium ion sensor is a useful tool in environmental pollution control, [2] food and clinical analyses [3] and other industry applications. [4]

On the other hand, calixarenes have attracted tremendous attention for several decades and calixarene chemistry has become an indispensable part of supramolecular science.[5] they can provide useful building blocks for host-guest type receptors through appropriate modification. For example, calix[4]arene derivatives incorporating crown ethers, amides, esters, and carboxylic acid groups have been shown to selectively extract metal ions.[6] The hexahomotrioxacalix[3]arene which are structurally related to the calixarenes and the crown ethers, have a three dimensionalcavity with a potentially C_3-symmetric structure, and are intriguing ligands for metal cations,[7] ammonium cations,[8] and fullerene derivatives.[9]

Cations recognition by artificial receptors has attracted increasing attention because of the important roles played by ions in both environment and biological systems.[10] all the known modes of cation binding by native and functionalized calixarenes exploiting cation-π, induced dipole, or electrostatic interactions.[11] the most important calixarene-based cation receptors are obtained by the introduction of chelating units at the lower rather than at the upper rim. For example, Calixarenes fully functionalized at the lower rim with ether groups show a affinity for alkali metal ions,[12] Shinkai et al. reported a series of calix[4]arene-crown-4 derivatives among which the partial cone derivative exhibits an exceptional Na^+/K^+ selectivity, as determined by ion-selective electrodes (ISEs). we also have developed a series of triazole-derived chemosensors for selective binding of heavy metal ions based on calixarene scaffolds.[13] For example, chemosensors derived from hexahomotrioxacalix[3]arene exhibited a highly selective affinity for the Pb^{2+} cation through enhancement of the monomer emission of pyrene in both organic and organic-aqueous solution.

On the other hand, Hexahomotrioxacalix[3]arene derivatives with C_3 symmetry can selectively bind ammonium ions, which play an important role in both chemistry and biology. The formation of intracavity endo-complexes of the resulting ammonium ions was observed, tripodal $NH^+ \cdots O$ interactions with the phenolic oxygen atoms and CH-π interactions were supposed to stabilize the complex.[14] Recently, our group reported the construction of C_3 symmetrically functionalized

hexahomotrioxacalix[3]arenes, which selectively recognized primary ammonium ions.[15]

Additionally, click chemistry has attracted considerable attention recently and has been applied in a wide range of fields for its efficiency, region selectivity, and compatibility with reaction conditions.[16,17] For example, Rao groups designed and synthesized a lower rim triazole-linked Schiff base calixarene as the primary fluorescence switch-on chemosensor for Zn^{2+} ions.[18] Therefore, we hypothesized that suitably arranged functionalized ligand moieties containing nitrogen atoms attached to homooxacalix[3]arene should be a good receptor candidate for metal cations or ammonium cations. Therefore, with this in mind, we have synthesized compound **L** and studied their cation-binding affinity.

4.2 Result and discussion

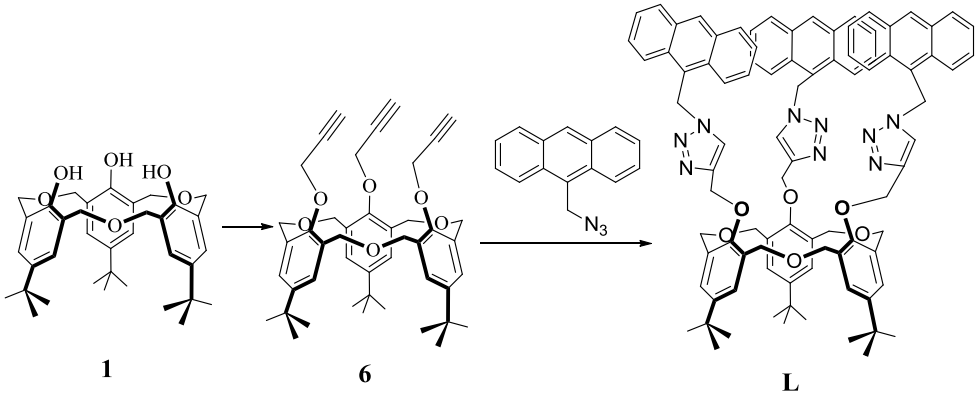

Scheme 4.1

The synthesis of **L** was carried out as shown in Scheme 4.1 which was discussed in chapter 3. fluorescent compound **L** can be obtained from the reaction of **6** with 9-azidomethylanthracene under standard conditions for Click chemistry. The coupling of **3** with 9-azidomethyl-anthracene afforded *cone* conformation compound **L** in 75 % yield. ^{1}H NMR spectrum of **L** shows a singlet for the *tert*-butyl protons at δ 0.94 ppm, and a doublet at δ 4.03 ppm for the bridge protons, and ^{13}C NMR spectrum of **L** exhibits two peaks for the methyl and the quaternary carbon atoms of the *t*-Bu groups at δ 31.32, 34.04 ppm, three peaks for methylene carbon at 45.51, 66.94, 68.87 ppm and 14 peaks for aromatic carbon. respectively, indicating a C_3–symmetric structure for sensor **L**. And the anthracene moieties appended on **L** were sterically-fixed to be in close proximity to allow the formation of π–π stacking between the anthracene moieties.

4.2.1 Fluorescent Receptor for Ammonium Ions

Dilution experiments at different concentrations of **L** were prepared as follows. Test

solutions were prepared by taking 70 mL of the calixarene stock solution in a 10 mL volumetric flask, adding 0, 0.2, 0.4, 0.6, 0.8 and 1.0 mL of stock solution, and making up to the volume with CH_3CN. On the basis of these observations, the fluorescent behaviors of **L** toward ions were studied in an organic solution CH_3CN.

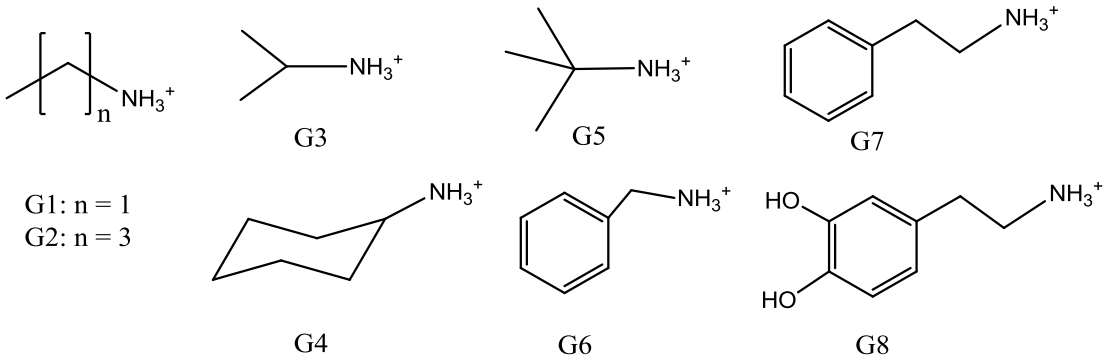

Scheme 4.2

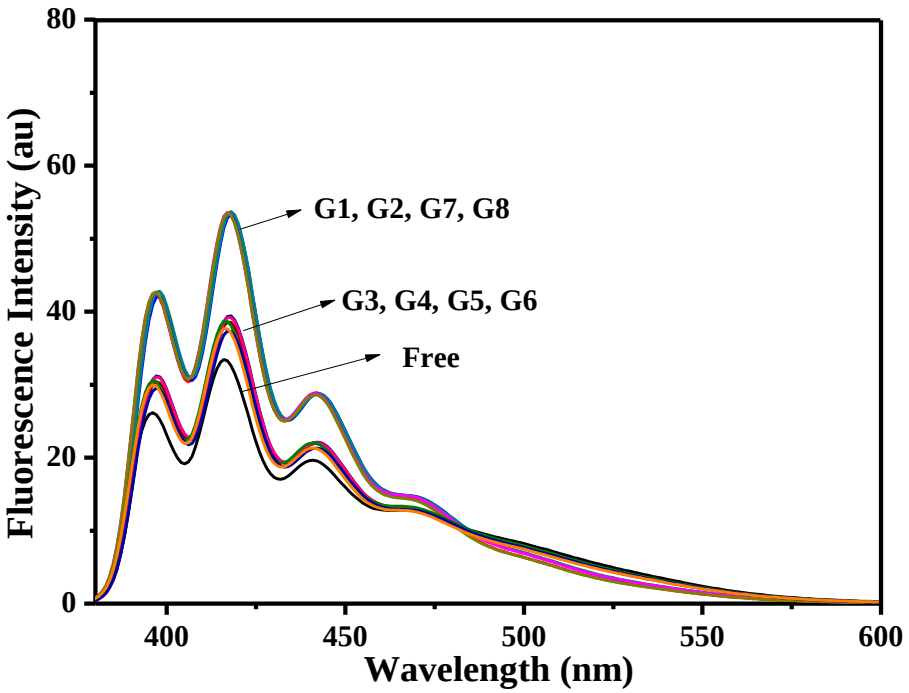

Figure 4.1. Fluorescence intensity changes of receptors **L** (0.1 mM) in CH_3CN at 298 K upon addition of various ammonium guest ions **G1-G8** (10 equiv.)

A preliminary screening of the binding affinity of **L** for the picrate salts of ammonium guest ions (G1 – G8, Scheme 4.2) using the fluorescence. Figure 4.1 shows the fluorescence intensity changes of the emission for receptors **L** in the presence of various ammonium guest ions. There was minor variation in the fluorescence intensity of branched-chain ammonium guest ions after adding 10-fold

relative to receptors **L**, and the relative standard deviation was less than 5%. Interestingly, when adding linear-chain ammonium guest ions to the solution of receptors **L**, it led to a fluorescence enhancement under the same conditions. The significantly different spectral change in the receptors **L** solution upon addition of either linear-chain and branched-chain ammonium guest ions indicates that receptors **L** is a sensitive functional chemosensor for ammonium guest ions, and **L** can distinguish between linear-chain and branched-chain ammonium guest ions.

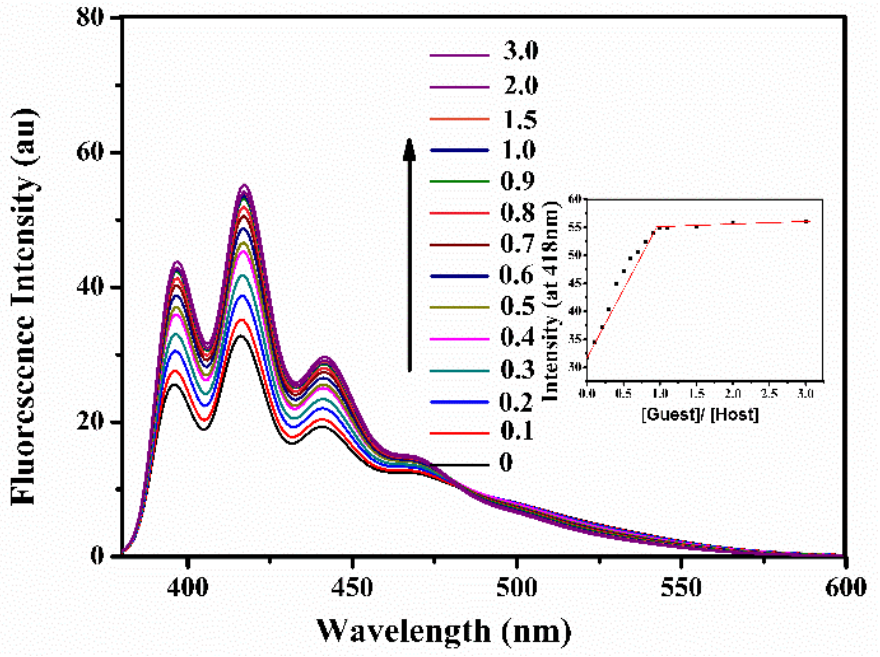

Figure 4.2. Fluorescence spectra of receptor **L** (0.01 mM) upon addition of increasing concentrations of n-$BuNH_3^+$in CH_3CN. λ_{ex} = 365 nm

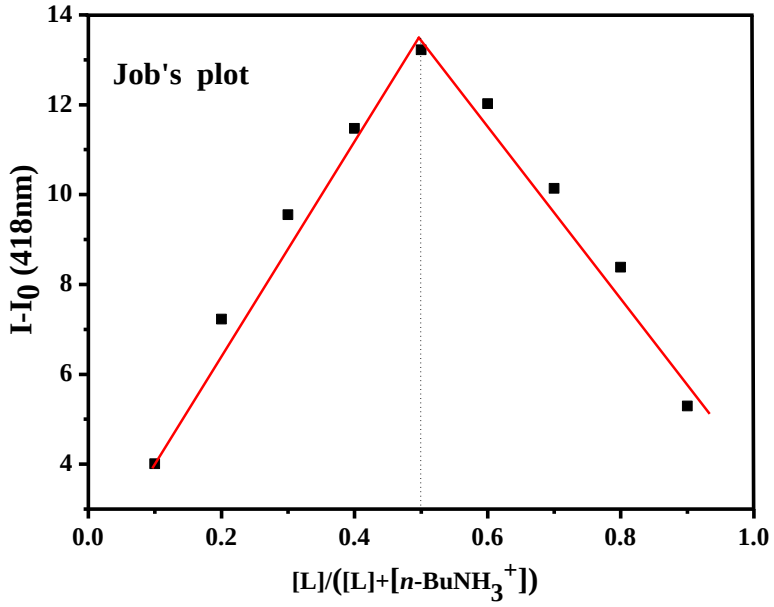

Figure 4.3. Job's plot showing the 1:1 binding of **L** to *n*-$BuNH_3^+$ ion.

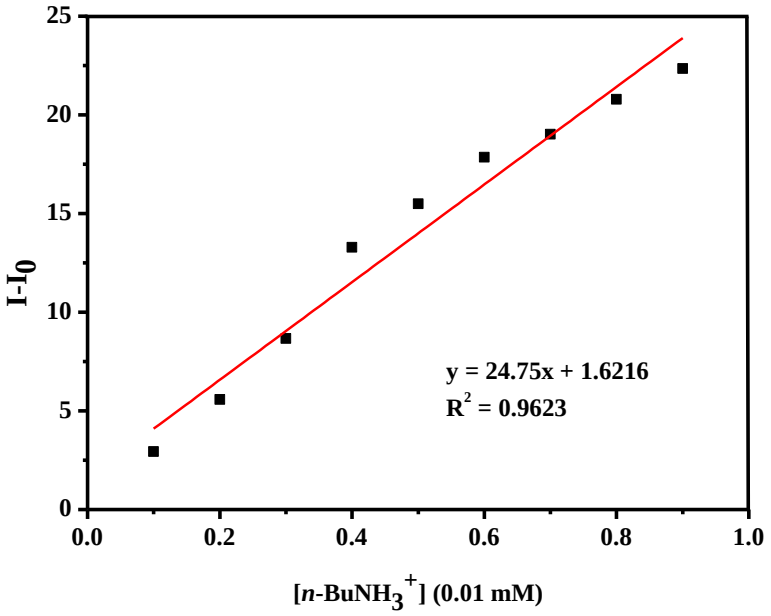

Figure 4.4. Linear concentration range of *n*-$BuNH_3^+$ with **L**. The detection limit of *n*-$BuNH_3^+$ was calculated to be 2.90 × 10^{-7} M by the formula (3σ/K).

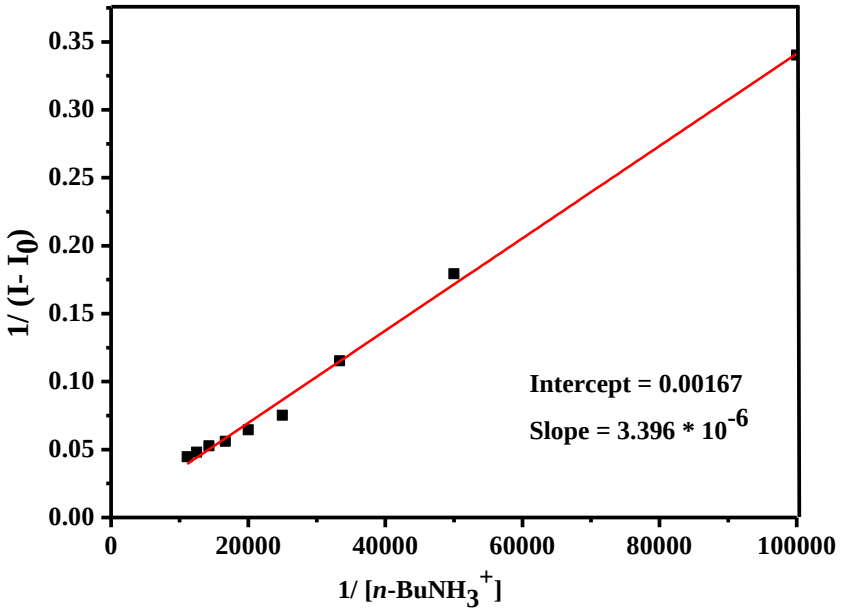

Figure 4.5. The binding constants of **L** with *n*-$BuNH_3^+$ in different concentrations. The K_a of *n*-$BuNH_3^+$ was calculated to be 4.91 × 10^3.

Figure 4.2 shows the fluorescence spectra of receptor **L** by the addition of increasing concentrations of *n*-$BuNH_3^+$. Upon addition of *n*-$BuNH_3^+$, the fluorescence intensity of the receptor **L** solution increased gradually. The saturation behavior of the

fluorescence intensity after adding 2 equivalents of *n*-$BuNH_3^+$ reveals that a 1:1 stoichiometry is best for the binding mode of *n*-$BuNH_3^+$ and L, which is also supported by the Job's plot data (Figure 4.3). According to the 1:1 model, the stability constant (K_a) of **L** with *n*-$BuNH_3^+$ was calculated to be 4.91 $\times 10^3$ M^{-1} (error < 10%), the low detection limit of 2.90 $\times 10^{-7}$ M and the quantum yield of **L** is Φ = 0.15. And the same phenomenon has been found in the case of $EtNH_3^+$ (Figure 4.6).

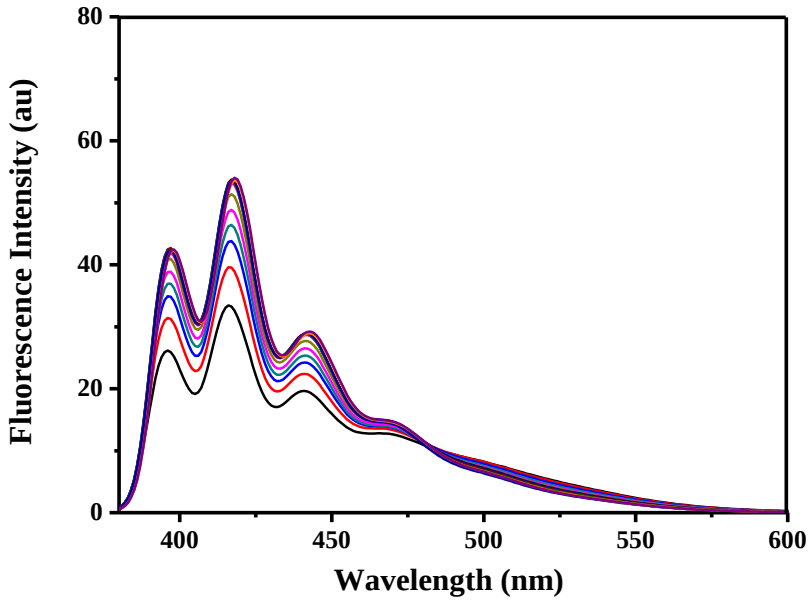

Figure 4.6. Fluorescence spectra of receptor **L** (0.01 mM) upon addition of increasing concentrations of $EtNH_3^+$in CH_3CN. λ_{ex} = 365 nm

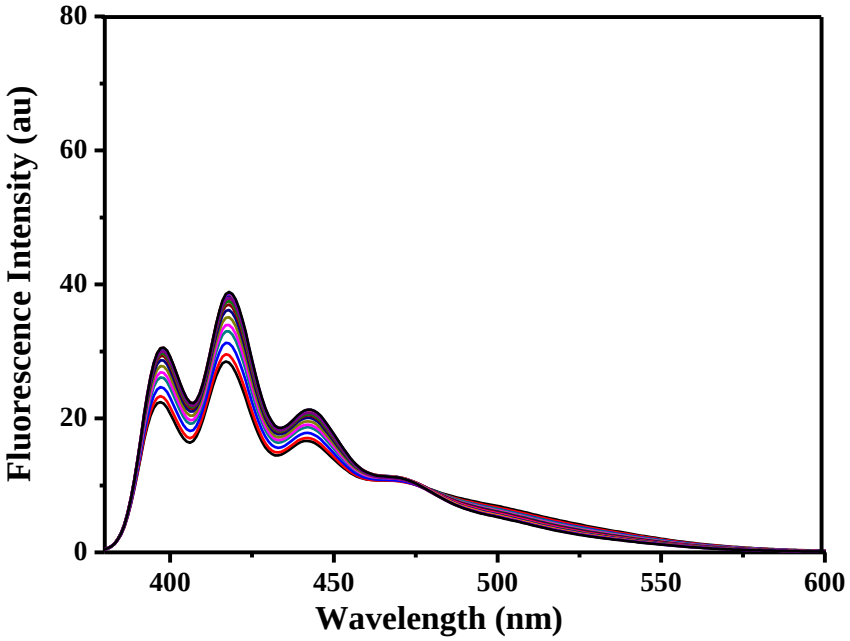

Figure 4.7. Fluorescence spectra of receptor **L** (0.01 mM) upon addition of increasing concentrations of t-$BuNH_3^+$ in CH_3CN. λ_{ex} = 365 nm

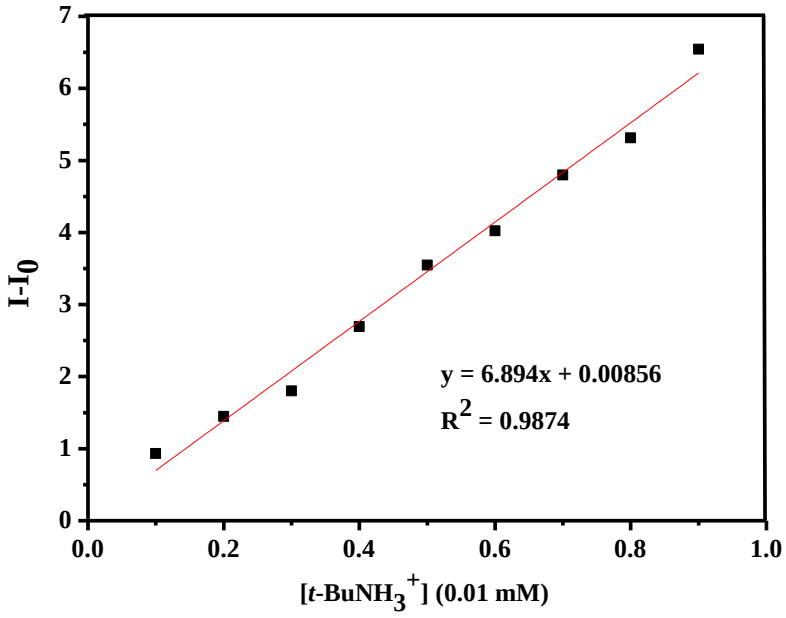

Figure 4.8. Linear concentration range of *t*-$BuNH_3^+$ with **L**. The detection limit of *t*-$BuNH_3^+$ was calculated to be 1.05 × 10^{-6} M by the formula (3σ/K).

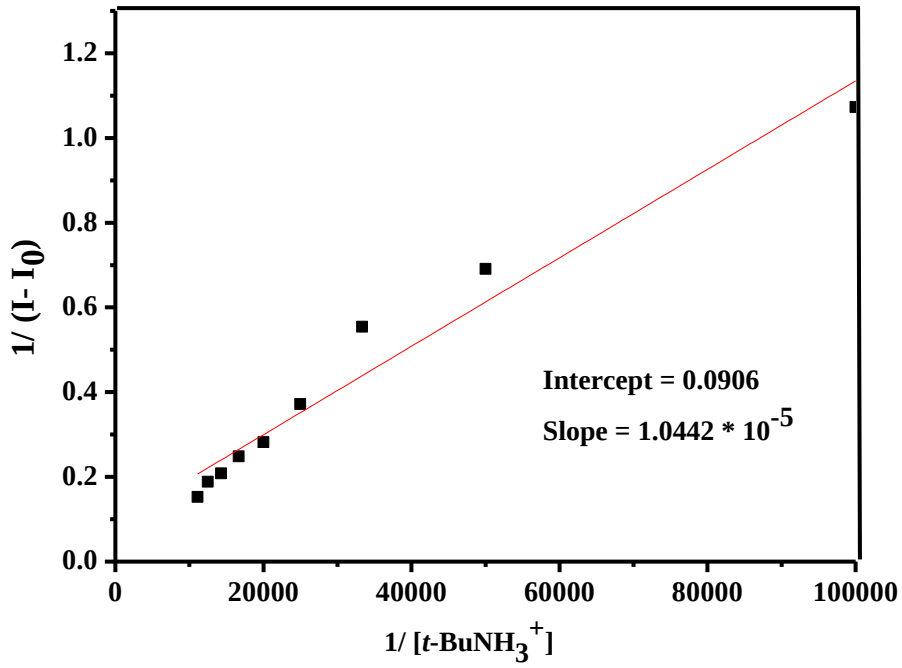

Figure 4.9. The binding constants of **L** with *t*-$BuNH_3^+$ in different concentrations. The K_a of *t*-$BuNH_3^+$ was calculated to be 8.6 × 10^3.

On the other hand, Figure 4.7 shows the fluorescence spectra of receptor **L** by the addition of increasing concentrations of *t*-$BuNH_3^+$. Upon addition of *t*-$BuNH_3^+$, the fluorescence intensity of the receptor **L** solution increased gradually. The saturation

behavior of the fluorescence intensity after adding 2 equivalents of *t*-$BuNH_3^+$ reveals that a 1:1 stoichiometry is best for the binding mode of *t*-$BuNH_3^+$ and **L**. According to the 1:1 model, the stability constant (K_a) of **L** with *t*-$BuNH_3^+$ was calculated to be 8.6 × 10^3 M^{-1} (error < 10%), the low detection limit of 1.05 × 10^{-6} M. And the same phenomenon has been found in the case of G3, G4, and G6 (Figure 4.10).

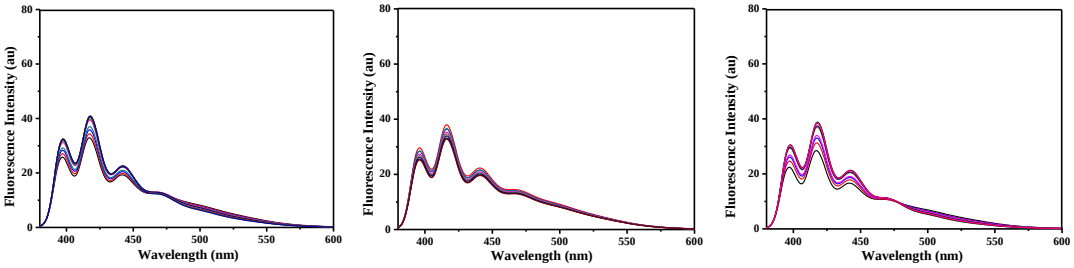

(a) (b) (c)

Figure 4.10. Fluorescence spectra of **L** (0.01 mM) upon addition of increasing concentrations of G3 (a), G4 (b), G6 (c) in CH3CN. λex = 365 nm.

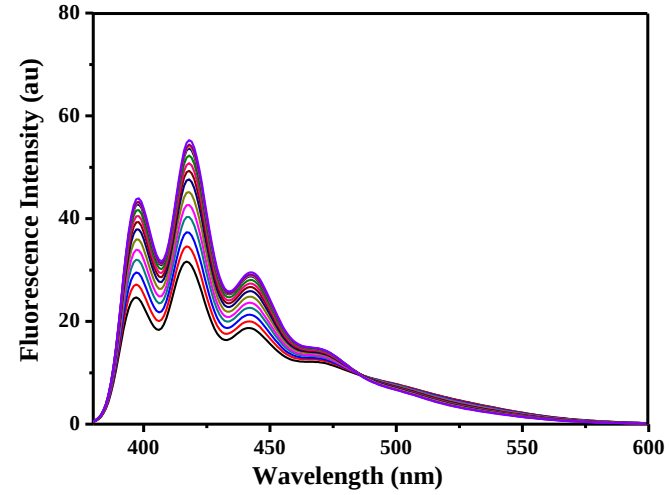

(a)

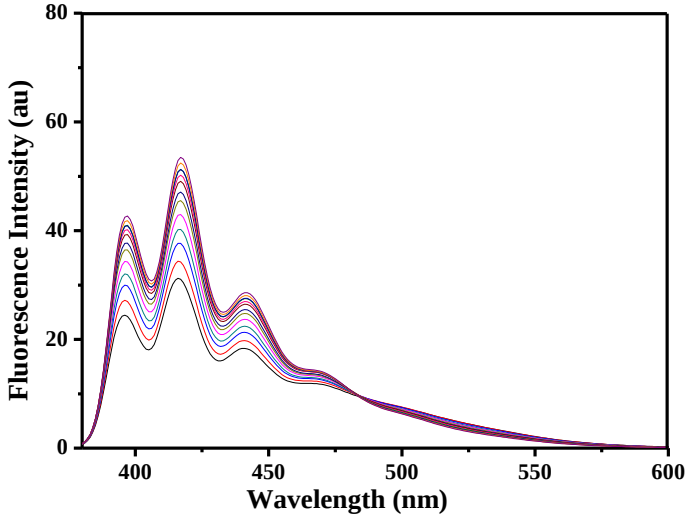

(b)

Figure 4.11. Fluorescence spectra of **L** (0.01 mM) upon addition of increasing concentrations of G1 (a), G3 (b), G4 (c) and G5 (d) in CH3CN. λex = 365 nm.

In the case of G7 (phenethylamine) and G8 (dopamine), Upon addition of G7 and G8, the fluorescence intensity of the receptor **L** solution increased gradually (Figure 4.11). The saturation behavior of the fluorescence intensity after adding 2 equivalents of G7 and G8 reveals that a 1:1 stoichiometry is best for the binding mode of G7, G8 and **L**.

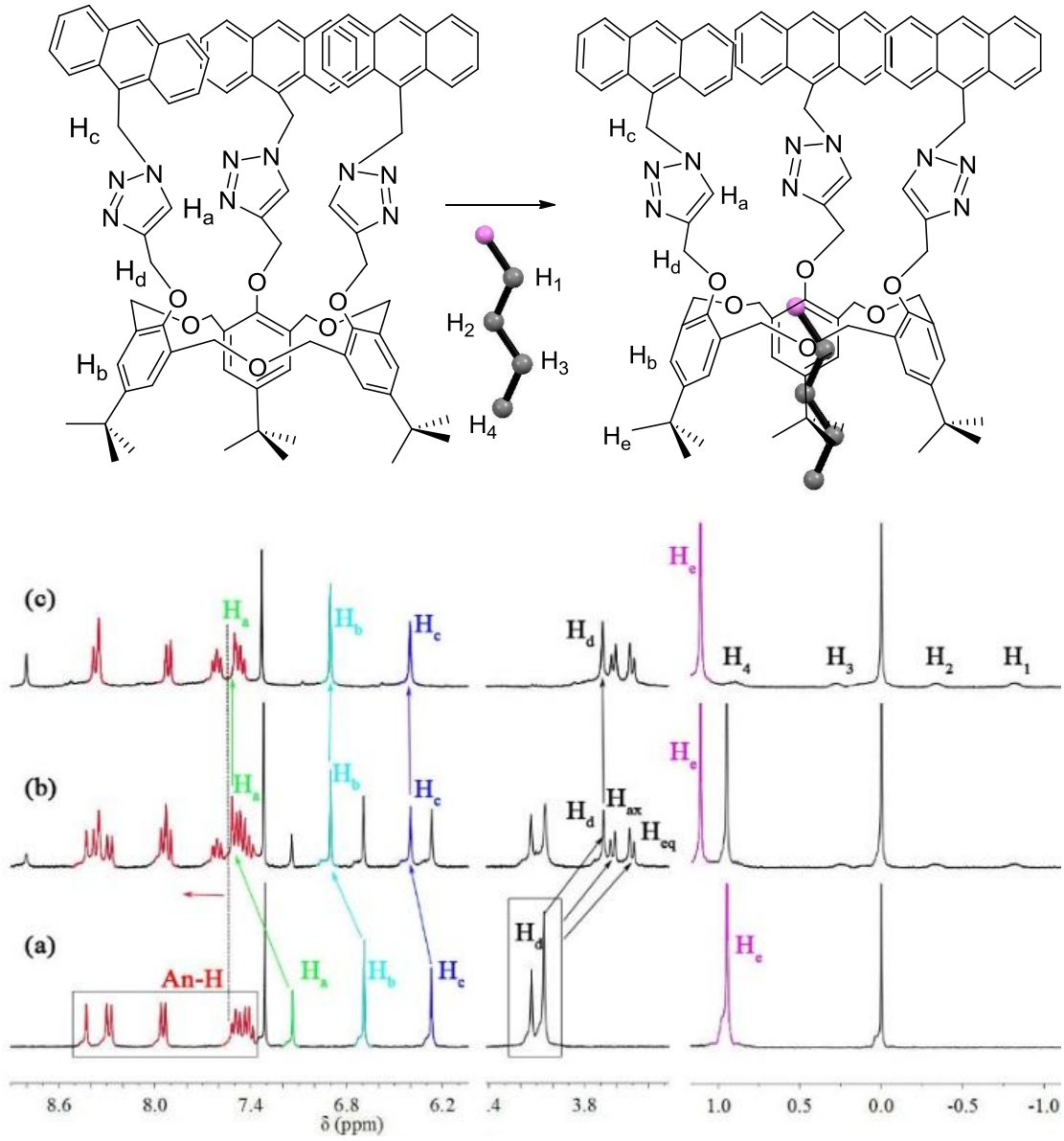

Figure 4.12. Plausible complexation of **L** for *n*-$BuNH_3^+$ ion, and partial ^{1}H NMR spectra of **L** in $CDCl_3/CD_3CN$ (10:1, v/v) upon addition of n-BuNH3+ at 298 K. (a) Free **L**, (b) **L** ⊂ *n*-$BuNH_3^+$ (0.5 equiv.), and (c) L ⊂ *n*-$BuNH_3^+$ (1.0 equiv.).

To confirm the binding mechanism, ^{1}H NMR spectra of the **L**, **L**•*n*-$BuNH_3^+$ complex were measured in a mixture of $CDCl_3$ /CD_3CN (10:1, v/v). As shown in Figure 4.12, upon gradual addition of *n*-$BuNH_3^+$ salt (0.5 equiv.) to a solution of **L**,

the resonances corresponding to the protons of receptor **L** were split into two sets of signals. After addition of 1 equiv. *n*-$BuNH_3^+$ in receptor **L** the original proton signals disappeared. This result suggests the presence of the complexed form between L•*n*-$BuNH_3^+$ and the uncomplexed form of free **L**. Moreover, the $\Delta\delta_H$ value for H_{ax} and H_{eq} of the ArCH_2O methylene protons changed to 0.12 ppm, the large $\Delta\delta_H$ value for H_{ax} and H_{eq} indicated that the phenol groups in the complex are positioned in a more-upright form, the calix cavity changed from a "flattened-cone" to a more-upright form that is similar to the previously reported examples. [19]

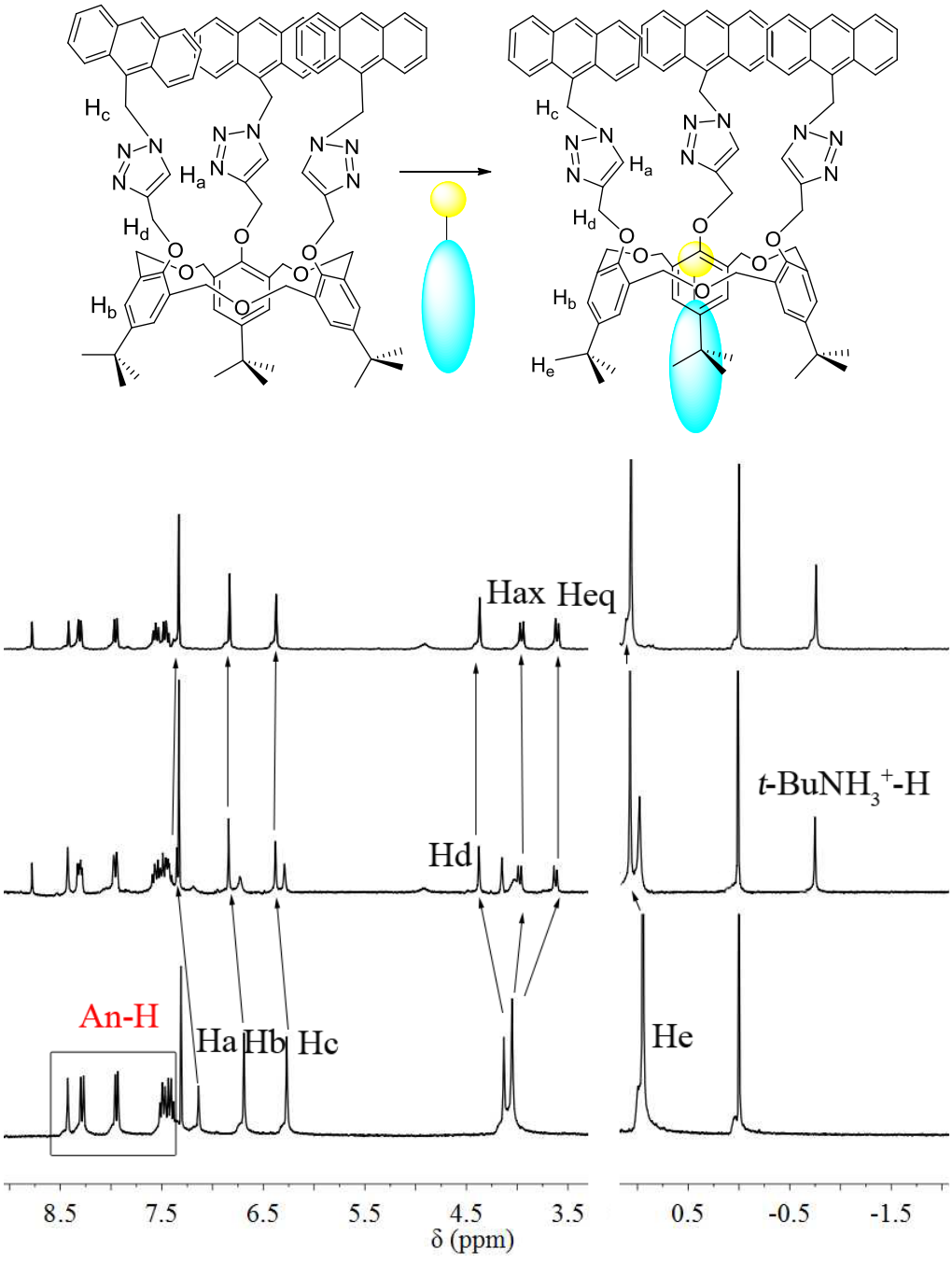

Figure 4.13. Plausible complexation of **L** for *t*-$BuNH_3^+$ ion, and partial ^{1}H NMR

spectra of **L** in $CDCl_3/CD_3CN$ (10:1, v/v) upon addition of *t*-$BuNH_3^+$ at 298 K. (a) Free **L**, (b) **L** ⊂ *t*-$BuNH_3^+$ (0.5 equiv.), and (c) **L** ⊂ *t*-$BuNH_3^+$ (1.0 equiv.).

On the other hand, addition of n-$BuNH_3^+$ to **L** resulted in the formation of endo-cavity inclusion complexes, unambiguously confirmed by the appearance of high-field resonances (δ = 0.91 to 0.20 and –0.32 to –0.81 ppm, respectively), for the methylene hydrogen atoms of the included alkylammonium guest ions experiencing the shielding effects of the calixarene aromatic units. Similar ^{1}H NMR titration experiments were carried out for **L**•*t*-$BuNH_3^+$ (Figure 4.13). The guest proton of *t*-$BuNH_3^+$ is shifted to δ –0.76 ppm, it is strongly suggesting the formation of endo-cavity inclusion complexes.

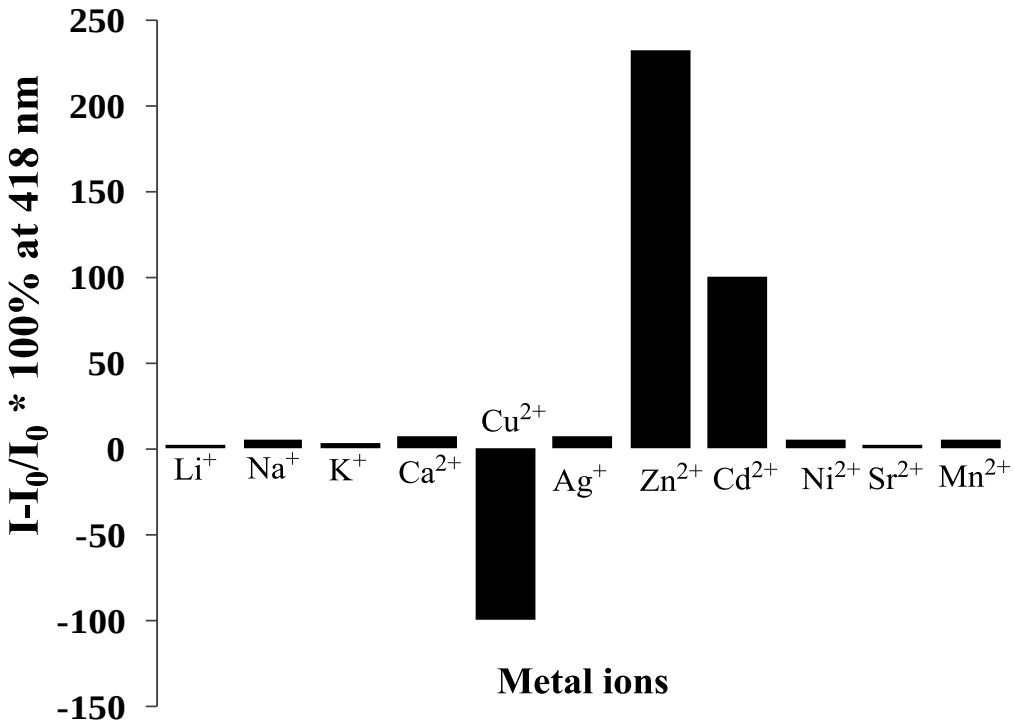

Figure 4.14. Fluorescence intensity changes ($(I - I_0)/I_0 \times 100\%$) of **L**•n-$BuNH_3^+$ (0.01 mM) in CH_3CN at 298 K upon addition of various metal perchlorates (10 equiv.). I_o is fluorescence emission intensity at 418 nm for **L**•n-$BuNH_3^+$, and I is the fluorescent intensity after adding metal ions. λ_{ex} = 365 nm.

4.2.2 Fluorescent receptor for both Zn^{2+} and ammonium ions

Interestingly, the fluorescence intensity changes of the emissions of **L**•n-$BuNH_3^+$ ([L]/ [n-$BuNH_3^+$] = 1:1, [L] = 0.1 mM) upon addition of metal ions, such as K^+, Na^+, Ca^{2+}, Mn^{2+}, Ni^{2+}, Sr^{2+}, Ag^+, Cu^{2+}, Cd^{2+} and Zn^{2+} (1.0 mm), determined as their perchlorate salts in CD_3CN, are summarized in Figure 4.14. We found that upon excitation at 365 nm, enhancement of the fluorescence intensity was observed upon

addition of about 10 equiv. of Zn^{2+} and Cd^{2+} compared to that of only complex **L**•n-$BuNH_3^+$. These results suggested that complex **L**•n-$BuNH_3^+$ has a high selectivity for the Zn^{2+} ion by enhancement of fluorescence intensity.

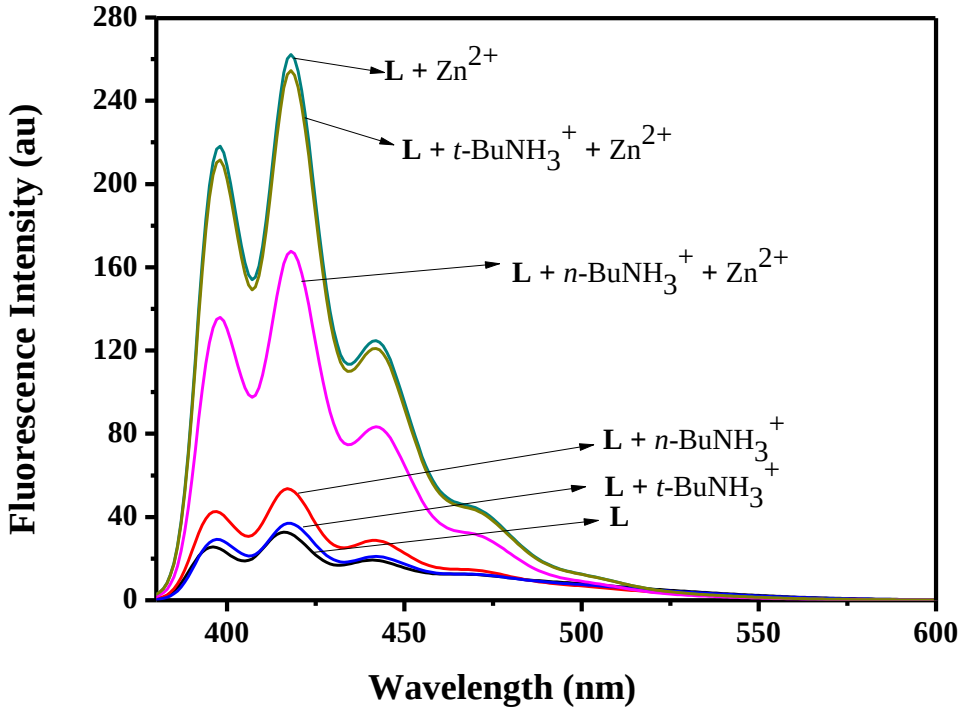

Figure 4.15. Fluorescence spectra of receptor **L** (0.01 mM) (a) in CH_3CN at 298 K upon addition of *n*-$BuNH_3^+$, *t*-$BuNH_3^+$ and Zn^{2+}. λex = 365 nm.

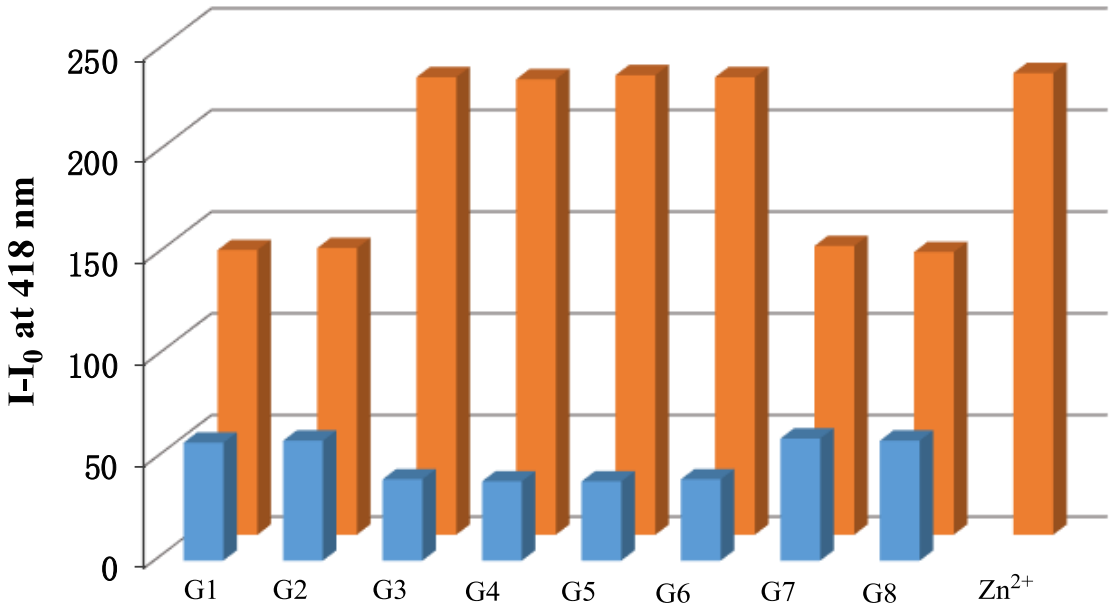

Figure 4.16. Percentage fluorescence intensity of **L** (0.01 mM) by the addition of 10 equiv. of various ions. Bule bars, L ⊂ 2 equiv. of various ammonium guest ions (G1 – G8); yellow bars, L ⊂ 2 equiv. of various ammonium guest ions (G1 – G8) ⊂ 10 equiv. of Zinc ion. Excitation wavelength was 365 nm.

Similar fluorescence experiments were carried out for **L**•(G1-G8) (Figure 4.15 and Figure 4.16). In the case of linear-chain ammonium guest ions, the addition of Zn^{2+} caused fluorescence emission spectra similar with **L**•n-$BuNH_3^+$•Zn^{2+}. The result indicated **L** possesses a high affinity and selectivity for linear-chain ammonium guest ions and Zn^{2+} ions by enhancement of fluorescence intensity in organic solution. In the case of branched-chain ammonium guest ions, the addition of Zn^{2+} caused fluorescence emission spectra similar with **L**•Zn^{2+}. The result indicated **L** possesses a high affinity and selectivity for linear-chain ammonium ions and Zn^{2+} ions by enhancement of fluorescence intensity in organic solution, and **L** can distinguish between linear-chain and branched-chain ammonium guest ions.

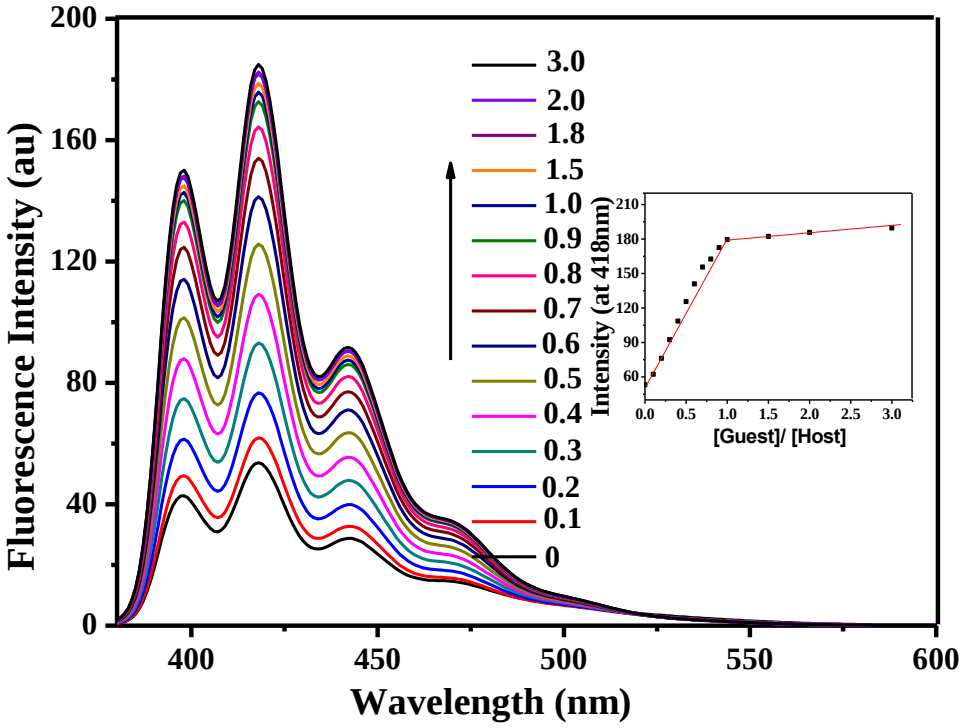

Figure 4.17. Fluorescence spectra of **L**•*n*-$BuNH_3^+$ ([L]/ [*n*-$BuNH_3^+$] = 1:2, [**L**] = 0.1 mM) upon addition of increasing concentrations of Zn^{2+} in CH_3CN. λ_{ex} = 365 nm.

Figure 4.17 illustrates the fluorescence titration experiments of receptor **L**•n-$BuNH_3^+$ with the Zn^{2+} ion in neutral solution. No shift of the maximum of emissions was observed upon the addition of Zn^{2+} ion with excitation wavelength at 365 nm, However, when increasing concentrations of Zn^{2+} were added to the solution of **L**•*n*-$BuNH_3^+$, the fluorescence intensity gradually increased and reached a plateau upon adding about 10 equiv. of Zn^{2+} ion. The association constant of **L**•*n*-$BuNH_3^+$ with Zn^{2+} was calculated to be 7.0 $\times 10^3$ M^{-1} (error < 10%). And the same phenomenon has been found in the case of G3, G4, and G6.

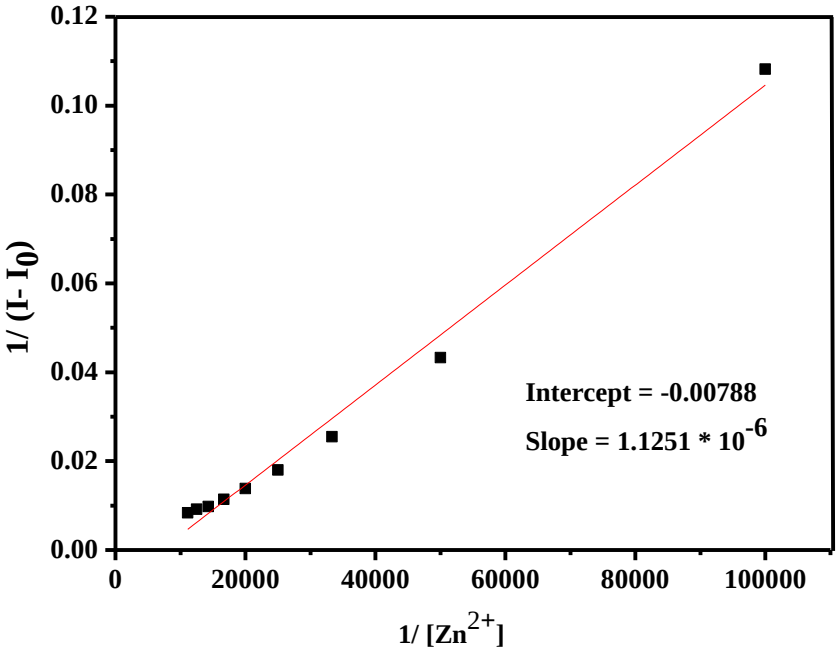

Figure 4.18. The binding constants of **L**•*n*-$BuNH_3^+$ with Zn^{2+} in different concentrations. The K_a of Zn^{2+} was calculated to be 7.0×10^3.

On the other hand, Figure 4.19 illustrates the fluorescence titration experiments of receptor **L**• Zn^{2+} with the n-$BuNH_3^+$ ion in neutral solution. No shift of the maximum of emissions was observed upon the addition of n-$BuNH_3^+$ ion with excitation wavelength at 365 nm, However, when increasing concentrations of n-$BuNH_3^+$ were added to the solution of **L**• Zn^{2+}, the fluorescence intensity gradually increased and reached a plateau upon adding about 10 equiv. of n-$BuNH_3^+$ ion. Similar fluorescence experiments were carried out for n-$BuNH_3^+$, Cd^{2+} and **L** (Figure 4.20 and 4.21)**.**

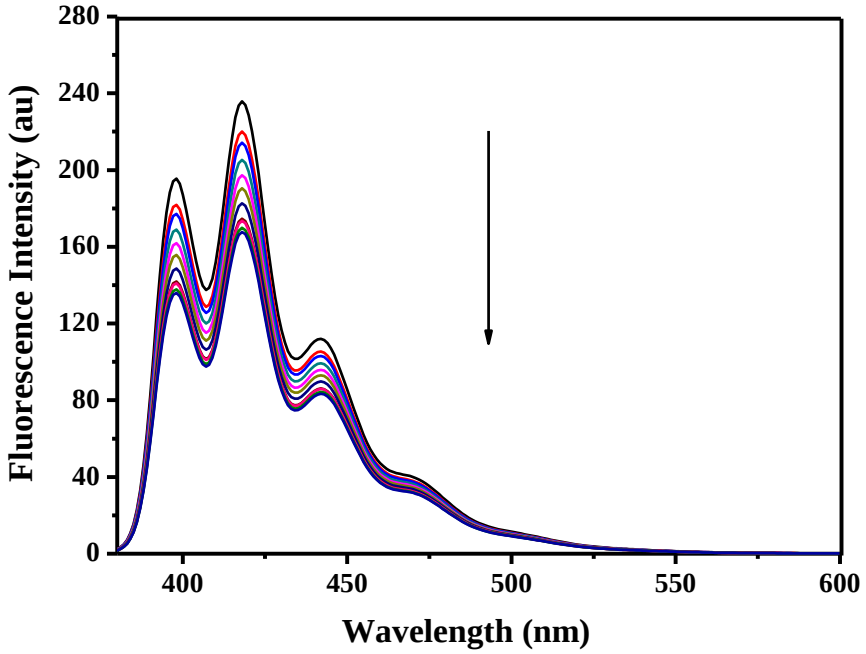

Figure 4.19. Fluorescence spectra of **L**• Zn^{2+} ([L]/ [Zn^{2+}] = 1:2, [L] = 0.01 mM) upon addition of increasing concentrations of *n*-$BuNH_3^+$ in CH_3CN. λ_{ex} = 365 nm.

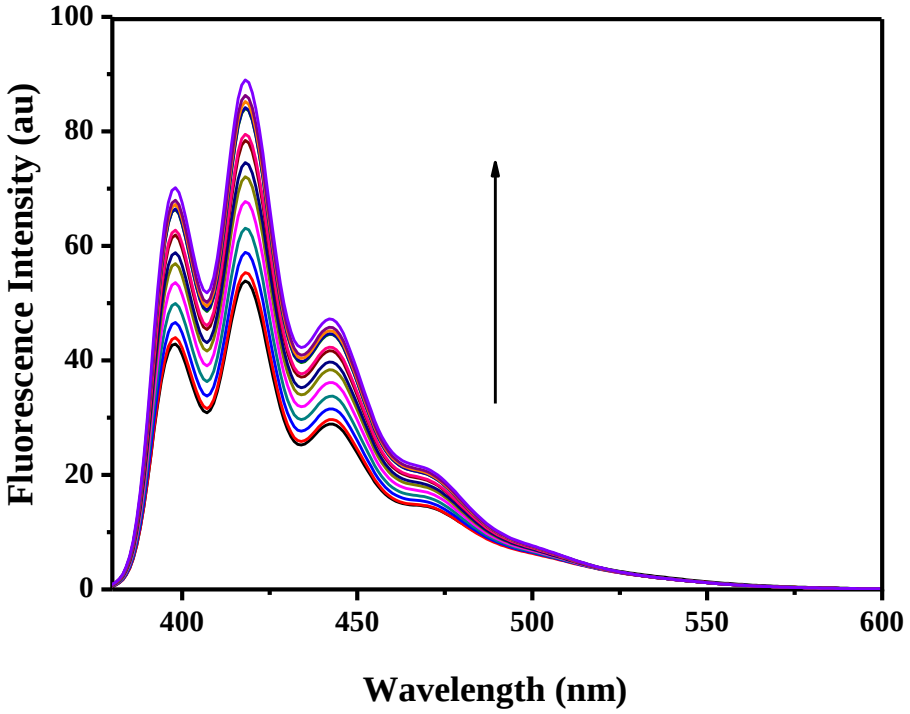

Figure 4.20. Fluorescence spectra of **L**•*n*-$BuNH_3^+$ ([L]/ [*n*-$BuNH_3^+$] = 1:2, [L] = 0.01 mM) upon addition of increasing concentrations of Cd^{2+} in CH_3CN. λ_{ex} = 365 nm.

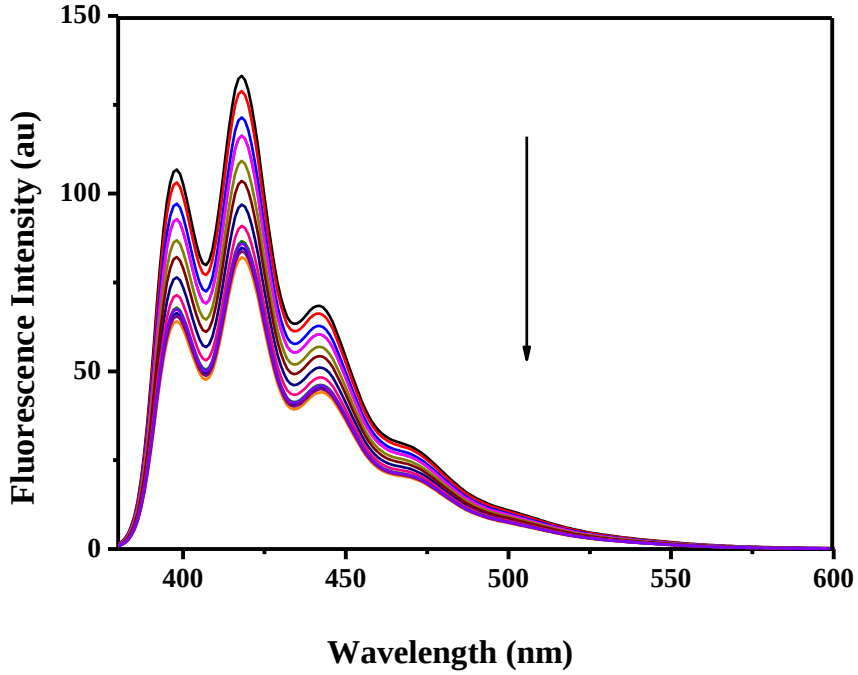

Figure 4.21. Fluorescence spectra of **L**• Cd^{2+} ([L]/ [Cd^{2+}] = 1:2, [L] = 0.01 mM) upon addition of increasing concentrations of *n*-$BuNH_3^+$ in CH_3CN. λ_{ex} = 365 nm

In an effort to gain more detailed information on the interactions between **L**•n-$BuNH_3^+$ and Zn^{2+} ion, ^{1}HNMR spectroscopic studies were carried out in $CDCl_3/CD_3CN$ (10:1, v/v). The spectral differences are shown in Figure 4.22. the peak of the proton H_a on the triazole ring is shifted downfield from δ 7.47 to 7.54 ppm, whereas the O*CH*$_2$-triazole linker proton H_d and the H_c proton proximal to the anthracene moiety are shifted down-field by 0.76 ppm and 0.53 ppm. These spectral changes suggested that the Zn^{2+} ion is selectively bound by the nitrogen atoms on the triazole rings.

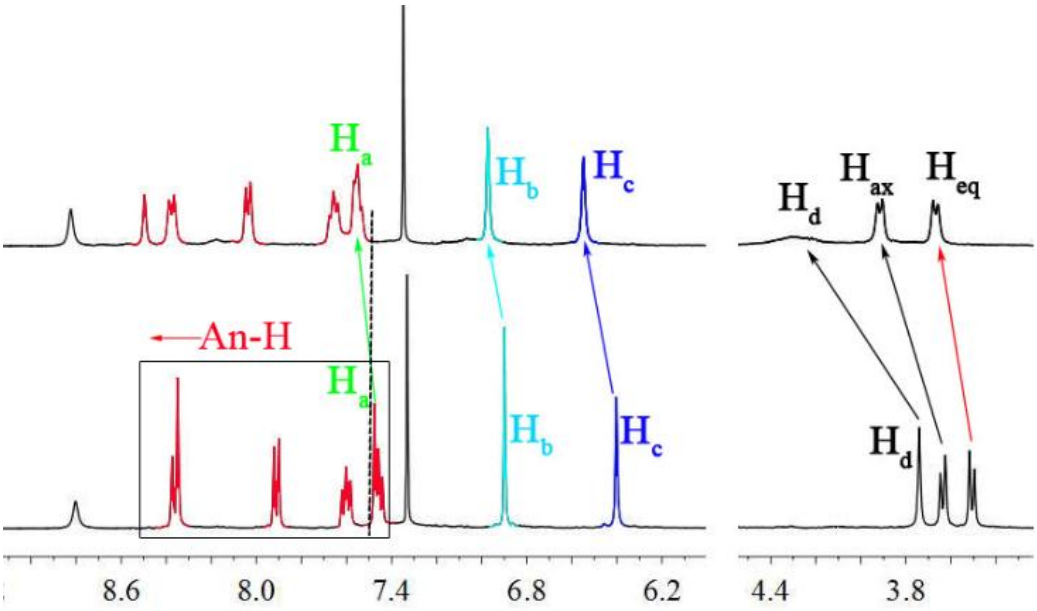

Figure 4.22. Partial ^{1}H NMR spectra of **L**•*n*-$BuNH_3^+$ in $CDCl_3/CD_3CN$ (10:1, v/v) upon addition of Zn^{2+} at 298 K. (a) **L** ⊂ *n*-$BuNH_3^+$ (1.0 equiv.), and (b) **L** ⊂ *n*-$BuNH_3^+$ (1.0 equiv.) ⊂ Zn^{2+} (1.0 equiv.

Table 4.1. Selected proton chemical shifts (δ, ppm) (300 MHz, $CDCl_3$:CD_3CN, 10:1 v/v, 27 °C) of **L.**

	n-$BuNH_3^+$				*t*-$BuNH_3^+$
	H_1	H_2	H_3	H_4	$H_{t\text{-Bu}}$
L⊂ *n*-$BuNH_3^+$	-0.81	-0.32	0.20	0.91	--
L ⊂ *n*-$BuNH_3^+$⊂ Zn^{2+}	-0.81	-0.32	0.20	0.91	--
L ⊂*t*-$BuNH_3^+$	--	--	--	--	-0.76
L⊂ *t*-$BuNH_3^+$ ⊂Zn^{2+}	--	--	--	--	1.40

On the other hand, the signal for the proton on the anthracene moiety revealed a down-field shift and the $\Delta\delta_H$ value for H_{ax} and H_{eq} of the Ar*CH*$_2$O methylene protons

changed from 0.12 ppm to 0.26 ppm, the binding mode of **L**•*n*-$BuNH_3^+$ with Zn^{2+} explore that the phenol groups in the complex are situated as an upright form and also the anthracene moieties are distant apart from each other to weaken the π–π stacking in presence of Zn^{2+} which results the fluorescence enhancement. On the other hand, because of the formation of endo-cavity inclusion complexes, the protons of guest still appeared at high-field resonances (δ = 0.91 to 0.20 and –0.32 to –0.81 ppm, respectively, Table 4.1). Based on the above results, a plausible binding mode of **L**•*n*-$BuNH_3^+$ with Zn^{2+} is therefore depicted in Figure 4.23.

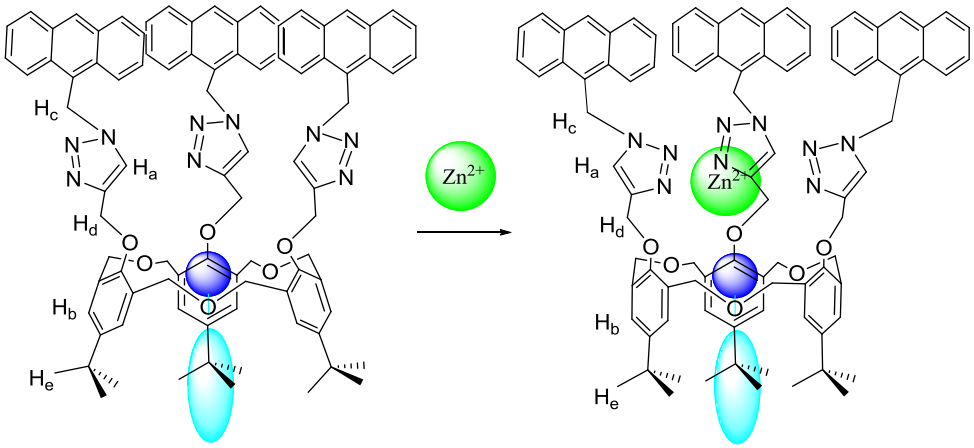

Figure 4.23. Plausible complexation of **L**•*n*-$BuNH_3^+$ for Zn^{2+} ion.

4.3. Conclusions

In summary, we have prepared a new type of chemosensing ensemble probes based on homooxacalix[3]arene with a C_3 symmetric structure, which displayed ratiometric selectivity for linear-chain ammonium ions and Zn^{2+} ions in neutral solution. It possesses a high affinity and selectivity for linear-chain ammonium ions and Zn^{2+} ions by enhancement of fluorescence intensity in organic solution, and **L** can distinguish between linear-chain and branched-chain ammonium guest ions. Interestingly, upon addition of Zn^{2+} to this system, chemosensor **L** can be capable of binding a metal ions and alkylammonium cations simultaneously through positive allosteric effect. The successful performance of these probes suggested chemosensing ensemble method had great advantage and should play more roles in sensor design.

4.4. References

1. (a) U. Borgmann, *Environ. Pollut.* **1994**, *86*, 329–335; (b) V. Vallet and M. Masella, *Chemical Physics Letters* **2015**, *618*, 168–173; (c) K. Zare, H. Sadegh, R. Shahryari-ghoshekandi, M. Asif, I. Tyagi, S. Agarwal, V. K. Gupta, *J. Mol. Liq.* **2016**, *213*, 345–350.

2. (a) P.W. Alexander, T. Dikitrakopoloulos, D.B. Hibbert, *Electroanalysis* **1997**, *9*,

1331–1336; (b) A. Arslan, S. Veli, *J. Taiwan Inst. Chem. E.* **2012**, *43*, 393–398.

3. (a) J. Magalhaes, A. Machado, *Analyst* **2002**, *127*, 1069–1075; (b) J. Lima, C. Delerue-Matos, C.V.M. Cristina, *Anal. Chim. Acta* **1999**, *385*, 437–441.
4. (a) L. L. Tan, A. Musa, Y. H. Lee, *Sensors and Actuators B: Chemical* **2012**, *173*, 614–619; (b) A. Zazoua, I. Kazane, N. Khedimallah, C. Dernane, A. Errachid, N. Jaffrezic-Renault, *Materials Science and Engineering: C* **2013**, *33*, 5084–5089; (c) Y. C. Luo, J. S. Do, *Sensors and Actuators B: Chemical* **2006**, *115*, 102–108.
5. (a) K. Cottet, P. M. Marcos and P. J Cragg, *Beilstein J. Org. Chem.*, **2012**, *8*, 201–226; (b) L. Mutihac, J. H. Lee, J. S. Kim and J. Vicens, *Chem. Soc. Rev.*, **2011**, *40*, 2777–2796; (c) L. Baldini, A. Casnati, F. Sansone and R. Ungaro, *Chem. Soc. Rev.*, **2007**, *36*, 254–266.
6. (a) J. S. Kim and D. T. Quang, *Chem. Rev.*, **2007**, *107*, 3780–3799; (b) R. Joseph and C. P. Rao, *Chem. Rev.*, **2011**, *111*, 4658–4702; (c) M. Kumar, R. Kumar and V. Bhalla, *Org. Lett.*, **2011**, *13*, 366–369; (d) H. S. Jung, P. S. Kwon, J. W. Lee, J. I. Kim, C. S. Hong, J. W. Kim, S. Yan, J. Y. Lee, J. H. Lee, T. Joo and J. S. Kim, *J. Am. Chem. Soc.*, **2009**, *131*, 2008–2012.
7. (a) X.-L. Ni, M. Takimoto, X. Zeng and T. Yamato, *J. Inclusion Phenom. Macrocyclic Chem.*, **2011**, *71*, 231–237; (b) X.-L. Ni, J. Tahara, S. Rahman, X. Zeng, D. L. Hughes, C. Redshaw and T. Yamato, Chem. Asian J., 2012, 7, 519–527; (c) Alfonso, M.; Espinosa, A.; T_arraga, A.; Molina, P. Org. Lett. 2011, 13, 2078–2081.
8. (a) X.-L. Ni, X. Zeng, D. L. Hughes, C. Redshaw and T. Yamato, *Org. Biomol. Chem.*, **2011**, *9*, 6535–6541; (b) K. Tsubaki, T. Otsubo, T. Morimoto, H. Maruoka, M. Furukawa, Y. Momose, M. H. Shang and K. Fuji, *J. Org. Chem.*, **2002**, *67*, 8151–8156; (c) T. Yamato, S. Rahman, F. Kitajima, Z. Xi and J. T. Gil, *J. Chem. Res.*, **2006**, 496–498;
9. (a) A. Ikeda, T. Hatano, S. Shinkai, T. Akiyama and S. Yamada, *J. Am. Chem. Soc.*, **2001**, *123*, 4855–4856; (b) A. Ikeda, M. Yoshimura, H. Udzu, C. Fukuhara and S. Shinkai, *J. Am. Chem. Soc.*, **1999**, *121*, 4296–4297;
10. (a) F. P. Schmidtchen, M. Berger, *Chem. Rev.*, **1997**, *97*, 1609; (b) P. D. Beer, P. A. Gale, *Angew. Chem., Int. Ed.*, **2001**, *40*, 486.
11. (a) C. D. Gutsche, Calixarenes. An Introduction, ed. J. F. Stoddart, The Royal Society of Chemistry, Cambridge, 2008; (b) F. Sansone, L. Baldini, A. Casnati, and R. Ungaro, *New J. Chem.*, **2010**, *34*, 2715.
12. (a) F. Sansone, L. Baldini, A. Casnati, and R. Ungaro, *New J. Chem.*, **2010**, *34*, 2715. (b) A. Casnati, F. Sansone, and R. Ungaro,. Cerberus Press Inc., South Miami, 2004, 9, 165–218. (c) J. F. Dozol and R. Ludwig, *Ion Exch. Solvent Extr.*,

2010, *19*, 195.

13. (a) X.-L. Ni, S. Wang, X. Zeng, Z. Tao and T. Yamato, *Org. Lett.*, **2011**, *13*, 552–555; (b) X.-L. Ni, X. Zeng, C. Redshaw and T. Yamato, *Tetrahedron*, **2011**, *67*, 3248–3253; (c) X.-L. Ni, X. Zeng, C. Redshaw and T. Yamato, *J. Org. Chem.*, **2011**, *76*, 5696–5702.
14. R. Ludwig and N. T. K. Dzung, *Sensors*, **2002**, *2*, 397.
15. (a) T.Yamato, F. Kitajima and J. T. Gil, *J. Inclusion Phenom. Macrocyclic Chem.*, **2005**, *53*, 257–262; (b) T. Yamato, F. Zhang, H. Tsuzuki and Y.Miura, Eur. *J. Org. Chem.*, **2001**, 1069–1075.
16. (a) K. Araki, N. Hashimi, H. Otsuka, S. Shinkai, *J. Org. Chem.* **1993**, *58*, 5958–5963; (b) D. Garozzo, G. Gattuso, A. Notti, A. Pappalardo, S. Pappalardo, M. F. Parisi, M. Perez, I. Pisagatti, *Angew. Chem.* **2005**, *117*, 4970–4974.
17. (a) M. M. Song, Z. Y. Sun, C. P. Han, D. M. Tian, H. B. Li, J. S. Kim, *Chem. Asian J.* **2014**, *9*, 2344–2357; (b) X. L. Ni, X. Zeng, C. Redshaw, T. Yamato, *J. Org. Chem.* **2011**, *76*, 5696–5702; (d) C. Wu, Y Ikejiri, J. L. Zhao, X. K. Jiang, X. L. Ni, X. Zeng, C. Redshaw, T. Yamato, *Sensors and Actuators B: Chemical* **2016**, *228*, 480–485; (e) F. J. Miao, J. Y. Zhan, Z. L. Zou, D. M. Tian, H. B. Li, *Tetrahedron* **2012**, *68*, 2409–2413.
18. (a) R. K. Pathak, S. M. Ibrahim, C. P. Rao, *Tetrahedron Lett.* **2009**, *50*, 2730–2734; (b) R. K. Pathak, A. G. Dikundwar, T. N. G. Row, C. P. Rao, *Chem. Commun.* **2010**, *46*, 4345–4347; (c) N. M. Feng, L. Luo, G. F. Zhang, F. J. Miao, C. Wang, D. M. Tian, H. B. Li, *RSC Adv.* **2013**, *3*, 19278–19281. (d) N. M. Feng, H. Y. Zhao, J. Y. Zhan, D. M. Tian, H. B. Li, *Org. Lett.* **2012**, *14*, 1958–1961.
19. R. K. Pathak, K. Tabbasum, A. Rai, D. Panda, C. P. Rao, *Anal. Chem.* **2012**, *84*, 5117–5123

Summary

Calixarenes are an important class of macrocyclic compounds and are ideal platforms for the development of cation, anion, and neutral molecule recognition. Calixarenes and their derivatives are also attractive compounds for use in host–guest and supramolecular chemistry. In particular, hexahomotrioxacalix[3]arene derivatives with *C3*-symmetry can selectively bind ammonium ions which play important roles in both chemistry and biology. Furthermore, the incorporation of two types of recognition sites via the introduction of different ionophores on the hexahomotrioxacalix[3]arene will create potential hetero-ditopic receptors with the capability of binding cations and anions, e.g. ammonium ions and halides. Therefore, many fluorescent chemosensors based on calixarenes, which show highly selective recognition of metal cations, ammonium cations, and fullerene derivatives, have been reported. Many approaches such as atomic absorption, ICP atomic emission, UV-vis absorption, and fluorescence spectroscopy have been employed to detect low limits. Among these methods, fluorescence spectroscopy is widely used because of its high sensitivity, facile operation, and low cost.

Click chemistry has attracted considerable attention recently and has been applied in a wide range of fields for its efficiency, regioselectivity, compatibility with reaction conditions and especially for its ions binding ability. Click chemistry has also been used to synthesize calixarene conjugates of chromophores and bioactive molecules such as glycosides,[12] sialoclusters,[13] and amino acids.[14] Because of the highly selective nature of the alkyne-azide cycloaddition, the Click reaction is a general method to introduce various functional groups/moieties at the upper or lower rim of calixarenes. Recently, heteroditopic chemosensors have received much interests and design, synthesis of heteroploytopic chemosensors will open a new gate for metal ions recognition.

Thus, against this background, several kinds of heteropolytopic chemosensors or fluorescent chemosensors for metal ions and ammonium cations were designed and synthesized based on hexahomotrioxacalix[3]arene in this dissertation. The sensitivity and selectivity properties of these receptors to the target analytes were carefully evaluated.

In chapter 1, a shortly review of the recently development of fluorescent receptors for cations and anions based on calixarene, fluorescent recognition for cations: Zn^{2+}, Cu^{2+}, Ag^{+}, alkali metal, ammonium ions and anions: Cl^{-}, Br^{-}, H_2PO4^{-} and so on. Many coupling methods have been reported such as Click chemistry reactions forming triazo rings that can bind to metal ions and act aschromophore. In this part,

we also introduce the reported works about recognition of amino acids and anions by the metal ions complexes.

In chapter 2, *O*-alkylation of 7,15,23-tri-*tert*-butyl-25,26,27-trihydroxy-2,3,10,11,18,19-hexahomo-3,11,19-trioxacalix[3]arene (**1**H_3) with 9-chloromethyl-anthracene **5** was carried out under the different reaction conditions. The number of anthrylmethyl group introduced to the phenolic oxygen of hexahomo-trioxacalix[3]arene **1**H_3 was achieved through selective *O*-alkylation with stoichiometric amounts of 9-chloromethylanthracene **5** in the acetone system to give mono-*O*-alkylated product **2**H_2An, di-*O*-alkylated product **3**HAn_2 and *tri*-*O*-alkylated product *partial-cone*-**4**An_3, and their structures were confirmed by ^{1}H NMR, ^{13}C NMR, IR, MS spectroscopy and X-ray analysis. Interestingly, **2**H_2An, **3**HAn_2, and *partial-cone*-**4**An_3 was synthesized from compound **1**H_3 through selective alkylation in the acetone system whereas by using acetone /benzene (1: 1 v /v) mixed solvent system, the *cone*-**4**An_3 was produced. These results suggest that the solvent can also control the conformation of the *O*-alkylation products, the solvent effects on this reaction in aprotic solvents has revealed hydrogen bond donor and acceptor abilities and polarity of solvent. The possible reaction routes of the *cone*-**4**An_3 and *partial-cone*-**4**An_3 were also discussed.

However, it should be noted that there are relativity few example of receptors for ammonium ions with ratiometric fluorescence sensor. Because of the conformation can decide the binding ability to ammonium ions.

In chapter 3, a new type of selective and sensitive fluorescent sensor having triazole rings as the binding sites at the lower rim of a hexahomotrioxacalix[3]arene scaffold in a *cone* conformation was synthesized. The selective binding behaviour of chemosensor **L** has been evaluated by fluorescence spectra and ^{1}H NMR spectroscopic analysis. This sensor has desirable properties for practical applications, including selectivity for detecting Zn^{2+} and Cd^{2+} in the presence of excess competing metal ions at low ion concentration or as a fluorescence enhancement type chemosensor due to the cavity of calixarene changed from a "flattened-cone" to a more-upright form and inhibition of photoinduced electron transfer (PET). In contrast, the results suggested that receptor **L** is highly sensitive and selective for Cu^{2+} and Fe^{3+} as a fluorescence quenching type chemosensor due to the photoinduced electron transfer (PET) or heavy atom effect.

In chapter 4, chemosensor **L** displayed ratiometric selectivity for linear-chain ammonium ions and Zn^{2+} ions in neutral solution. It possesses a high affinity and selectivity for linear-chain ammonium ions and Zn^{2+} ions by enhancement of fluorescence intensity in organic solution, and **L** can distinguish between linear-chain

and branched-chain ammonium guest ions. Interestingly, upon addition of Zn^{2+} to this system, chemosensor **L** can be capable of binding a metal ions and alkylammonium cations simultaneously through positive allosteric effect. The successful performance of these probes suggested chemosensing ensemble method had great advantage and should play more roles in sensor design.

In summary, homooxacalix[3]arene have two conformation isomers, and the cone results can formed when a template metal is present in the reaction system or using solvent effect. Chemosensor **L** in cone conformation were designed and synthesized based on hexahomotrioxacalix[3]arene, Click chemistry. It has been use to recognize metal cation and ammonium cations. In these research fields, there are relativity few example and will open a gate for chemical research on chemosensors based on calixarene.

Publications

1. Synthesis and structures of O-anthrylmethyl-substituted hexahomotrioxacalix[3]arenes

Xue-Kai Jiang, Yusuke Ikejiri, Xi-Long Ni, Xi Zeng, Carl Redshaw and Takehiko Yamato,

Journal of Molecular Structure, 1120, 274–280, 2016.

2. Synthesis and evaluation of a novel fluorescent sensor based on hexahomotrioxacalix[3]arene for Zn^{2+} and Cd^{2+}

Xue-Kai Jiang, Yusuke Ikejiri, Cheng-Cheng Jin, Chong Wu, Jiang-Lin Zhao, Xin-Long Ni, Xi Zeng, Carl Redshaw, Takehiko Yamato

Tetrahedron, 72, 4854–4858, 2016.